Universitat Autònoma de Barcelona

Study of urine extracellular vesicles-derived protein biomarkers for the non-invasive monitoring of kidney-transplanted patients

Laura Carreras Planella

Study of urine extracellular vesicles-derived protein biomarkers for the non-invasive monitoring of kidney-transplanted patients

Laura Carreras Planella

Doctoral thesis

Badalona, 20th October 2020

Thesis directors:

Francesc Enric Borràs Serres, PhD

Maria Isabel Troya Saborido, PhD

PhD programme in Advanced Immunology
Department of Cellular Biology, Physiology and Immunology
Universitat Autònoma de Barcelona

Study of urine extracellular vesicles-derived protein biomarkers for the non-invasive monitoring of kidney-transplanted patients

Estudi de biomarcadors proteics derivats de vesícules extracel·lulars de la orina per la monitorització no invasiva de pacients trasplantats de ronyó

Thesis presented by Laura Carreras Planella to qualify for the PhD degree in Advanced Immunology by the Universitat Autònoma de Barcelona

The presented work has been performed in the ReMAR-IVECAT group at the Germans Trias i Pujol Health Sciences Research Institute (IGTP) under the supervision of Dr. Francesc Enric Borràs Serres, as tutor and co-director, and Dr. Maria Isabel Troya Saborido as co-director.

Laura Carreras was sponsored by the Spanish Government with an FPU grant ("Formación de Personal Universitario", FPU17/01444) and by La Fundació Cellex during the development of the PhD project.

This work supported in part by grants from project PI13/ 00050 integrated in the National R+D+I and funded by the ISCIII and the European Regional Development Fund (http://www.isciii.es), the SGR program of Generalitat de Catalunya (2017-SGR-301 REMAR Group), the ISCIII-REDinREN (RD16/0009 Feder Funds), and Fundació Cellex. The project leading to these results has also received funding from "la Caixa" Foundation (ID 100010434), under agreement LCF/TR/CI19/52460021. This activity has received funding from the European Institute of Innovation and Technology (EIT), which is supported by the European Union's Horizon 2020 research and innovation program.

The European Patent Application Number 19 383 190.6, related to the use of vitronectin as biomarker for kidney fibrosis, was developed at the Institut d'Investigació en Ciències de la Salut Germans Trias i Pujol (IGTP).

Samples used in this thesis were obtained from a collaboration with the Nephrology Dept. of the Hospital Universitari Germans Trias i Pujol, the Nephrology Dept. of the Hospital Clínic de Barcelona and the Biobank of the Hospital Universitari de Girona Dr. Josep Trueta and Institut d'Investigació Biomèdica de Girona Dr. Josep Trueta.


IGTP
Germans Trias i Pujol Research Institute


UAB
Universitat Autònoma
de Barcelona


REMAR


iVECAT


Germans Trias i Pujol
Hospital


CLÍNIC
BARCELONA
Hospital Universitari


Hospital Universitari de Girona
Doctor Josep Trueta


Fundació Privada
CELLEX


Red de
Investigación
Renal
redinRen


IDIBGi
Institut d'Investigació
Biomèdica de Girona
Dr. Josep Trueta


Unión Europea
Fondo Europeo de
Desarrollo Regional
"Una manera de hacer Europa"


AGAUR
Agència
de Gestió
d'Ajuts
Universitaris
i de Recerca


Generalitat de Catalunya
Departament d'Empresa i Coneixement
Secretaria d'Universitats i Recerca


CaixaBank


Caixa impulse
innovation for society

TABLE OF CONTENTS

ABBREVIATIONS

Abbreviation	Description
ABMR	antibody-mediated rejection
aCNIT	acute calcineurin inhibitors toxicity
ACR	acute cellular rejection
ah	arterial hyalinosis
ANOVA	analysis of variance
cCNIT	chronic calcineurin inhibitors toxicity
CD	cluster of differentiation
cg	chronic glomerular lesions
CHAPS	3-[(3 cholamidopropyl) dimethylammonio]-1 propanesulfonate
ci	chronic interstitial lesions
CKD	chronic kidney disease
CNIT	calcineurin inhibitors toxicity
ct	chronic tubular lesions
cv	chronic vascular lesions
DSA	donor-specific antibodies
DTT	dithiothreitol
ELISA	enzyme-linked immunosorbent assay
ERA-EDTA	European Renal Association - European Dialysis and Transplant Association
EV	extracellular vesicles
FDR	false discovery rate
GO	Gene Ontology
GSEA	Gene Set Enrichment Analysis
HCA	hierarchical clustering analysis
HLA	human leukocyte antigens
iBAQ	intensity-based absolute quantification
IFTA	interstitial fibrosis and tubular atrophy
IL	interleukin
ISEV	International Society of Extracellular Vesicles
LC-MS/MS	liquid chromatography followed by tandem MS
miRNA	micro ribonucleic acid
MFI	mean fluorescence intensity
mm	mesangial matrix increase
MS	mass-spectrometry

mTOR	mammalian target of rapamycin
NIH	National Institute of Health
NKF	normal kidney function
OCATT	Organització Catalana de Trasplantaments
ONT	Organización Nacional de Trasplantes
PAS	periodic acid Schiff
PCA	principal component analysis
PEG	polyethylene glycol
PROSPR	protein organic solvent precipitation
RIPA	radioimmunoprecipitation assay
RNA	ribonucleic acid
ROC	Receiver Operating Characteristics
RRT	renal replacement therapy
RT-qPCR	real-time quantitative polymerase chain reaction
SEC	size-exclusion chromatography
SEN	Sociedad Española de Nefrología
SRM	Selected Reaction Monitoring
TCMR	T-cell-mediated rejection
TGF	transforming growth factor
THP	Tamm-Horsfall urinary glycoprotein
UC	ultracentrifugation
uEV	urinary extracellular vesicles
UF	ultrafiltration
WB	western blot

ABSTRACT

Chronic rejection in kidney transplantation is the main cause of graft failure. Since renal biopsy -the current gold standard diagnostic method- is invasive, costly, entails a high subjectivity factor and is not representative of the whole kidney, there is a clear need for more precise, non-invasive and cost-effective diagnosis tests. To meet this need, the objective of this thesis was to find protein biomarkers that could be utilized as a non-invasive diagnosis method of renal alterations in kidney-transplanted patients.

Urine has been extensively investigated to find biomarkers of different renal alterations in kidney transplantation because it provides a holistic view of the whole urinary system, and it can be collected non-invasively, and repeatedly. However, the complex constituents of urine can hamper the detection of lower abundant proteins by proteomic technologies. In this sense, the analysis of extracellular vesicles (EV) found in urine provides an attractive solution. Since the composition of EV varies upon the origin and physiological state of the producing cell, urinary EV (uEV) are an ideal source of biomarkers for renal alterations. Moreover, high abundance contaminant proteins are usually removed during the isolation process, while the protein cargo of uEV remains protected.

The introduction of the thesis contains a brief history of the kidney and kidney transplantation, which although interesting for the reader, it is not strictly relevant for the comprehension of the results. The "formal" introduction focuses on the epidemiology of kidney transplantation, types of graft rejection, current diagnosis methods and defines the problem to solve. The results and

discussion of the project were divided into three parts based on the structure of published articles, with some modifications to accommodate to the structure of a doctoral thesis.

The study exposed in this thesis follows a common pipeline for protein biomarker search, consisting of a discovery phase, a verification phase and a validation phase. In each phase, we analysed the uEV proteome from kidney-transplanted patients using mass-spectrometry (MS) or antibody-based techniques. Patients were classified into four groups according to their renal alteration diagnosed by biopsy and clinical parameters: normal kidney function (NKF), interstitial fibrosis and tubular atrophy (IFTA), calcineurin inhibitors toxicity (CNIT) and acute cellular rejection (ACR).

The first part is focused on CNIT, a kidney alteration of poorly characterized mechanisms, diagnosis and treatment. Although in kidney biopsy CNIT often shows IFTA lesions, the treatment is consistently different. We scanned the CNIT uEV proteome by MS searching for differences with IFTA group that could reveal potential biomarkers of CNI nephrotoxicity. The results showed upregulation of terms related to epithelial processes and overexpression of uroplakins and plakins in the CNIT group uEV, suggesting the participation of these proteins specifically in CNIT, but not in the development of fibrotic lesions.

In the second part, we expose other proteins differentially expressed in pathological samples compared to NKF patients found in the discovery phase. Then, a second phase (verification phase) was set up using targeted MS in a bigger cohort of patients to confirm the results of the candidate proteins

selected from the first phase. Among other findings, vitronectin was found to be more expressed in patients with high degree of kidney fibrosis (defined by Banff histological criteria), pointing out the potential of this protein as a biomarker for renal fibrosis.

Finally, in the third part, we carried out a pilot study to demonstrate the detection of urinary vitronectin using ELISA. With this method, much more cost-efficient than MS, we can make the findings in this project more translationable to the clinical practice.

RESUM EN CATALÀ

El rebuig crònic en el trasplantament renal és la causa principal de fallada de l'empelt. Donat que la biòpsia renal (l'actual mètode diagnòstic considerat com a el "gold standard") és invasiva, costosa, implica una alta subjectivitat i no és representativa de tot el ronyó, hi ha una necessitat clara de desenvolupar testos diagnòstics no invasius i rendibles. Per cobrir aquesta necessitat, en aquesta tesis ens vam proposar com a objectiu trobar biomarcadors proteics que es puguin utilitzar com a un mètode diagnòstic no invasiu d'alteracions renals en pacients trasplantats de ronyó.

L'orina s'ha investigat extensament buscant biomarcadors de diverses alteracions renals en el context del trasplantament perquè proporciona una visió holística de tot el sistema urinari. A més, es pot mostrejar de manera no invasiva i repetidament. No obstant, els complexos constituents de l'orina poden dificultar la detecció de proteïnes menys abundants mitjançant tècniques de proteòmica. En aquest sentit, l'anàlisi de vesícules extracel·lulars (VE) presents en l'orina profereix una solució atractiva. Degut al fet que la composició de VE varia segons l'estat fisiològic i l'origen de la cèl·lula productora, les VE urinàries (uVE) són una font ideal de biomarcadors urinaris. A més, durant el procés d'aïllament de les uVE es retiren proteïnes contaminants altament abundants de l'orina, alhora que el contingut proteic de les uVE es manté protegit.

La introducció de la tesis conté una breu història del ronyó i del trasplantament de ronyó que, malgrat que poden ser interesants pel lector, no és necessari per poder comprendre els resultats. La introducció "formal" se

centra en l'epidemiologia del trasplantament renal, els tipus de rebuig, els mètodes diagnòstics actuals i defineix els problemes a solucionar. Els resultats i discussió del projecte s'han dividit en tres parts basats en l'estructura d'articles publicats, amb algunes modificacions per acomodar-ho a l'estructura d'una tesi doctoral.

L'estudi exposat en aquesta tesi segueix un sistema comú en la recerca de biomarcadors proteics, que consisteix en una fase de descobriment, una fase de verificació i una fase de validació. En cada fase, vam analitzar el proteoma de les uVE de pacients trasplantats de ronyó utilitzant espectrometria de masses (EM) o tècniques basades en anticossos. Els pacients van ser classificats en quatre grups segons l'alteració renal que patien, diagnosticada a partir de biòpsia renal i paràmetres clínics (les sigles dels grups deriven de la terminologia anglesa): funció renal normal (NKF), fibrosi intersticial i atròfia tubular (IFTA), toxicitat per inhibidors de la calcineurina (CNIT) i rebuig cel·lular agut (ACR).

La primera part es focalitza en la CNIT, els mecanismes de la qual estan poc caracteritzats, així com també el seu diagnosis i tractament. Malgrat que en la biòpsia renal de CNIT sovint apareixen signes de IFTA, el tractament és ben diferent. Vam investigar el proteoma de uVE de CNIT mitjançant EM per buscar diferències amb el grup de IFTA que poguessin representar biomarcadors de CNIT. Els resultats van mostrar que hi havia una major regulació de proteïnes relacionades amb processos epitelials, de uroplaquines i plaquines en les uVE de CNIT, el que suggereix la participació d'aquestes proteïnes en la CNIT específicament però no en el desenvolupament de lesions fibròtiques.

A la segona part es descriuen altres proteïnes diferencialment expressades en mostres patològiques en comparació amb el grup NKF trobades en la fase de descobriment. Vam procedir amb una segona fase (fase de verificació) mitjançant proteòmica dirigida en una cohort de pacients més gran per confirmar els resultats de les proteïnes seleccionades de la primera fase. Entre altres troballes, la vitronectina es va trobar més expressada en pacients amb un alt grau de fibrosi renal (definida segons paràmetres histològics de Banff), assenyalant el potencial d'aquesta proteïna com a biomarcadors de fibrosi renal.

Finalment, a la tercera part, vam dur a terme un estudi pilot per demostrar la detecció de vitronectina segons el grau de fibrosi renal utilitzant un assaig d'ELISA. Amb aquest mètode, molt més rendible que l'EM, aconseguim apropar les troballes del projecte a la pràctica clínica.

INTRODUCTION

Real things in the darkness seem no realer than dreams.

— Murasaki Shikibu, The Tale of Genji

1 BRIEF HISTORY OF THE KIDNEY

The text in this section has been published in:

Carreras-Planella L, Franquesa M, Lauzurica R, Borràs FE. *A brief history of kidney transplantation*. **Hektoen International** Journal, 2020 Sep. Summer 2020, Nephrology and Hypertension. ISSN 2155-3017.

We may think of renal transplantation as routine therapy today, but this procedure has taken centuries to develop and is marked by important events in the history of science. An ancient description of the kidneys is found in the Egyptian Ebers Papyrus, dated to 1550 BC and discovered by the German Egyptologist Georg Ebers (1837-1989). It contained observations made by ancient physicians and included illustrations of human mummies with conditions such as renal cysts or stones. In mummification rites the ancient Egyptians removed all organs from the body except the heart and the kidneys.[1] The kidney was believed to be a means of judgment in the afterlife, [2], [3] a belief shared by the Jews of Egypt and described in the Old Testament and other ancient writings. The two kidneys were thought to represent good and evil; the right kidney giving a person good advice and the left kidney bad advice. In the afterlife, the kidneys and the heart would be examined to decide the fate of the soul.[4] A similar concept is found in traditional Chinese medicine, where the two kidneys represent balance and harmony, hold the *yin* and *yang* of the body, determine life and death, and are a reservoir of energy.[5]

The ancient Greek physician Hippocrates of Kos (460-370 BC) also described diseases and conditions of the kidney and urinary bladder in his *Corpus Hippocraticum*.[6] Aristotle (387-322 BC) proposed an anatomy of the human kidney based on empirical observations of fish and birds. Galen of Pergamum (130-201 AD), one of the most famous Greek physicians and the surgeon of emperors and gladiators, was the first to observe that the major function of the kidneys was to produce urine.[7]–[10] He even introduced the idea that the kidney functioned as a filter. In fact, the word "nephrology" comes from then ancient Greek "νεφρός" (*nephros*), which is derived from the word "νεφός" (*nephos*, meaning cloud), and was a metaphorical description of the kidneys producing urine as clouds produce rain.[11]

Some centuries later Oribasius (326-403 AD), physician to the Roman emperor Julian the Apostate, explored the function of the kidneys in *Collectiones Medicae*. He endeavored to describe the renal circulation, stating that the kidneys absorbed urine from the blood, and also defined the ureters and the urethra.[12], [13] Although the anatomy had not yet been defined, many disorders and treatments had nevertheless been described. Theophilus Protospatharius (6^{th}-7^{th} century AD) is regarded as the most important uroscopist of the Byzantine Empire; even Emperor Heraklios wished to have him as the physician of the court. Early uroscopists examined the urine for color, turbidity, and sediment to diagnose abnormalities of the kidneys and urinary tract. As this practice evolved, conditions such as diabetes, pregnancy, and liver failure were also diagnosed by uroscopy. Theophilus Protospatharius wrote *De Urinis* (*On Urine*), a short book describing findings in urine and renal problems in the elderly. Those descriptions and practices were used by

teachers of Western medicine for more than 500 years in famous medical schools such as the *Schola Medica Salernitana* in Salerno, Italy.[14], [15]

One of the most exceptional physicians in history was Avicenna, also known as Abu Ali al-Husayn ibn-Abdullah ibn Sina, who lived in Persia from 980-1037 AD. He incorporated medical knowledge from his predecessors in ancient Persia and Greece and expanded it with research of his own.[16] He even performed clinical trials that were noticeably advanced for that time. His particular focus was the anatomy of the abdomen and the description of the digestive apparatus and associated organs.[17], [18] Avicenna stated that the liver was the main metabolic organ and that its processed products were filtered and excreted by the kidneys as urine. He hypothesized that since the liver indirectly contributed to the production of urine, analysis of urine could also indicate the health of the liver.[19] He compiled his observations in the famous *Canon of Medicine*.[20]

During the Renaissance, there were many breakthroughs in anatomy and medicine. Andreas Vesalius (1514-1564), regarded as the father of anatomy, recorded 200 drawings of anatomical structures including the kidney in his masterpiece *De Humani Corporis Fabrica*.[21] He challenged and changed existing theories, such as the concept of sieving through a membrane (*membrana cribri malo*), which had been incorrect.[22], [23] In Bologna Marcello Malpighi (1628-1694), who introduced microscopic anatomy, wrote and illustrated documents about the anatomical structure of the kidney. Malpighi identified the glomerulus (also known as the Malpighian corpuscles) and renal tubules. [24], [25]. Other microscopic structures of the kidney were identified later by Jacob Henle (1809-1885) [26] and William Bowman (1816-

1892) [27], [28] among others, who made precise drawings and detailed descriptions of their histologic observations of animal and human kidneys.

Around 1820, advances in the clinical field came from Thomas Hodgkin (1798–1866), Thomas Addison (1793-1860), and Richard Bright (1789-1858). They made great contributions to the field of nephrology while working at Guy's Hospital in London. Richard Bright, who is considered the father of modern nephrology, developed a hospital research unit where he conducted autopsies and described the symptoms of renal diseases.[29], [30] He was the first to note that albuminuria and edema could be markers of a renal condition that became known as Bright's disease. [31]

In the field of physiology, Claude Bernard (1813-1878) described how the cells of an organism maintain their function thanks to the constancy of the environment found in the surrounding extracellular fluid space. This state was called *Milieu Intérieur* (interior milieu), now known as homeostasis and further defined by the American physiologist Walter Bradford Cannon (1871-1945) who also coined the term "fight or flight."[32] This dynamic state of stability is maintained by the kidneys thanks to their capacity for keeping the right amount and composition of substances in the extracellular fluid.[33]

At the beginning of the twentieth century it was still not clear how secretion and reabsorption could occur at the same time through the epithelium of the kidney tubules, a theory that Arthur Robertson Cushny defended in his monograph *The Secretion of Urine* published in 1917.[34] He also reported the acids found in the urine of humans and other carnivores, whereas herbivores had alkaline urine unless fed a protein diet. Soon after this, Wearn

and Richards studied the excretory system of amphibians. Using the recently invented micropuncture technique,[35] they sampled fluid filtered through the glomeruli of frogs and reported that its composition was similar to blood except for a lack of proteins.[36] Arthur M. Walker and others used oil droplets to block certain segments of the nephron, then injected and collected a known fluid to observe the modifications in that segment and elucidate how the fluid was processed to become urine in the bladder.[37] After World War II, Hans Ussing studied the transport of solutes and ions across epithelia.[38] and two decades after Burg[39], [40] developed new techniques for the exploration of the kidney. Devices such as the flame photometer permitted the refined measurement of solutes and led to the understanding of regulation and transport of substances across nephron tubule sections.[33]

These experiments, descriptions, and inventions have formed the base of our present knowledge about renal pathophysiology and replacement therapy. A timeline with the most remarkable hallmarks in the history of the kidney from year 1550 BC to the present is depicted in Figure 1. Dialysis and transplantation are the currently available therapeutic options for end stage renal disease. Of these, transplantation is the best treatment in terms of survival rate, cost-effectiveness, and quality of life. Today over 70,000 kidney transplantations are performed every year worldwide.[41]–[43]

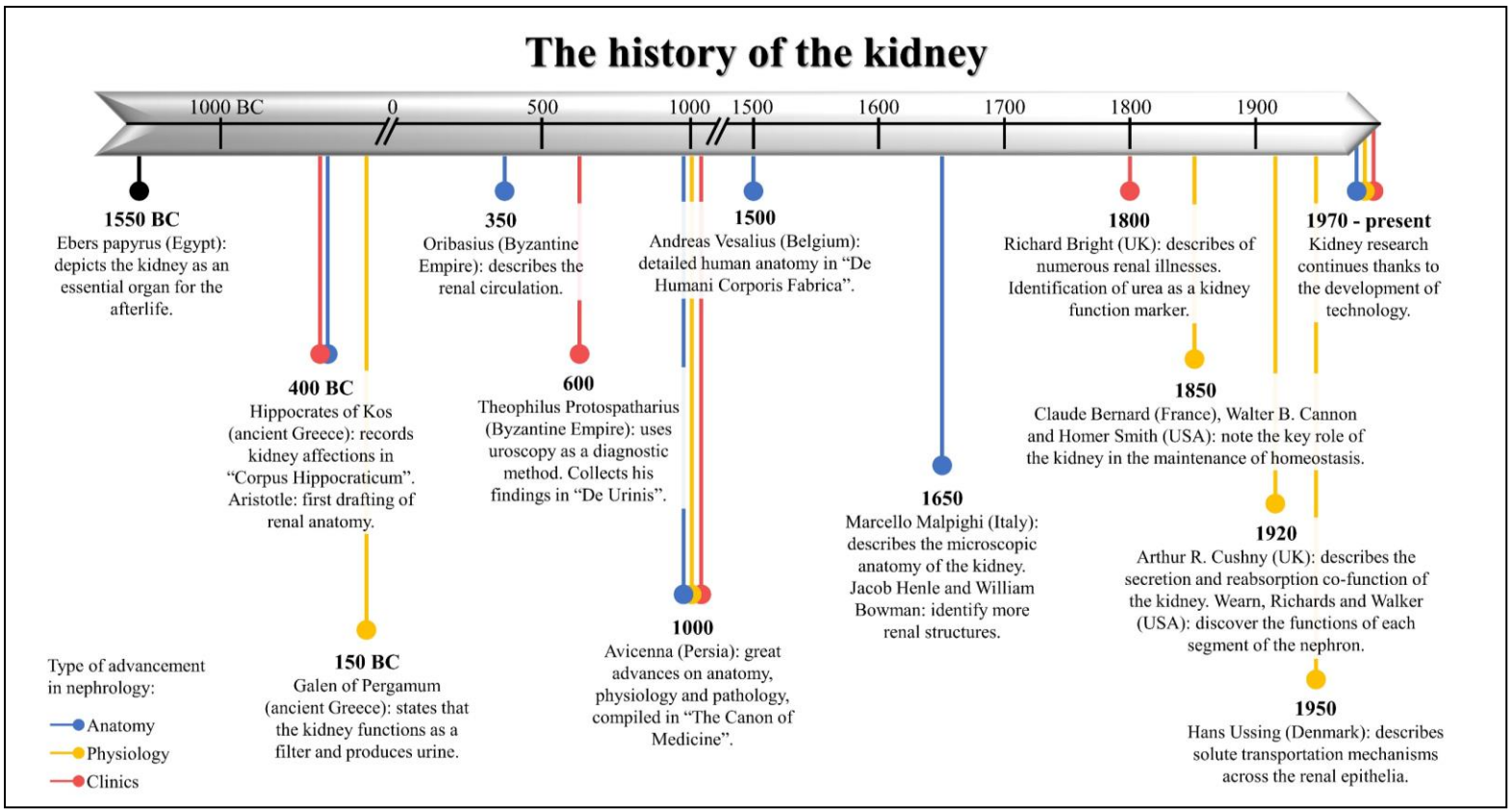

Figure 1. Timeline with the most remarkable hallmarks in the history of the kidney from year 1550 BC to the present. Colours denote the type of advancement in nephrology.

1.1 BRIEF HISTORY OF KIDNEY TRANSPLANTATION

The history of kidney transplantation as we know it today began in the 1950s, but other key attempts were made earlier in the twentieth century. The first successful organ transplant was performed by Emerich Ullmann from the Vienna Medical School in 1902 when he auto-transplanted a kidney in a dog from its normal location to the vessels of the neck, where it produced some urine.[44], [45] In the same year, dog-to-dog and dog-to-goat kidney transplants were performed by Ullmann and Alfred von Decastello, who was known for his study of blood groups. In the early 1900s, Alexis Carrel worked closely with the physiologist and surgeon Charles Claude Guthrie, making crucial breakthroughs in vascular surgery such as anastomosis and other techniques for blood vessel preservation. In 1906 Mathieu Jaboulay, with Carrel as assistant surgeon (both of them Nobel laureates), performed the first kidney transplantations from goats and pigs to the arms and thighs of humans. Each kidney worked for one hour only, but these and attempts with other species were performed by pioneers such as Ernst Unger, improving the knowledge of surgical technique.[46] The first transplantation from a human cadaver was attempted in the USSR by Yurii Voronoy in 1939, although the organ was rejected because of blood group incompatibility and the patient died after two days.[47] Immune mechanisms involved in the grafting of the transplanted organ were poorly understood at the time, as described by Alexis Carrel two years later in a lecture to the International Surgical Society: "The surgical side of the transplantation of organs is now completed, as we are now able to perform transplantations of organs with perfect ease and with excellent results from an anatomical standpoint. But as yet [...] transplantations are almost

always unsuccessful from the standpoint of the functioning of the organs. All our efforts must now be directed toward the biological methods which will prevent the reaction of the organism against foreign tissue and allow the adapting of homoplastic grafts to their hosts."[48], [49]

Investigations resumed after World War II with other attempts at human kidney transplantation, especially by two groups in Europe and the United States. In 1946 a human kidney allograft was transplanted to blood vessels in the arm under local anesthesia by a team in Boston.[50] The graft only functioned for a short time, but it was long enough to help the patient recover from acute renal failure. This achievement attracted major interest, as did the first transplantation from a live donor performed by Jean Hamburger (who defined the term "nephrology") in Paris from a mother to her sixteen-year-old son. The transplanted kidney functioned for twenty-two days.[51] In 1950, Lawler in Chicago was the first to attempt intra-abdominal kidney transplantation.

In 1954 at Peter Bent Brigham Hospital (later Brigham and Women's Hospital) in Boston, Joseph Murray performed the first truly successful living donor kidney transplantation. He received the Nobel prize for this achievement in 1990. The transplant was performed from one monozygotic twin to the other, so there was no histo-incompatibility. This was the first time that a transplanted patient, who had been dying from renal failure, survived for years after the transplant.[52] The procedure was met with growing success - one kidney recipient even had a successful pregnancy and delivery - and expanded to other hospitals.[53] The first kidney transplantation in Spain was performed in 1965 at the Hospital Clínic de Barcelona by Antoni Caralps, Pedro Pons, Gil-

Vernet, and Magriñá, followed by eight additional transplantations at the same hospital that year.

However, even though transplantation surgical techniques had greatly improved, good immunosuppressive regimens were still lacking. The use of the newly available azathioprine, prednisolone, or total body irradiation helped during the initial crucial rejection period between identical twins or siblings.[54] In the mid-1960s, great improvements were made in the pre-treatment of patients with hemodialysis to enhance health before surgery; organ transportation between hospitals; identification of HLA antigens, discovered by Jean Dausset; development of tissue-typing and lymphocytotoxicity testing; and an increase in kidney transplants, which provided valuable data for improvement.[55]–[57] Methodologies and management were consolidated in the 1970s, and saw the beginning of transplantations from cadaveric donors.

But the most remarkable breakthrough of this period was the introduction of the calcineurin inhibitors cyclosporine A and tacrolimus. Cyclosporine A was first isolated in 1971 from a soil fungus (*Hypocladium inflatum gams*) in Norway and studied by Jean-Francois Borel and Hartmann F. Stähelin at Sandoz (now Novartis).[58], [59] The importance of this drug was reflected in the speed at which it was approved and released to the market in 1983. This small cyclic polypeptide made it possible to reduce the percentage of rejection in the first year after transplantation from 80% to 10%.[60] Tacrolimus, somewhat better than cyclosporine A in reducing acute rejection and improving graft survival,[61] was isolated from *Streptomyces tsukubaensis* in the soil of Tsukuba, Japan in 1987. The name tacrolimus derives from "Tsukuba

macrolide immunosuppressant," although it was initially called FK506 because of its target FK506 binding protein (FKBP).[62], [63], [57] Mycophenolic acid, which was first isolated in 1893 from *Penicillium glaucum* in spoiled corn, was found to possess antibiotic activity but carried many adverse effects.[64]. A century later, its ester derivate mycophenolate mofetil was synthetized as a safer drug with immunosuppressant action.[65], [66] Rapamycin, also known as sirolimus and a current first-line immunosuppressant, was first found to be an antifungal metabolite of *Streptomyces hygroscopicus.* Discovered in Rapa Nui (formerly named Easter Island) in 1964, the name rapamycin comes from the site of its discovery.[67]–[69] It is also abbreviated as mTOR because *tor* in German means door, and this protein serves as a gateway to cell growth and proliferation.[70] Other analogues such as everolimus were synthesized later and are also routinely used in kidney transplantation.[71] Although many immunosuppressive drugs are now in use, cyclosporine A and tacrolimus are still key in preventing organ rejection, even fifty years after their discovery.

The modern success of kidney transplantation would not be possible without the previous knowledge acquired by brave, enthusiastic, and brilliant people throughout history who made their findings available for future generations. Discoveries over millennia have made possible a science that today saves thousands of lives.

2 RENAL PHYSIOLOGY

Each kidney is composed of about 1 to 1.2 million nephrons[72], the smallest functional unit of the kidney (depicted in Figure 2). All nephrons present in

the adult life are completely formed by the end of gestation [73]. Each nephron (approximately 200 μm in size) includes a renal corpuscle (or Malpighian corpuscle), composed by a glomerulus (mesh of capillaries) embraced by the Bowman's capsule, where blood is filtered to enter the kidney. Most renal corpuscles are located in the renal cortex, but around 20% of the nephrons are found in the medulla. These are called juxtamedullary nephrons ("juxta" meaning "next to", in contraposition to cortical nephrons) and contain the juxtaglomerular apparatus, essential for water balance regulation [74]. Every day about 180 L of fluid pass through the glomeruli to enter the nephron through the Bowman's space [75]. In this first step, water, glucose and electrolytes pass by freely, while cells, some proteins and other large molecules are retained in blood. Glomerular and tubular epithelial cells determine which molecules pass through, basically depending on their size and charge [76]. The size filter consists of pores in the basal membrane and pores of around 42 Å in the endothelial cells [77] that usually let molecules of less than 25 kDa pass by but holds those larger than 70 kDa [78], [79]. The charge barrier is formed by polyanionic glycosaminoglycans located on the basal membrane [80]. Experiments using different size ferritin molecules with neutral, positive or negative charge helped to understand why some molecules in blood such as albumin, which measures 39 Å but is polyanionic, do not pass through the glomerulus [77].

The filtrate flows along the different sections of the tubular structure of the nephron, each composed of a monolayer of specialized cells with specific characteristics. Their main mission is to reabsorb water (the 90-99% of the filtered water is returned to blood along the tubules [75]) and essential

substances which arrive to the extracellular space to be reabsorbed by the net of capillaries embracing the nephron. The first segment encountered after the glomerulus is the proximal tubule, composed of epithelial cells highly permeable to water due to high expression of aquaporin 1 [81]. Around 60-70% of the water is reabsorbed by sodium gradients [82]. Besides, the proximal tubule carries out other functions: metabolization of 1,25-dihydroxy-vitamin D and its precursor 25-hydroxy-vitamin D [83]; gluconeogenesis similarly to the liver [84], [85]; secretion of erythropoietin, renin and Klotho into the blood; and the production of hormones such as dopamine, endothelin, prostaglandins or angiotensin II [86]–[88]. More water is reabsorbed in a similar way in the next segment of the nephron: the descending limb of the loop of Henle. The ascending limb of the loop and the final portion of the nephron (the distal convoluted tubule) are impermeable to water. Distal convoluted tubule from surrounding nephrons connect with the collecting tubules, to transport urine finally to the urinary bladder [89].

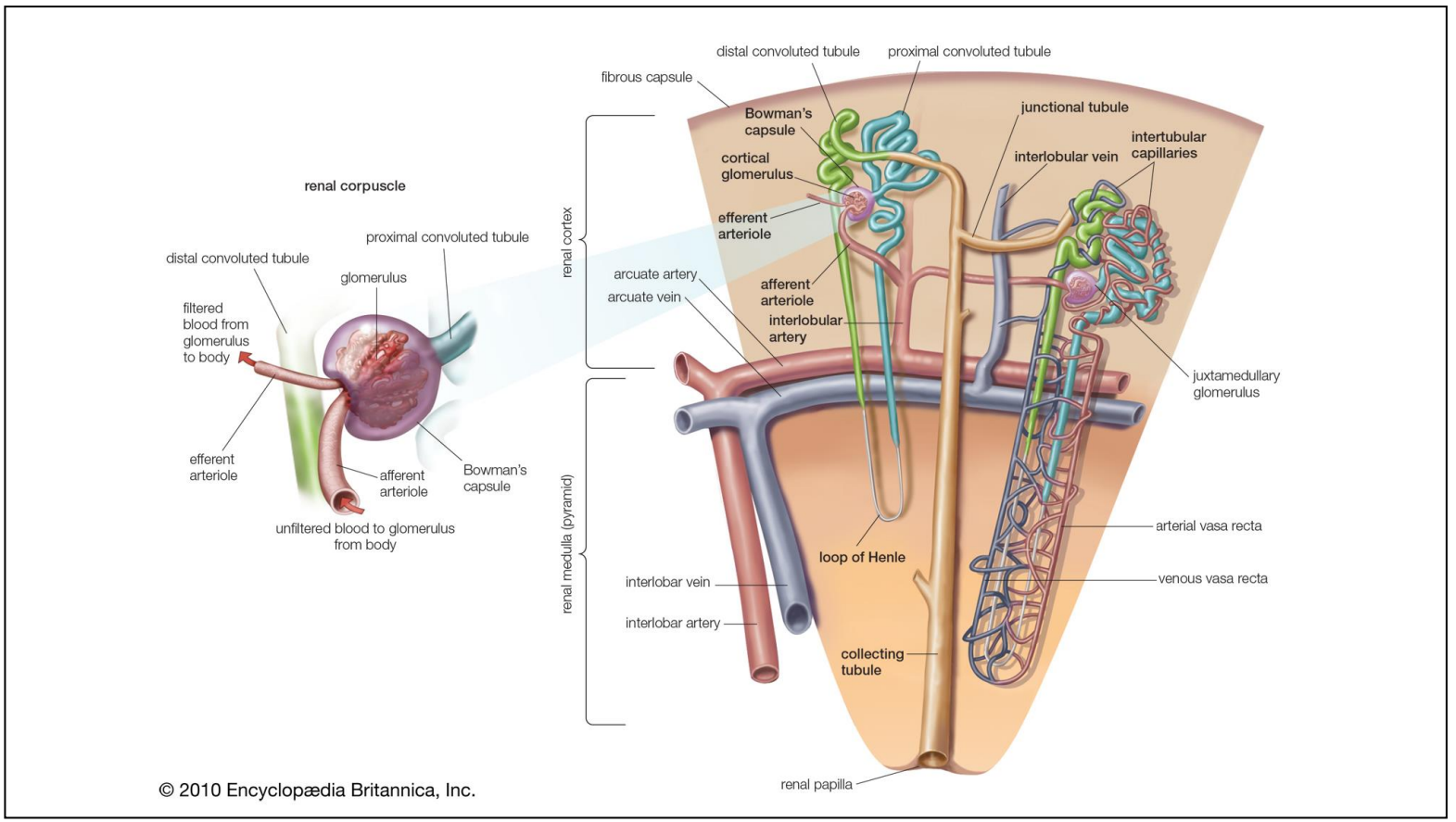

Figure 2. Scheme of the parts of the nephron and detail of the renal corpuscle. Image from Encyclopaedia Britannica.

3 RENAL FAILURE AND KIDNEY TRANSPLANTATION

All renal structures work coordinately, but if any of them fails and the others cannot overcome the problem, a pathological state will appear. For example, a damaged glomerular filtration barrier would lead to leakage of low molecular weight proteins like albumin. Large quantities of albumin can overload the protein reabsorption capability of the proximal tubule, leading to proteinuria. If proteinuria is prolonged in time, hypoproteinaemia, reduction of the plasma oncotic pressure and loss of antithrombin can occur and cause nephrotic syndrome (generalized oedema, ascites, pleural effusion and hypercholesterolemia) [90]. On a longer term, chronic kidney disease (CKD) is a pathological state defined by a low glomerular filtration rate (<60 mL/min/1.73 m^2)[91] and/or damage in the kidney structure or function persisting for more than 3 months. The most common causes of CKD are diabetes and hypertension [92], [93]. The prevalence of CKD worldwide is estimated to be between 8-16% [94], but due to its increasing tendency it could extend from being the 13th cause of death worldwide to the 5th in 2040 [95]–[99]. There are almost no treatments to effectively treat or slow down CKD, and its progression can end up into chronic kidney failure or end-stage kidney disease [91]. At this point, the patient needs invariably a renal replacement therapy (RRT), which can be haemodialysis, peritoneal dialysis or kidney transplantation. The 5-years survival rate of patients on dialysis is around 45%, while the equivalent for transplanted patients is more than 90% [100], [101]. In kidney-transplanted patients, the survival rate depends greatly on the number of human leukocyte antigens (HLA) matched between the

donor and the receptor of the organ, as discovered by Prof. Jon J. van Rood. Being aware of the large number of existing HLA types and the difficulty of finding a good donor-patient match, Rood founded in 1967 the Eurotransplant International Foundation (Eurotransplant). The foundation started with 12 centres from 3 countries, but now 7 countries participate in the network: Austria, Belgium, Croatia, Germany, Hungary, Luxembourg, the Netherlands and Slovenia. They work with kidney, pancreas, liver, intestines, heart and lung donation centres to crossmatch information with the aim of finding the best donor for the patients in the waiting list.

4 CURRENT PICTURE OF KIDNEY TRANSPLANTATION EPIDEMIOLOGY

There are more than 850 million people with CKD, acute kidney injury or on RRT worldwide, a considerable number that represents about twice the estimated amount of people with diabetes mellitus and is more than 20 times higher the number of people with acquired immune deficiency syndrome (AIDS) [95]. In Europe, the European Renal Association - European Dialysis and Transplant Association (ERA-EDTA) [102]–[104] produces annual reports collecting epidemiological information on kidney diseases and RRT of their country members. These reports are created in the Department of Medical Informatics of the Amsterdam University Medical Centre and can be consulted on their webpage [100]. Such work is of utmost importance to know the incidence of kidney diseases, how hospitals implement RRT in different countries, details about each therapy, etc. Countries submit their data registries

as a whole or by internal regions. In the case of Spain, each autonomous community provides individual patient data, and aggregated data are generated by the Spanish National Transplant Organization ("Organización Nacional de Trasplantes", ONT [105]) and the Spanish Society of Nephrology ("Sociedad Española de Nefrología", SEN [106]).

The ERA-EDTA 2018 annual report, that includes data collected in 2016, shows the number of transplantations in each country per million population (Figure 3). The country with the highest transplantation rate was Spain, being Catalonia the region with the highest transplantation rate in all Europe (94 transplants per million population). This fact could be due to the effectivity of the donation network as well as to the relatively better coverage of the Spanish health system compared to the other member countries.

Catalonia, and especially Barcelona, has always been on the edge of transplantation. The first renal transplantation in Catalonia performed in 1965 by Josep Maria Gil-Vernet Vila and Antoni Caralps Riera [107] was a milestone that would open the door to pancreas, testicle, liver and heart transplantations and would transform Barcelona in a worldwide recognized capital of organ transplantation [108]. The "Organització Catalana de Trasplantament" (OCATT) creates an annual report on donation and transplant activity in Catalonia, which is publicly available in three languages (Catalan, Spanish and English). In 2018, 773 renal transplantations were performed, what corresponds to a transplantation rate of 101.7 per million inhabitants. The percentage of renal transplantations from living donor was 16%, almost twice that in Spain (9%) (Figure 4).

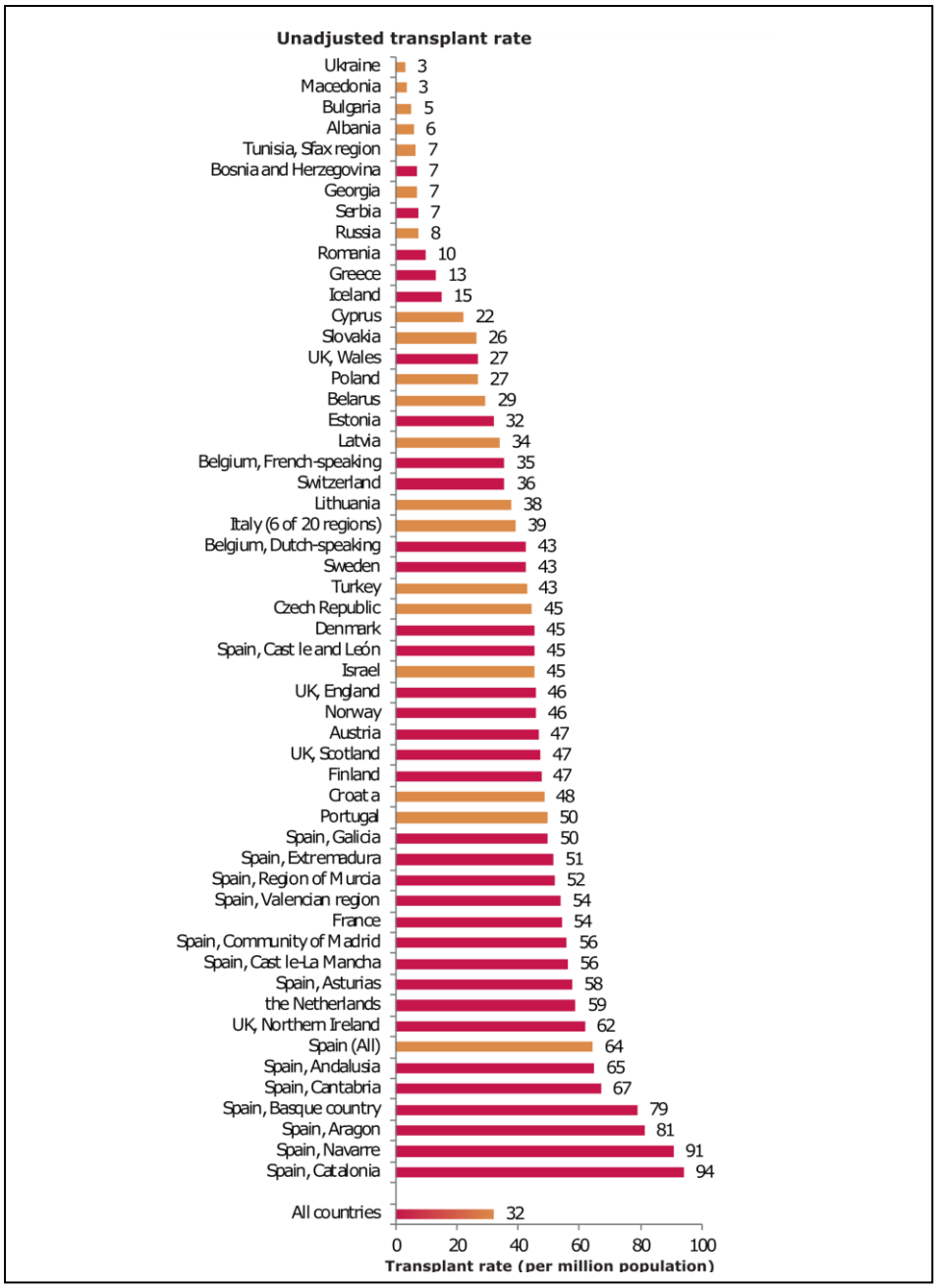

Figure 3. ERA-EDTA 2016 annual registry of the transplant rate (number of kidney transplantations per million inhabitants) in each country. Registries providing individual patient data are shown as red bars, and registries providing aggregated data, as orange bars.

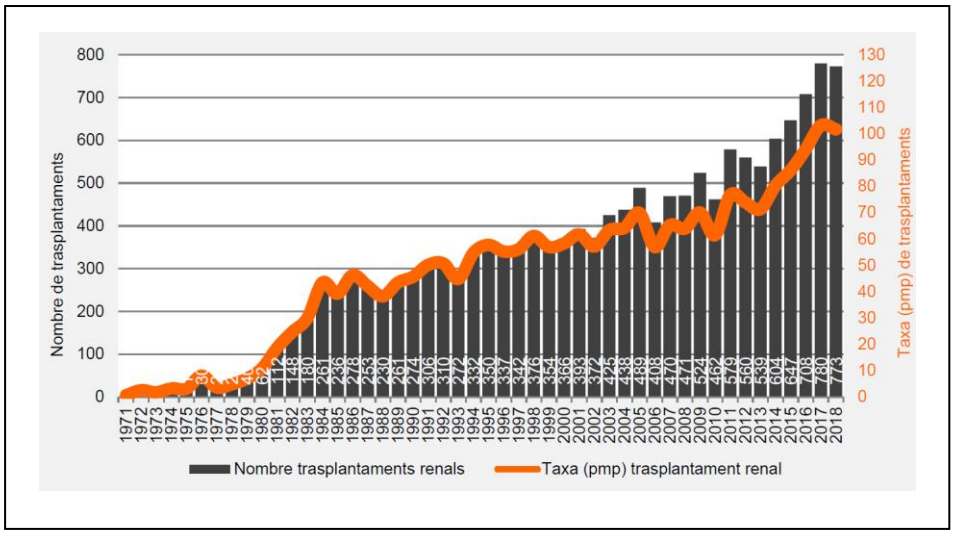

Figure 4. Evolution of the number of transplants (in white on the black bars) and transplantation rate (orange line) in Catalonia.

5 GRAFT FAILURE IN KIDNEY TRANSPLANTATION

According to the ERA-EDTA reports at 5 years after transplantation, the mean graft survival probability is around 80.9% in deceased donor and 86.7% in living donor and the mean patient survival time is 91.9% in deceased donor and 94.6% in living donor [100]. Nevertheless, due to the sheer fact that transplanted tissues or cells to a genetically different organism are recognised as an alloantigen, the recipient's immune system (both adaptive and innate responses) develops a response against it. This process is called allograft rejection. If the receptor presented blood type incompatibility or donor-specific antibodies (DSA), the immune system would develop a hyperacute rejection within minutes after the transplantation. This is a seldom event nowadays [109]. On a longer time lapse, although T cells are the main

mediators in the recognition of the allograft, there are multiple cells, cytokines and co-stimulatory molecules that orchestrate pathological changes, which can eventually lead to renal dysfunction or, in the worst cases, allograft loss or patient's death [110], [111]. Upon immunological and histopathological characteristics, kidney graft rejection can be broadly classified in [112]:

1. **Acute rejection:** usually occurs within days or weeks after transplantation or due to non-adherence to immunosuppressive treatment [113]. It can be broadly classified into:
    a. Acute T-cell-mediated rejection (TCMR): can be detected by the presence of infiltrating immune cells in the tubular, interstitial and/or vascular compartments.
    b. Acute antibody-mediated rejection (ABMR): caused by antibodies against donor-specific HLA molecules, blood group antigens (ABO)-isoagglutinins or endothelial cell antigens. It can be diagnosed by the presence of DSA, C4d positivity and evidence of glomerulitis or peritubular capillaritis [114], [115].
2. **Chronic allograft rejection:** it develops within months to years after transplantation. The main manifestations are arteriosclerosis (progressive narrowing of the graft vessels lumen) and fibrosis.
3. **Acute rejection concurrently with chronic rejection**

Decades after the first kidney transplantation, acute rejection (ABMR or TCMR) has been harnessed – it accounts for only 12% of graft failure cases - with the appearance and use of immunosuppressive drugs [52], [54], [116], [117]. However, there has been little improvement on the management of chronic allograft rejection and graft loss on the long term, and there is still a 10%

graft rejection rate per year after transplantation, as widely reported [116], [118]–[121]. Chronic allograft rejection is an entity with multiple complex causes that unfortunately lack precise biomarkers [122]. In addition, the lack of effective therapies have caused disparity of opinions about its management [123].

This thesis focuses on two main entities that participate in chronic allograft rejection in order to find biomarkers that can help the non-invasive monitoring of patients and improve the therapeutic regimes.

5.1 INTERSTITIAL FIBROSIS AND TUBULAR ATROPHY

A persistent injury to the renal tissue can lead to the appearance of interstitial fibrosis and tubular atrophy (IFTA) in an attempt of the kidney to compensate the loss of function and scar the injured tissue [124], [125]. The injuries to the kidney can include both immune-related and non-immune-related causes such as: chronic antibody-mediated rejection, ischemia-reperfusion injury, polyoma virus, vascular, malignant or infectious diseases, pre-existing donor kidney lesions, non-adherence to the immunosuppressive treatment, hypertension or calcineurin inhibitors toxicity [119], [124], [126], [127]. IFTA can be present in the kidney alone or concomitantly with other lesions [128]. When the kidney is damaged and there is loss of functional nephrons, compensatory mechanisms such as hyperfiltration are initiated by the unaffected nephrons, but these changes can lead to hypertensive damage. Then, regenerative mechanisms are activated, but if the level of physiological repair is exceeded, that will result in fibrosis, which is a progressive loss of organ architecture and loss of functional tissue by deposition of extracellular matrix (ECM) [129]–[131].

Fibrogenesis is orchestrated by a myriad cells and cellular pathways, out of which the transforming growth factor (TGF)-β1 pathway is considered as the main regulator [132]. TGF-β1 binds to a serine-threonine kinase type II receptor results in the recruitment and phosphorylation of a type I receptor, which in turn phosphorylates SMADs, thereby initiating signalling cascades [129], [133] and a plethora of cells such as fibroblasts, pericytes, tubular epithelial cells, lymphatic and vascular endothelial cells, immune cells and resident or infiltrating stem cells [134]–[136]. In the event of tissue injury, tubular epithelial cells and T cells secrete TGF-β1 that induces the transformation of fibroblasts to myofibroblasts and leads to an excess of extracellular matrix deposit [137], [138]. Collagens are essential for the structural maintenance of the tissue, but under profibrotic conditions, they participate in pathological conditions such as fibrosis, glomerulosclerosis or vascular sclerosis [135] (Figure 5). Due to the non-functionality of fibrotic tissue, IFTA in transplanted patients is associated with worse renal function and it accounts for two thirds of failed grafts when associated with chronic allograft dysfunction. [139]. Severe fibrosis has a negative prognostic value for functional decline and graft survival [137], [140]–[147] and it can eventually lead to graft failure, independently of the initial cause [117], [148], [149]. Currently fibrosis is not reversible, so it has become a focus of concern for transplantation nephrologists, as evinced by the more than 20 ongoing clinical studies on renal antifibrotic interventions in humans [137], [150].

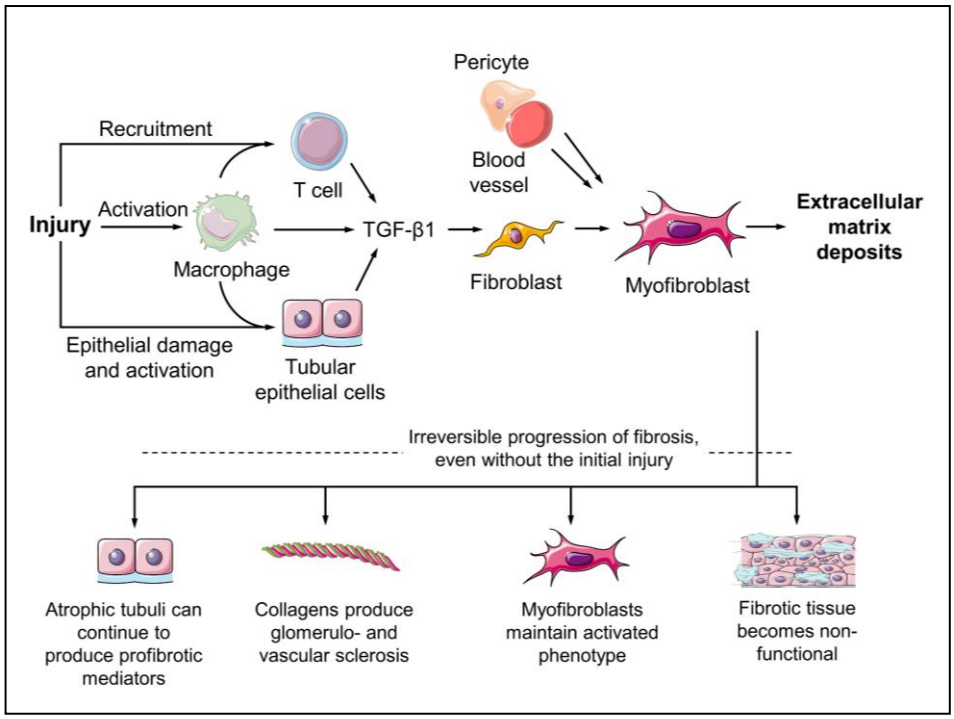

Figure 5. Simplified diagram of renal fibrogenesis. Most injuries promote an inflammatory response with recruitment of immune cells and activation of epithelial cells. These cells produce profibrotic mediators such as TGF-β1 that induce fibroblasts differentiation into myofibroblasts that produce extracellular matrix. This process may progress until an irreversible state even when the initial injury has disappeared. Adapted from Vanhove et *al.*, 2017. This figure was created using images from Servier Medical Art Commons Attribution 3.0 Unported License. (http://smart.servier.com). Servier Medical Art by Servier is licensed under a Creative Commons Attribution 3.0 Unported License.

5.2 CNIT

Cyclosporine A [58], [60] and tacrolimus are first-line immunosuppressive agents in kidney transplantation [57], [62], [63] - 94% of renal-transplanted patients receive a CNI-based immunosuppressive regime [151] - and are largely responsible for the increase in early graft survival over the last three

decades [152]. At the same time, they represent a thread to the kidney due to their nephrotoxicity. The management of the so-called calcineurin inhibitors toxicity (CNIT) is another source of debate among transplantation nephrologists due to its interindividual variability and mechanisms complexity. The mechanism of action of CNI is based on the disruption of T-cell activation and proliferation by inhibiting calcineurin, an enzyme that causes dephosphorylation and activation of NFATc, which in turn triggers the transcription of interleukin (IL)-2. The IL-2/IL2R interaction induces T-cell activation and proliferation by clonal expansion via the mammalian target of rapamycin (mTOR), what represents the first step in graft rejection [153]. TGF-β1 is a key contributor in CNIT pathology since cyclosporine-A and tacrolimus induce its expression in the tubule directly and independently of the other mechanisms [154]. Thus, lesions similar to IFTA pathology will appear. In parallel, they affect the activity of some ion transporters leading to metabolic alterations such as hyperuricemia, hyperglycaemia, hypertension, hyperkalaemia, hyperpotassaemia, hypomagnesemia and hyperchloremic metabolic acidosis [155] (Figure 6).

Upon conditions of appearance, CNIT can be acute or chronic. Acute CNIT (aCNIT) is usually easy to detect and solve by reducing CNI doses. The diagnosis of chronic CNIT (cCNIT) is not so straight forward, but strong correlations in CNI concentration-rejection and CNI concentration-toxicity for cyclosporine A and tacrolimus have been observed, so it is mandatory to maintain CNI levels in patients within a narrow therapeutic window. However, there is still controversy in the precise way to diagnose, monitor and treat CNIT, because a reduction of CNI can adversely produce graft rejection [156].

Another big challenge is the high inter- and intraindividual pharmacokinetic variability of these drugs [157], [158]. A more precise knowledge about the mechanisms that contribute to CNIT should enable the identification of new biomarkers for a better monitoring.

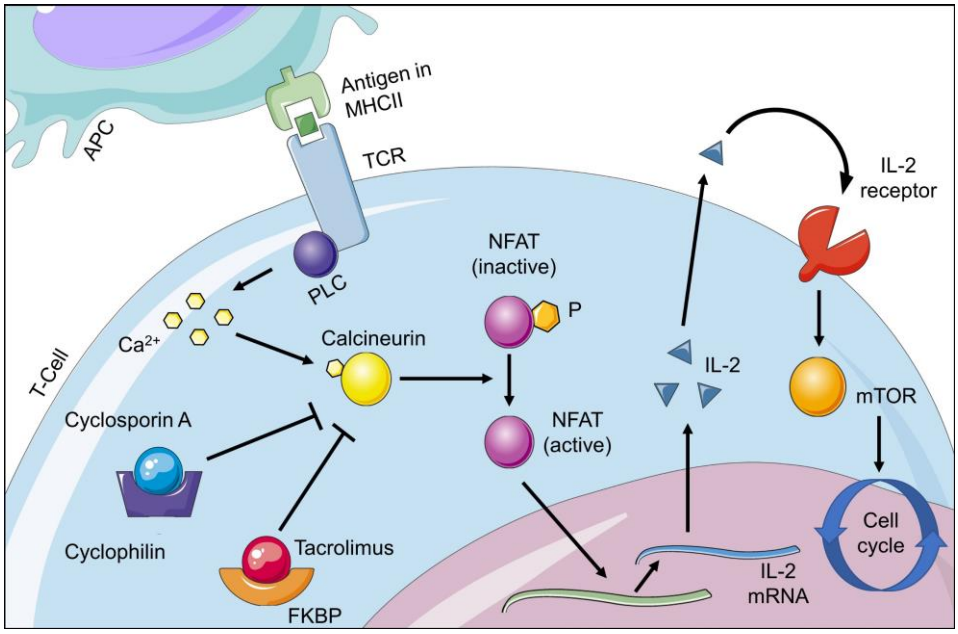

Figure 6. Mechanism of action of the calcineurin inhibitors cyclosporin A and tacrolimus. APC, antigen presenting cell; MHCII, major histocompatibility complex class II; TCR, T-cell receptor; PLC, phospholipase C; NFAT, nuclear factor of activated T-cells; mTOR, mammalian target of rapamycin. This figure was created using images from Servier Medical Art Commons Attribution 3.0 Unported License. (http://smart.servier.com). Servier Medical Art by Servier is licensed under a Creative Commons Attribution 3.0 Unported License.

5.3 DIAGNOSIS, MONITORING AND HISTOPATHOLOGICAL EVALUATION OF THE TRANSPLANTED KIDNEY

After renal transplantation, patients require periodic tests to monitor the function of the kidney even in the absence of clinical signs as they only appear

once the damage to the kidney is well advanced [159]. These tests are based on the determination of serum creatinine concentration, estimated glomerular filtration rate and proteinuria at different time intervals. The skeletal muscle metabolizes creatinine and continuously releases it into the blood. When it reaches a healthy kidney, it is normally filtered freely through the glomeruli, without being reabsorbed or metabolized. If the kidney is not functioning properly, creatinine will remain and accumulate in the serum. Patients have their creatinine levels analysed every 2-3 months and yearly for proteinuria after the first year post-transplant. Renal failure is considered when serum creatinine levels rise over 1.7 mg/dL. An estimated glomerular filtration rate below 40 ml/min/1.72m^2 and a proteinuria greater than 500 mg/day from the first year post-transplant would suggest chronic allograft dysfunction according to the international guidelines of the Kidney Disease Improving Global Outcomes group (KDIGO) [160]. However, serum creatinine is far from being the ideal marker for renal transplanted patients due to its delay in change, its misestimation - and usually, underestimation - of the renal lesion and its non-specificity about the cause [124], [161]. Similarly, the appearance of proteinuria is an unspecific sign of graft damage [162] and of potential graft-loss [163].

Renal biopsy is the current gold standard test for diagnosis of transplanted kidney alterations, nowadays essential to define the diagnosis and the most appropriate treatment [164]. Renal biopsy became a widespread technique in in the 1950s for the great value it provides for diagnosis, prognosis and response to treatment [165]. Still being used today, the technique consists of the collection of a 2-4 mm piece of renal cortex. In some centres, per-cause

kidney biopsies are performed when the renal analytes indicate a problem in renal function. Otherwise, protocol biopsies are implemented, which consist of performing a biopsy usually every six months even when there are no signs of rejection. It has been shown that this enables the identification of many subclinical rejection cases, that is, seeing lesions in the kidney before there is any clinical manifestation [147], [166], [167]. Early detection of kidney rejection is key for graft survival since the physician will be able to start an early treatment to stop the rejection process preventing the loss of the graft [168], [169].

In 1991, a meeting was organized in Banff where experts in the field of nephrology developed a series of criteria and nomenclature to evaluate biopsies of transplanted kidneys in a standardized way worldwide. The Banff scoring guides or criteria help not only to improve the diagnosis and management of patients, but also to better understand the physiopathology. Hence, they are being revised continuously to adapt them with the emerging discoveries [112], [161], [170].

A renal biopsy specimen must contain at least 10 glomeruli and 2 arteries to be "adequate" for the histopathological evaluation under Banff criteria. It is stained with haematoxylin and eosin, Periodic acid–Schiff (PAS) and gomori trichrome to be observed under light microscope. A series of histopathological parameters that describe interstitial, tubular, glomerular and vascular lesions are evaluated and scored from 0 (absence) 3 (severe presence) [171]. Figure 7 shows the mean of Banff chronic lesions scores along time, which increase especially after the second year after transplantation. IFTA is a lesion of the renal tissue which can be, among many other causes, produced by CNIT, so

their histopathological characteristics present similarities. However, in order to apply the correct treatment an assertive diagnosis is paramount.

5.3.1 *HISTOPATHOLOGICAL MANIFESTATION OF IFTA*

Kidney fibrosis or interstitial fibrosis and tubular atrophy (IFTA) is the histological finding of chronic allograft lesions with no known aetiology [171]. Under Banff criteria, IFTA appears microscopically as chronic interstitial lesions (ci, IF) and chronic tubular lesions (ct, TA). These two lesions almost always appear concomitantly [137] and IFTA grade is determined as the mean of the two parameters [172]. A grade of 2 or 3 has a probability of appearing in the grafted kidney of around 35% from the first year after transplantation [117]. Other chronic lesions in the Banff classification are (with abbreviation and other descriptive names when appropriate): chronic vascular lesions (cv, arterial fibrous intimal thickening), arterial hyalinosis (ah), mesangial matrix increase (mm) and chronic glomerular lesions (cg, transplant glomerulopathy) [173]. These lesions are highly correlated in terms of appearance except for cg, which is an independent pathologic entity with individual prognosis [140], [174]. When there is deterioration of the allograft's structure, IFTA is usually the most noticeable manifestation because the tubular and interstitial compartments comprise the 90% of the kidney volume, although other chronic lesions can progress parallelly [137]. In non-transplanted kidneys, conventional staining with haematoxylin and eosin, periodic acid Schiff (PAS) or trichrome are routinely used to determine the extension of fibrosis [175]. Quantification of fibrosis is PAS staining is the most used method, but it entails subjectivity-related errors [176].

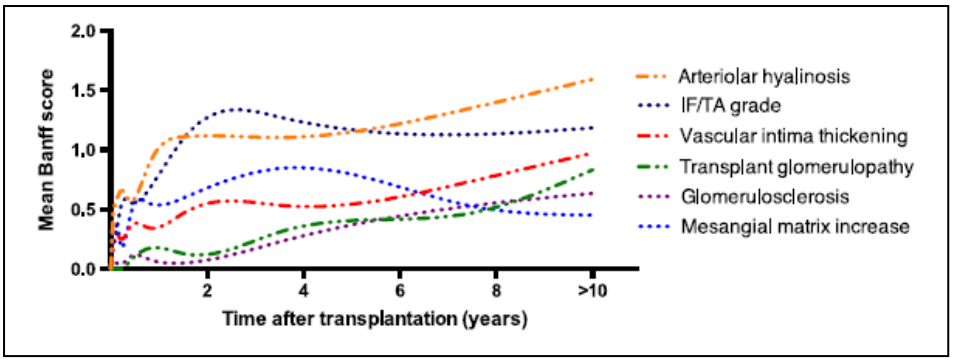

Figure 7. Mean chronic Banff score lesions in Naesens et *al.* 2014 study of biopsies performed in 1,200 kidney transplanted patients. IF/TA grade represents the mean of ci and ct scores.

5.3.2 *Histopathological manifestation of CNIT*

The main signs of aCNIT are arteriolar hyalinosis (ah), isometric tubular vacuolization and thrombotic microangiopathy [177]–[179]. Thrombotic microangiopathy is a lesion on capillaries or arterioles that causes thickening of the wall and intraluminal platelet thrombosis with partial or complete obstruction of the vessel [180]. In a study by Kambham et *al.* [181], the lesion that better correlated with CNIT was arteriolar hyalinosis. But this lesion is chronic, appears when the renal damage is well advanced and is, in general, irreversible. When cCNIT takes on, it can produce irreversible damage to all compartments of the kidney: vascular (arteriolar hyalinosis), interstitial (interstitial fibrosis), tubular (tubular atrophy) and glomerular (Bowman's capsule fibrosis and focal or segmental glomerular sclerosis) [141], [182]. However, these lesions are not only specific of cCNIT as they are also present in diabetic nephropathy, hypertension or chronic antibody mediated rejection or they can be a sequel present already in the donor kidney [183]. In addition,

the effects mentioned for aCNIT can also be caused by other drugs, ischaemia-reperfusion injury or other causes.

5.3.3 *Drawbacks of renal biopsy*

Despite being the gold-standard diagnostic, there are notable drawbacks for kidney biopsies that have not been solved, starting with the uncomfortable pain caused by the large diameter needles. There is a risk of 6% of minor and major complications [184], [185] such as haematuria, arteriovenous fistula, ileus, renal pelvic rupture, or even renal loss [186]. In addition, there are situations where percutaneous biopsy is contraindicated due to the condition of the patient, like in uncontrolled severe hypertension, pregnancy, urinary tract infections or severe obesity [187], [188]. The recovery time - 1 to 3 days in hospital plus 1-week rest - also entails economical expenses [189]. The quality of the taken sample is a determinant factor for the success of the method. In addition, there is no assurance that the examined tissue is representative of the alterations happening in the whole organ because of the small proportion sampled (10 glomeruli from the estimated 1 million glomeruli) and because in a transplanted kidney, lesions are not spread homogeneously in the tissue, several injuries can occur concomitantly and they can vary in a relatively short time [190]. Moreover, histological evaluation is subjected to sampling error (maybe forcing its repetition) and inter-observer variability, which has been reported to be around 20% [185], [191]. In spite that almost all studies affirm that renal biopsy can improve clinical management of patients, there is no consensus about specific indications of this procedure, so it remains a personal or single centre decision [192].

6 NEW BIOMARKERS OF KIDNEY DAMAGE

The drawbacks of the current diagnosis methods are clear. A non-invasive, objective, precise, early and repeatable better and earlier diagnosis would enable the optimization of the treatment [193], what would translate into an improvement of graft and patient survival, in addition to easing the pain of the biopsy procedure. The National Institute of Health (NIH) Biomarkers Definitions Working Group defines a biomarker as "a characteristic that is objectively measured and evaluated as an indicator of normal biological processes, pathogenic processes or pharmacological responses to a therapeutic intervention" [194]. By now, perfect biomarkers for kidney-transplanted patients have not been discovered, though they may not exist. Probably, a panel of proteins rather than a single one would provide more precise information.

Several studies searched for molecular biomarkers of rejection in "protocol" kidney biopsies and have provided much information regarding the long-term evolution of the transplanted graft [159], [191], [192], [195]–[198] as well as having reduced the inter-observer variability associated with the biopsy [185], [191]. Yet, provided they reached the clinics, it would also be subjected to the quality of the collected sample and it would still be an invasive procedure.

Given that urine is a fluid directly generated by the kidney and it can be collected non-invasively, easily and repeatedly, it is the ideal source of biomarkers of kidney rejection. Although more validation experiments are lacking, many studies have already demonstrated that changes happening in the kidney are reflected in the urinary proteome [199]. Markers such as cystatin

C, which seems to indicate loss of renal function [200] or proteins like kidney injury molecule-1 (KIM-1) [201], neutrophil gelatinase associated lipocalin (NGAL) [202], [203], n-acetil-b-(D)-glucosaminidasa (NAG) [204], interleukin 18 (IL-18) [205] and fatty acid binding protein (FABP) [206], have been proposed as biomarkers of alteration of the tubular compartment metabolism. Currently, none of these markers that can differentiate concise renal alterations.

6.1 EXTRACELLULAR VESICLES

Included in the material excreted in urine are extracellular vesicles (EV), which have been under the focus of attention in the field of biomarkers for the last decade due to their biophysical properties. These lipid-bilayered vesicles that measure 50 to 200 nm of diameter, are produced by practically all cells in the organism and released into the extracellular space, so they can be found in most biological fluids, including urine [207], [208]. The term EV technically includes three types of vesicles: exosomes, microvesicles and apoptotic bodies [209]. The International Society of Extracellular Vesicles (ISEV) has set the standards for the experimental characterization of EV [210]. However, there is no consensus about the specific way to differentiate the different types of EV, so the use of the generic term EV is recommended [211]. EV have been studied in immunology, neurobiology, stem cell and tumour biology. Their content includes proteins, miRNA or lipids, and interestingly, this composition varies upon the cell of origin and its physiological state [209], [212]. The knowledge about the content of EV from studies worldwide is collected on extensive databases such as Exocarta [213], Vesiclepedia [214] and EVpedia [215], [216].

The first demonstrations of the existence of EV in urine were made in 2002 [217] and 2004 [218], when it was confirmed that membrane proteins were present in an ultracentrifugation-derived pellet. EV are too large to be filtered from plasma through the kidney, although some may be transported by transcytosis through podocytes [219]. Urinary EV (uEV) contain cell-specific markers from cells of all nephron segments and cells composing the excretory system such as renal epithelial cells, glomerular podocytes, renal tubule cells, cells lining the urinary drainage system and immune infiltrating cells. Therefore, uEV mirror a holistic view of the kidney's pathophysiological state [218], [220], [221].

6.1.1 CONSIDERATIONS FOR THE USE OF URINE SAMPLES IN UEV RESEARCH

Urine samples should be collected, processed and stored using standardized methods for the isolation of uEV. Three of the most important steps for their storage are 1) keeping the samples at a stable temperature of -80ºC, where they can last for years [222]; 2) vortexing samples thoroughly after thawing for uEV isolation [223], [224]; and 3) reducing the interference of uromodulin. Uromodulin (or Tamm-Horsfall urinary glycoprotein (THP)) is the most abundant protein in urine that is synthesized in the thick ascending limb of the loop of Henle [208]. Uromodulin forms polymers that can entrap uEV hindering proteomic analysis. Treating urine with dithiothreitol (DTT), that acts as a reducing agent, or the zwitterionic detergent 3-[(3 cholamidopropyl) dimethylammonio]-1 propanesulfonate (CHAPS) breaks uromodulin polymers and it has been shown to increase the yield of uEV [225]. Besides, urine contains proteases and RNases that will require specific inhibition depending on the desired downstream analyses [224].

6.1.2 ISOLATION OF UEV

Several methods have been developed to isolate uEV based on their physicochemical properties. Even for each method, research groups and laboratory companies usually implement their own protocols or combination of techniques [226], what means that still a consensus on a general method for EV isolation is yet to be achieved [227]. To date, the type of isolation used will depend on the intended downstream analyses as well as the facilities of the research center. The most commonly used methods are briefly described below [228], [229]:

a. **Ultracentrifugation (UC):** sequential centrifugations are used to first remove cells and debris at low speeds (3,000x *g* followed by 17,000x *g*), followed by higher speed centrifugations (100,000-200,000x *g*) to pellet uEV. It requires high-cost equipment. If not combined with other purification techniques, in the pellet there are a mix of EV types with other proteins and particles [222]. UC would not be suitable for downstream proteomics analyses for patients with nephrotic syndrome due to the large amounts of proteins released in urine that would impede the detection of lower abundant proteins [230].

b. **Density gradient isolation:** based on the use of a density gradient media like iodixanol combined with centrifugation steps to separate EV upon buoyant density. Then, UC is used to extract those EV of a determined density range. It decreases the quantity of protein contaminants [231] and co-isolated lipoproteins, what is especially important in sera samples [232]. This method is practical for large volumes of samples, such as cell culture media [233]. However, the resulting EV can be partially lost during

the separation steps and other particles of similar density (such as viruses) can be co-isolated [232].

c. **Antibody-based affinity capture:** based on the isolation of uEV by specific EV markers, promises to be a valuable method. It still has some bundles to surpass because of the high heterogeneity in EV [234]–[236].

d. **Ultrafiltration (UF):** it is faster and requires less high-cost equipment than UC. Samples are filtered through a nanomembrane filter of usually 100 kDa cut-off to concentrate uEV [237]. An RNA yield similar to UC is obtained with this method [238], but still a significant amount of proteins contaminates the isolated uEV, so it would not be valid for patients with nephrotic syndrome [239]. Another problem of using UF with urinary samples is that subsets of uEV containing AQP2 and TSG101 get trapped in the nanofilter and are extremely difficult to separate [228].

e. **Polymer-based precipitation methods:** some commercial reagents based on polymer precipitation (most commonly polyethylene glycol (PEG), protein organic solvent precipitation (PROSPR) and NaAc-based water exclusion) have been developed to isolate uEV. They bring high RNA and miRNA yields [240]. Nevertheless, the physicochemical properties of uEV become affected [229] and numerous contaminant proteins as well as some other membranous organelles are co-isolated [241] and. It seems that this method precipitates mostly (cluster of differentiation (CD)9 containing uEV and leaves out CD63 containing uEV, what raises concern considering that they are both important tetraspanin uEV [241].

f. **Size-exclusion chromatography (SEC):** this method isolates uEV based on their size. The pre-processing of samples usually involves some centrifugations to remove cells and debris and UF to concentrate the sample before loading it onto the SEC column [242]. Mechanistically, the column consists of a matrix (stationary phase) with pores that separates particles passing through with an elution buffer (mobile phase). Particles that are bigger than the matrix's fractionation range elute faster, while particles that are smaller are slowed by the matrix's pores and elute later [243]. With this method, uEV can be purified almost without contaminant soluble proteins [244]–[246]. It is especially useful for protein biomarker research to detect lower abundance proteins even from patients with nephrotic syndrome or other protein rich samples [230]. For all its advantages and adequation to the sample type, downstream analyses and purpose, SEC was the method used in this project.

6.1.3 Analysis of uEV content

Systems biology approaches use high throughput techniques, named "omics", to discover biomarkers for many different medicine specialities. In genomics, the development in genomics of RNA-sequencing has allowed the analysis of microRNA (miRNA), which are short (20-25 bp) non-coding nucleotide sequences that regulate negatively the translation of mRNA to proteins. miRNA are relatively simple, suffer no post processing modifications, are stable and are found in many body fluids including urine. Thus, miRNA are being investigated for being promising biomarkers or potential therapeutic targets and to help understand the pathophysiology of diseases. A study by Lozano-Ramos et *al.* revealed that there are minimal differences in the uEV miRNA of

cadaveric versus living donors' kidneys [244]. In another study, the group of Llorente identified five miRNA in uEV that were downregulated in prostate cancer patients compared to healthy controls, and validated two of them by RT-qPCR (real-time quantitative polymerase chain reaction) showing their potential as prostate cancer biomarkers [247].

Proteomics is on the leading edge for biomarkers research [248]. Since the first attempt by Tanaka et *al.* to analyse biomolecules as large as proteins using mass-spectrometry (MS) in 1988 [249], there have been large improvements on the technique. Now, MS enables the detection of thousands of proteins in one sample with high precision, sensitivity and throughput [250], providing a photography of the state of the cell of origin. The current most used pipeline for biomarker search (Figure 8), which is the followed in this thesis project, usually begins with a "discovery phase", where the proteins in a group of samples of interest are compared to control samples [251]. Usually, the proteins in a sample are fractioned into peptides by enzymatic digestion and then analysed by semiquantitative liquid chromatography followed by tandem MS (LC-MS/MS) contrasted against a protein database. Bioinformatics analysis identify those proteins that are differentially expressed from the huge number of proteins detected. Finally, candidate proteins are selected. In the following step, the "verification phase", other samples are screened to confirm the previous findings. This frequently employs a higher-specificity and quantitative MS technique [252]. Several different methodologies called "targeted proteomics" have appeared over the last years and rapidly established for their usefulness to detect and most importantly quantify determined proteins of interest within a complex sample [253]. After that, a

"validation phase" that bridges basic research with the clinics is performed. In this stage, cheaper techniques (usually antibody-based techniques such as enzyme-linked immunosorbent assay (ELISA), western blot (WB) or immune-electron microscopy) are used to confirm the previous results and to proof the applicability of that biomarker in the clinics. The number of patients and samples usually increases over the phases of the pipeline [254].

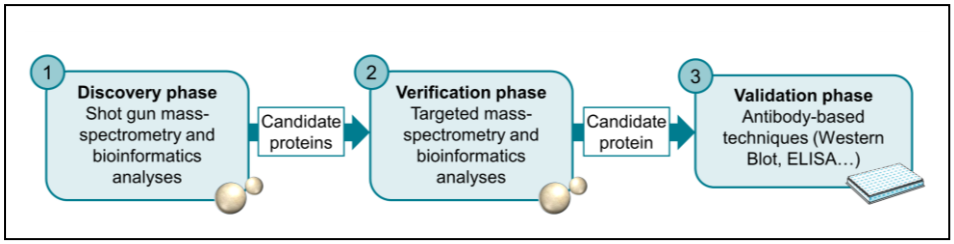

Figure 8. Standard pipeline used for biomarker discovery in proteomics.

6.1.3.1 Normalization

Normalization of proteomics values is necessary in the biomarkers field to make the comparison between samples more reliable. It is especially relevant in urine due to its high variability between individuals, physiological variations in water excretion along the day or variations induced by pathologies [228]. Normalization can be applied based on creatinine, time or some constant protein in the sample. In addition, a pre-collection normalization can be applied by collecting samples around the same time of the day in all patients, for instance in the morning. Normalization of experimental protein biomarkers in urine by creatinine is commonly used because creatinine is secreted at a more or less constant rate in urine [255]. However, renal pathologies can induce large variations in its excretion [256]. In uEV, normalization by urinary creatinine has been shown to lead to bias in results interpretation [257].

Therefore, for proteomics analysis in uEV other methods have been proposed: normalization based on a certain protein found by MS such as uromodulin, uEV markers, or any other protein that proves to be useful to calculate a ratio that correlates with pathology [258], [259]. In our study, we have used the EV marker ezrin to normalize intensity values in mass-spectrometry analyses.

6.1.4 uEV FOR BIOMARKER DISCOVERY IN URINARY TRACT DISEASES

Protein biomarkers in uEV could provide a non-invasive diagnosis and/prognosis method that could be performed repeatedly and cost-effectively. Therefore, numerous studies have searched for biomarkers of different kidney diseases or transplanted graft alterations in uEV. A more frequent monitoring of patients promotes an early detection of abnormalities and increases the chances of successful treatment, so numerous groups are searching for biomarkers of renal allograft function in uEV that outdo the current analytical markers. The proteome of small uEV in living donor kidney-transplanted patients was analyzed by MS in a 12-months longitudinal study [260]. It allowed the identification of changes in protein patterns related with cellular processes and complement activation and the identification of phosphoenol pyruvate carboxykinase (PCK2) as biomarker of renal function. In another study, NGAL in uEV was proposed as a biomarker of kidney dysfunction after renal transplantation [221]. MS has prooved that the uEV proteome changes when the kidney suffers alterations, but these results have to be translated to the clinics in order to reach the patients. In a recent study, Jung et *al*. compared the uEV proteome from kidney-transplanted patients with CAMR with that of patients with long-term graft survival (some of them presenting IFTA without rejection). Using MS, they identified six proteins that

could differentiate CAMR and validated their results with Western Blot [261]. Park et *al*. took a different approach to diagnose acute graft rejection. They reasoned that T cells infiltrating in the kidney would secrete EV that could be found in urine. They designed a device to immune-magnetically detect CD3+ EV in urine samples in 2 hours with an accuracy of 91% [262].

Not only protein content of uEV change in the presence of pathologies but also their size or number. It has also been described that pathological tissues release more EV than healthy tissues [228], [263]. In a study in patients with or without renal failure as a complication of type 2 diabetes, results show that density and size of uEV could also be used as a biomarker since they reflected the state of renal function [264].

It is worth mentioning that in all the previously mentioned studies, although all the protocols were slightly different, isolation of uEV was based on UC. Sigdel et *al*. tested two methods to isolate different uEV populations in urine from kidney-transplanted patients with acute or non-acute rejection. One method was UC, but it did not recover enough EV protein for Western Blot and proteomic analyses as did the other method, based on concentration with nanomembrane filtration. They found differentially expressed proteins between groups, and between isolation methods [263]. This study highlights the importance of the uEV isolation method and how it can interfere in the results.

HYPOTHESIS AND OBJECTIVES

My life amounts to no more than one drop in a limitless ocean. Yet what is any ocean, but a multitude of drops?

— David Mitchell, Cloud Atlas

1 HYPOTHESIS

Based on the background exposed in the previous section, the following hypothesis was developed: The protein content of EV released by cells of the urinary system in urine depends on their pathophysiological state. Thus, the proteomic analysis of uEV could allow the identification of biomarkers of a given pathologic situation, specifically in kidney-transplanted patients.

2 OBJECTIVES

To prove the above-mentioned hypothesis, the objective of this thesis is to find protein biomarkers contained in uEV that could be utilized as a non-invasive diagnosis method of renal alterations in kidney-transplanted patients.

To accomplish the main purpose, specific objectives were set as follows:

1. To analyse the global uEV proteome from kidney-transplanted patients affected with different renal alterations and to detect distinctive proteins.
2. To verify the differentially expressed proteins in a new cohort of patients suffering similar renal alterations
3. To validate the results with a technique applicable to the clinical laboratory (cost- and time-effective).

4.

MATERIALS AND METHODS

「七転び八起き」

— Japanese proverb. English translation: *Fall seven times, stand up eight*.

1 PATIENTS AND STUDY DESIGN

Figure 9 shows the pipeline followed for the uEV proteomics study. Two independent cohorts of kidney transplanted patients participated in the study: the discovery phase cohort, which included 23 patients from the Germans Trias i Pujol University Hospital (Badalona, Spain), and the verification phase cohort, that included 41 patients from the Hospital Clínic (Barcelona, Spain) (Figure 9a). The study population was selected according to the following inclusion criteria: 1) male or female patients older than 18 years of age; 2) ability to give informed consent; 3) absence of urinary tract infection demonstrated by the presence of leukocyturia and/or bacteriuria; 4) absence of hematuria; 5) absence of DSA or either active or chronic antibody-mediated rejection. Morning mid-stream urine samples (approximately 75 mL) were collected right before the renal biopsy procedure or in a regular visit check-up (in the case of NKF group in the first cohort). All patients were receiving a similar immunosuppressive regime including CNI. For the discovery phase, biopsies were carried out under clinical indication (i.e. when serum creatinine and proteinuria were altered). For the verification phase patients, per-cause biopsies and also protocol biopsies were considered. Histopathological diagnoses were used following the same criteria to define four groups of patients: normal kidney function (NKF), interstitial fibrosis and tubular atrophy (IFTA), acute cellular rejection (ACR) and calcineurin inhibitors toxicity (CNIT). NKF was defined by the absence of alteration in clinical parameters (serum creatinine and proteinuria) in the discovery cohort and the absence of fibrosis and/or other findings at renal per-protocol biopsy in the verification cohort. ACR was defined in the presence of significant interstitial inflammation (>25%

of nonsclerotic cortical parenchyma, i2 or i3) and foci of moderate tubulitis (t2) [112]. Fibrosis was graded as 1) mild, less than 25% of parenchyma affected, 2) moderate, 26-50% of parenchyma affected and 3) severe, > 50% of parenchyma affected. CNIT was diagnosed by the determination of high serum CNI levels [265], [266], together with the presence of isometric tubular vacuolization in the case of acute CNIT, or by the presence of arteriolar wall hyalinosis in patients taking calcineurin inhibitors in the case of chronic CNIT.

This study was carried out in accordance with the Declaration of Helsinki[267] and the recommendations of Guideline for Good Clinical Practice from the "Comitè d'Ètica de la investigació clínica de l'Hospital Universitari Germans Trias i Pujol", who also approved the protocol. All patients were informed about the procedures and provided written informed consent to participate in the study. In order to protect human subject identity, an arbitrary code was employed for sample identification.

Figure 9. **(A)** Workflow of the study. Urine was collected from patients from the discovery cohort and the verification cohort classified into 4 groups according to their biopsy diagnosis. **(B)** Extracellular vesicles were isolated from urine (uEV) by size-exclusion chromatography (SEC). The plot shows on the left y-axis mean fluorescence intensity (MFI) of tetraspanin EV markers (CD9 and CD63) and on the right y-axis, protein concentration of the 20 SEC fractions. Both MFI and protein concentration are shown as the mean of all samples±SEM in relative values from 0 to 100. **(C)** Samples from the discovery cohort were analysed by shotgun mass-spectrometry. The bioinformatics analyses brought to the selection of 23 candidate proteins that were analysed by targeted proteomics mass-spectrometry (selected reaction monitoring (SRM) in samples from the verification cohort. **(D)** Potential candidate protein biomarkers were validated using western blot and ELISA, two techniques applicable to the clinical setting.

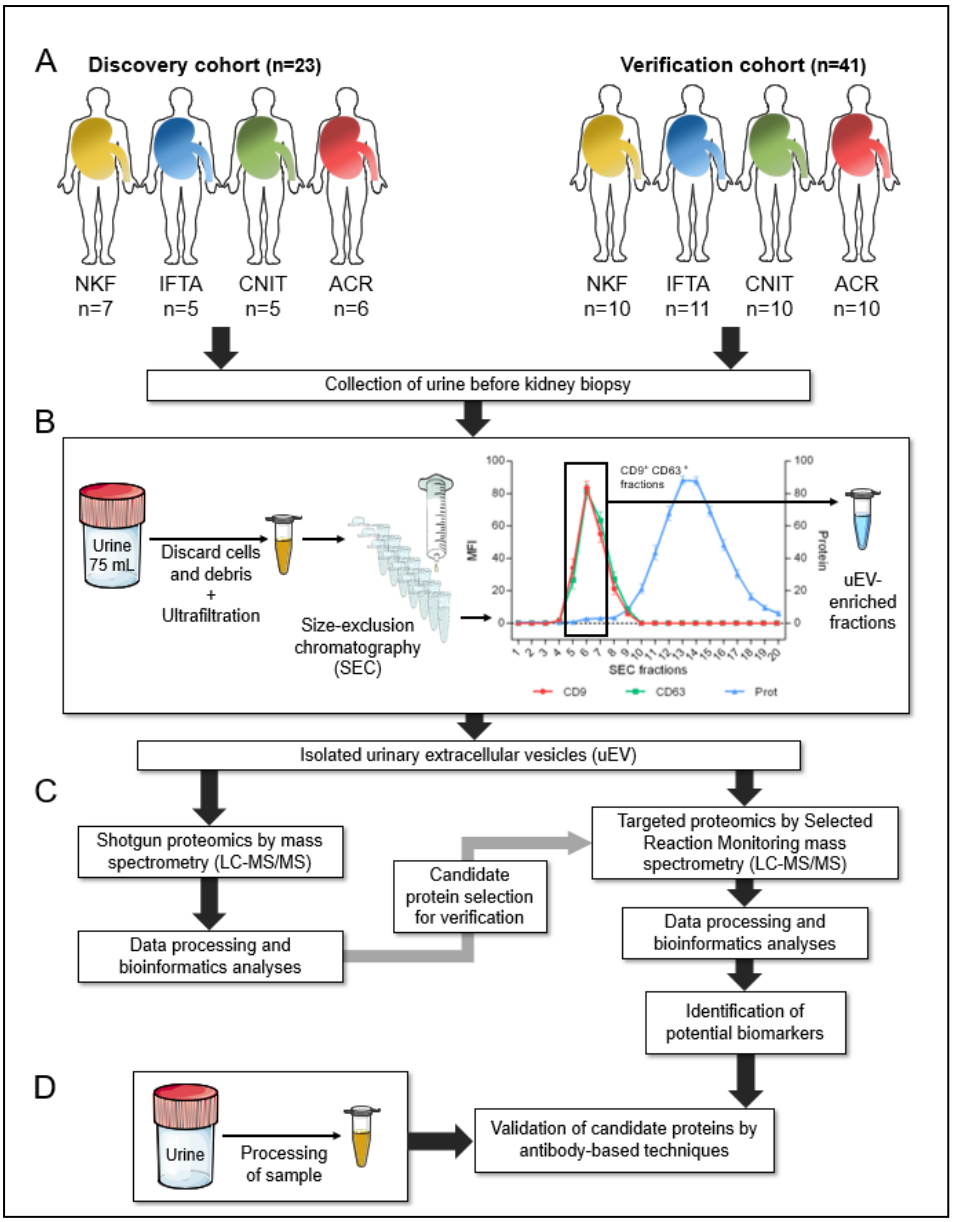
A
Discovery cohort (n=23)
Verification cohort (n=41)
NKF n=7
IFTA n=5
CNIT n=5
ACR n=6
NKF n=10
IFTA n=11
CNIT n=10
ACR n=10
Collection of urine before kidney biopsy
B
Urine 75 mL
Discard cells and debris + Ultrafiltration
Size-exclusion chromatography (SEC)
MFI
Protein
CD9+ CD63+ fractions
SEC fractions
CD9
CD63
Prot
uEV-enriched fractions
Isolated urinary extracellular vesicles (uEV)
C
Shotgun proteomics by mass spectrometry (LC-MS/MS)
Data processing and bioinformatics analyses
Candidate protein selection for verification
Targeted proteomics by Selected Reaction Monitoring mass spectrometry (LC-MS/MS)
Data processing and bioinformatics analyses
Identification of potential biomarkers
D
Urine
Processing of sample
Validation of candidate proteins by antibody-based techniques

2 ISOLATION OF EV FROM URINE BY SIZE-EXCLUSION CHROMATOGRAPHY

Urine samples were centrifuged (600× *g* 15 min) to eliminate cells and debris immediately after collection and frozen at -80ºC with protease inhibitor AEBSF (0.138 mg/mL; Roche, Basel, Switzerland). Urine was unfrozen overnight at 4ºC and processed following the protocol described by Puhka et *al.* in [268] to disrupt Tamm Horsfall polymers with some modifications. Then, urinary extracellular vesicles (uEV) were isolated by size-exclusion chromatography (SEC) and characterized based on the protocol described in detail by Lozano et *al.* [269] and Monguió-Tortajada et *al.* [242] with some modifications. Briefly, 40 mL of urine were centrifuged at 1,800× *g* for 10 min at 4ºC, the pellet was discarded and the supernatant was diluted 1/4 with Tris-EDTA buffer (20 mM, pH=9). After a 90-seconds vortex, each sample was centrifuged at 8,000× *g* for 15 min at 4ºC and the supernatant was concentrated using a 100 kDa cut-off Centricon filter unit (Millipore, Bedford, MA, USA). Then, 150 µL of the concentrate was loaded onto 1 mL sepharose CL-2B (Sigma-Aldrich, St. Louis, MO, USA) SEC columns and eluted with phosphate-buffered saline (PBS) to collect up to twenty 100 µL fractions (Figure 9b).

3 DETERMINATION OF UEV-ENRICHED FRACTIONS

Protein elution from SEC was determined by reading absorbance of 2 µL of each fraction at 280 nm with Nanodrop ND-1000 (Thermo Scientific, Waltham, MA, USA). In all cases, uEV eluted well before the bulk of soluble proteins,

which have a much smaller size (typically in fractions 5 to 8 and fractions 10 to 18, respectively) (Figure 9b). Next, fractions were analyzed for the expression of tetraspanin specific EV-markers CD9 and CD63 by bead-based assay flow cytometry on fractions 4 to 10 to determine the three most EV-enriched fractions. A 10% of SEC fractions volume was incubated with 4 µm aldehyde/sulphate-latex beads (Invitrogen, Carlsbad, CA, USA) for 15 min at room temperature and blocked with BCB buffer (PBS, 0,1 % BSA and 0,01% NaN3; Sigma-Aldrich) overnight at room temperature on rotation. After washing with BCB, EV-coated beads were incubated at 4ºC for 30 min with antibodies against the tetraspanin markers CD9 and CD63 (clones VJ1/20 and TEA 3/18, respectively), using goat-anti-mouse-FITC as secondary antibody (SouthernBiotech, Birmingham, AL, USA) and polyclonal mouse IgG as isotype control (Abcam, Cambrige, United Kingdom). In the flow cytometry analysis (FacsVerse, BD Biosciences, San Jose, CA, USA), 10,000 beads were acquired and FITC median fluorescence intensity (MFI) of singlet beads were measured for each fraction with FlowJo software (Tree Star, Ashland, OR, USA). For all samples, the fractions with the highest EV markers MFI were considered to contain EV, so they were pooled together rendering a volume of approximately 300 µL of which 150 µL were used for MS analysis.

4 MASS-SPECTROMETRY PROTEOMICS

The proteomics study design is depicted in the workflow in Figure 9c.

4.1 DISCOVERY PROTEOMICS

4.1.1 SAMPLE PREPARATION

For the discovery phase, 500 µL of uEV-enriched fractions from SEC were analyzed by shot gun proteomics with liquid chromatography followed by tandem mass spectrometry (LC-MS/MS). Samples were prepared for MS analysis, digested with LysC and Trypsin (Promega, Madison, WI, USA) and injected to an Orbitrap XL (Thermo Scientific). Data was analyzed using the Proteome Discoverer software (v2.0, Thermo Scientific) and proteins were identified using Mascot (Matrix Science, London, United Kingdom) against SwissProt human database (UniProtKB, April 2015; https://www.uniprot.org/) [270] with a false discovery rate (FDR) of 5%.

4.1.2 DATA PROCESSING

Raw data files derived from the MS analysis in the discovery phase were processed using MaxQuant software [271] (v1.5.3.30, https://www.maxquant.org/, Max Planck Institute of Biochemistry, Martinsried, Germany) and SwissProt human database (December 2015). Maximum FDR, which determines the expected proportion of type I errors, for peptides and proteins was set at 1%, so only those proteins with a q-value lower than 0.01 were kept. Other parameters set in the software include: (i) minimum peptide length of 7; (ii) minimum peptides per protein of 1 and minimum unique peptides per protein of 0; (iii) minimum score for modified peptides of 40; (iv) main search error was set to 4 ppm; (v) cysteine carbamidomethylation was

established as a fixed modification and methionine oxidation and acetylation of the N-terminus were established as variable modifications, with a maximum number of modifications per peptide set to 5. Proteins identified as potential contaminants, those only identified by site or identified with a reverse sequence were discarded, as well as proteins with less than 2 unique peptides. All the analyses were thereafter performed with intensity-based absolute quantification (iBAQ) values which were normalized with the EV marker ezrin. Although the selection of candidate proteins was eventually made on a presence-absence base, relative quantification of proteins for statistical analyses to demonstrate difference in the EV proteome between groups was based on iBAQ values. There are several ways to measure peptide intensity in label-free absolute quantification. iBAQ is calculated as the sum of intensities of all the tryptic peptides for each protein divided by the number of theoretically observable peptides, thus resulting in an accurate measure of the intensity of the proteins [272].

4.2 TARGETED PROTEOMICS

Twenty-three proteins (two peptides for each) were selected based on the results of the discovery phase to be analyzed with targeted mass spectrometry, a technique based on Selected Reaction Monitoring (SRM)[253] (Table 1).

Table 1. Proteins with their selected peptide pairs for verification by targeted proteomics.

Gene name	Protein name	NCBI Entry	Peptide sequence
ACE2	Angiotensin-converting enzyme 2	Q9BYF1	ISFNFFVTAP(K) SGENPYASIDIS(K)
ACTR3	Actin-related protein 3	P61158	DYEEIGPSI[C](R) LGYAGNTEPQFIIPS[C]IAI(K)
AFM	Afamin	P43652	ESLLNHFLYEVA(R) IAPQLSTEELVSLGE(K)
BASP1	Brain acid soluble protein 1	P80723	ESEPQAAAEPAEA(K) ETPAATEAPSSTP(K)
C5	Complement C5	P01031	IDTQDIEASHY(R) TDAPDLPEENQA(R)
C7	Complement component C7	P10643	LIDQYGTHYLQSGSLGGEY(R) NVVYT[C]NEGYSLIGNPVA(R)
CDC42	Cell division control protein 42 homolog	P60953	NVFDEAILAALEPPEP(K) T[C]LLISYTTN(K)
CST3	Cystatin-C	P01034	ALDFAVGEYN(K) TQPNLDN[C]PFHDQPHL(K)
CSTD	Cathepsin D	P07339	LVDQNIFSFYLS(R) VGFAEAA(R)
EZR	Ezrin	P15311	FYPEDVAEELIQDITQ(K) SQEQLAAELAEYTA(K)
IGFALS	Insulin-like growth factor-binding protein complex acid labile subunit	P35858	DLHFLEELQLGHN(R) LHSLHLEGS[C]LG(R)
ISLR	Immunoglobulin superfamily containing leucine-rich repeat protein	O14498	ALPGTPVASSQP(R) TVAAGALASLSHL(K)
LUM	Lumican	P51884	NIPTVNENLENYYLEVNQLE(K) SLEYLDLSFNQIA(R)
MB	Myoglobin	P02144	VEADIPGHGQEVLI(R) YLEFISE[C]IIQVLQS(K)
OGN	Mimecan	P20774	DFADIPNL(R)

			LSLLEELSLAENQLL(K)
PPL	Periplakin	O60437	EVVQEILQFQEDPQT(K) SLLGEVEQNLQAA(K)
PROM1	Prominin-1	O43490	AFTDLNSINSVLGGGILD(R) VLPIEQSLSTLYQSV(K)
RBP4	Retinol-binding protein 4	P02753	DPNGLPPEAQ(K) LIVHNGY[C]DG(R)
SERPINA4	Kallistatin	P29622	LGFTDLFS(K) VGSALFLSHNL(K)
SERPINC1	Antithrombin-III	P01008	AFLEVNEEGSEAAASTAVVIAG(R) TSDQIHFFFA(K)
TF	Serotransferrin	P02787	D[C]HLAQVPSHTVVA(R) DGAGDVAFV(K)
UPK1B	Uroplakin-1b	O75841	EPLNLEA[C](K) TENNDADYPWP(R)
VTN	Vitronectin	P04004	FEDGVLDPDYP(R) GQY[C]YELDE(K)

4.2.1 *Selection criteria of candidate proteins for the validation phase*

The criteria used for the selection of proteins to be analysed by targeted mass-spectrometry are the following:

1. Proteins that presented a significantly different expression between pathological processes and NKF and between pathologic groups.
2. Proteins with higher intensity in the mass spectrometry analysis had priority in order to decrease the number of false positives (a higher intensity in the mass-spectrometry analysis means that the mass-spectrometer has detected the peptides of that protein more times).
3. Biological significance of the protein regarding the process they seem to represent. Bibliography search was key for this purpose, as well as

resources such as UniProtKB [270] or Gene Cards (https://www.genecards.org/) [273].

Once candidate proteins for targeted proteomics validation were selected, two peptides for each of them were selected in accordance with the following criteria:

1. Unique peptides.
2. Peptides of 6 to 25-amino acids length.
3. Exclusion of peptides that contain some amino acids that could reduce the precision of the quantification analysis:
    3.1. The selected peptides cannot contain the amino acids methionine (M) or tryptophan (W), since they tend to suffer oxidations easily that would change the peptide mass, decreasing the precision of the quantification.
    3.2. Exclusion of peptides with missed cleavages, because it would also lead to imprecisions in the quantification. Trypsin cleaves peptides on the C-terminal side of lysine (K) and arginine (R). Trypsin can miss a cleavage in some situations, for instance if a proline (P) is on the carboxyl side of the cleavage site.
    3.3. Exclusion of peptides with two cysteine residues (C) together, since they tend to suffer modifications.
4. Peptides that tend to be more frequently read in mass-spectrometry experiments had priority. For this purpose, PeptideAtlas (http://www.peptideatlas.org/) [274] was consulted.

4.2.2 *SAMPLE PREPARATION AND DATA PROCESSING*

Purified uEV-enriched fraction samples (500 µL) were concentrated by ultrafiltration using 10kDa cut-off Amicon Ultra devices (Merck Millipore, Millerica, MA, USA), and the buffer was changed to 6M Urea, 50 mM ammonium bicarbonate. A known quantity of isotypic heavily labelled standard peptides (Thermo Scientific) was spiked into the samples prior to an in-gel (10% SDS-PAGE) trypsin digestion for LC-MS/MS analysis. Raw data was processed with the Skyline software (https://skyline.ms/) [275]. Ratios between the unlabeled endogenous peptide and the labeled internal standard were used to calculate endogenous peptide quantity in each sample (fmol/sample). Measured values were normalized by the peptide abundance across samples and by endogenous ezrin for each sample. Only those peptides that could be read in at least 90% of the samples with mass spectrometry were further analyzed, using the mean value of the peptide pair when possible.

5 WESTERN BLOT

One mL of uEV-enriched fractions was concentrated up to 25 µL using a 100 kDa-cut off Amicon Ultra filter unit (Merck Millipore) at 2,000x *g* for 20 minutes and further concentrated using SpeedVac vacuum concentrator (Thermo Scientific) up to 15 µL. Cell lysates from mesenchymal stem/stromal cells, JURKAT cells, A549 epithelial cell line or plasma were used as positive controls following the recommendations of the antibody manufacturer. One million cells were incubated with radioimmunoprecipitation assay (RIPA) buffer with proteases inhibitor on ice for 30 min. The lysed cells were then centrifuged

for 20 min 15,000x g at 4ºC and the supernatant was frozen at -20ºC until further use. Protein concentration of uEV samples and cell lysates was measured with Nanodrop ND-1000 (Thermo Scientific). Routinely, between 100-1,000 µg of uEV samples and 1,000 µg of cell lysate were used. Samples for western blot were mixed with Laemli buffer (Bio-Rad Laboratories, Hercules, CA, USA) 5% β-mercaptoethanol and denatured at 95ºC for 10 min. Then, samples and a molecular weight ruler were loaded into precast 10% tris-glycine gels (Bio-Rad Laboratories) and run at 170 V constant voltage for 1 hour in a western blot chamber (Bio-Rad Laboratories). Transfer to a low fluorescence polyvinylidene difluoride (PVDF, Sigma-Aldrich) membrane (0.2 µm pore, GE Healthcare, Life Sciences) was performed at 100 V for 30 min in a transfer chamber (Bio-Rad Laboratories). The membrane was blocked for 1 hour at room temperature before incubating with the primary antibody (Table 2) overnight at 4ºC. The membrane was washed three times and then incubated with a 1:15,000 dilution of the corresponding fluorescently conjugated secondary antibody (IRDye 680LT Goat anti-rabbit or IRDye 800CW Goat anti-mouse, both LI-COR Biosciences, Lincoln, NE, USA), washed three times and read with an Odyssey fluorescence scanner (LI-COR) at 700 nm or 800 nm.

Table 2. Details of the antibodies used in western blot analyses.

Target Protein	Gene name	H.	Clone	MW	Dilution
ADP-Ribosyltransferase 3	ART3	R	EPR7220(2)	41, 44	1/1,000
Alcohol Dehydrogenase 5 (Class III)	ADH5	R	EPR12885(B)	40	1/1,000
Capping Actin Protein, Gelsolin Like	CAPG	M	Polyclonal	39	1/500
Casein Kinase 2α'	CSKN2A2	R	Polyclonal	39, 41	1/1,000
Cathepsin D	CTSD	M	CTD-19	52	1/1,000
Cathepsin Z	CTSZ	M	AT6G11	33	1/1,000
CD44	CD44	M	106-405	82	1/100
CD44	CD44	M	33-3B3	82	1/100
CD44	CD44	M	156-3C1	82	1/100
CD44	CD44	R	EPR1013Y	82	1/5,000
CD5L	CD5L	R	1C8	40	1/1,000
Destrin	DSTN	R	EPR15827(B)	17-19	1/1,000
Ezrin	EZR	R	EP886Y	72	1/5,000
Galectin-3-binding protein	LGALS3BP	M	3G8	65	1/500
Glyceraldehyde-3-Phosphate Dehydrogenase	GAPDH	M	GA1R	36	1/500
Insulin-like growth factor-binding protein 2	IGFBP2	R	EPR3380(2)	35	1/10,000
Kallistatin	SERPINA4	R	Polyclonal	49	1/10,000
Kallistatin	SERPINA4	R	EPR15310	49	1/1,000
Kallistatin	SERPINA4	R	Polyclonal	49	1/500
Lumican	LUM	R	EPR8898(2)	50	1/1,000
Phosphoinositide-3-Kinase Interacting Protein 1	PIK3IP1	R	Polyclonal	12	1/100
Retinol binding protein 4	RBP4	R	EPR5879	23	1/10,000
Serine/Threonine Kinase 24	MST3	R	EP1468Y	52	1/5,000
Serpin B13	SERPINB13	R	Polyclonal	44	1/1,000
Tumor susceptibility gene 101	TSG101	M	4A10	44	1/500
Uroplakin Ib	UPK1B	R	EPR14451	25	1/10,000
Uroplakin IIIb	UPK3B	R	Polyclonal	34	1/1,000
Uteroglobin	SCGB1A1	R	EPR12008(B)	10	1/1,000

CD, cluster of differentiation; H., Host; R, Rabbit; M, Mouse; MW, molecular weight (kDa).

6 ENZYME-LINKED IMMUNOSORBENT ASSAY (ELISA)

One to two milliliters of urine were concentrated to 100 µL using an Amicon Ultra filter unit of 50 kDa cut-off at 2,000x *g* for 20 minutes and analyzed in 96-wells plates with a vitronectin ELISA kit (Cloud-Clone Corporation, USA), following the protocol recommended by the manufacturer. A standard curve provided in the kit was used to calculate vitronectin concentration in samples. Plasma samples at 1:100 dilution from healthy donors were used as positive controls. In the set-up phase, Amicon Ultra of 100 kDa cut-off and ExoGAG reagent (Nasasbiotech, A Coruña, Spain) were used.

7 STATISTICAL ANALYSES

Several types of plots and software were used to demonstrate the proteomic expression of uEV samples in both the discovery and validation phases. Enrichment analyses of Gene Ontology (GO) - Cellular Components were performed using the FunRich software (http://www.funrich.org, Melbourne, Australia) [276], [277]. The FunRich software annotates Gene Ontology – Cellular Component terms based on the data from the Gene Ontology database [276], [277], HPRD [280], Entrez Gene [281] and UniProt [282]. The number of shared proteins was calculated and represented with the online tool InteractiVenn (http://www.interactivenn.net/) [283]. The Perseus software [16] (v1.5.6.0 in the discovery phase or v1.6.1.3 in the verification phase, http://www.perseus-framework.org, Max Planck Institute of Biochemistry) was used for graphs representation and analyses. In the principal component

analysis (PCA), samples are distributed based on the so-called components, which explain a certain percentage of the variance between the samples. Components are numerated from the highest to the lowest percentage. GO terms to show enrichment of biological processes for each component were also annotated with Perseus. Non-supervised hierarchical clustering analysis (HCA) was also performed with the Perseus software after normalization of values with the z-score method. HCA was performed with no k-means and using Euclidean distance for both columns and rows. To represent differentially expressed proteins a volcano plot was used. It plots the fold-change difference is on the x-axis, and -$\log_2$(*p*-value) resulting from a two-sided unpaired t-test on the y-axis. Protein expression representations and other statistical tests were performed using GraphPad Prism software (v6.0 GraphPad Software, San Diego, CA, USA). After testing for normality, two-sided unpaired *t*-test (parametric) or Mann-Whitney (non-parametric) were used for the comparison of two groups of samples. In the case of multiple groups comparison, one-way analysis of variance (ANOVA) with Holm-Sidak's multiple comparison (parametric) or Kruskall-Wallis with Dunn's multiple comparison test (non-parametric) were performed. Hartigan test for unimodality was performed in R software (R Development Core Team, 2016; http://cran.r-project.org/) [285]. Receiver operating characteristics (ROC) curves were created with the SPSS statistical package (v15, SPSS Inc., Chicago, IL, USA) [286]. For combination of markers, first a binary linear correlation was calculated combining the two proteins of interest, and then ROC curves were calculated. Finally, Gene Set Enrichment Analysis software (GSEA v3.0, Broad Institute, Cambridge, MA, USA) [287] was used to compare enriched gene sets. The gene sets annotated

by GO-Biological Process were downloaded from GSEA molecular signatures database (MSigDB v6.2, Broad Institute) [288]. The normalized enrichment score (NES) accounts for differences between gene sets to allow comparisons between them. The FDR represents the nominal *p*-value adjusted for gene set size and multiple hypothesis testing. It is the estimated probability that a gene set with a given NES represents a false positive finding (significant FDR < 0.25, as recommended by the GSEA software).

RESULTS

Sometimes you win, sometimes you learn.

— Robert Kiyosaki, Rich dad poor dad

1 PART I: PROTEOMIC CHARACTERIZATION OF URINARY EXTRACELLULAR VESICLES FROM KIDNEY-TRANSPLANTED PATIENTS TREATED WITH CALCINEURIN INHIBITORS

The text in this section has been published in:

Carreras-Planella L, Juega J, Taco O, Cañas L, Franquesa M, Lauzurica R, Borràs FE. *Proteomic Characterization of Urinary Extracellular Vesicles from Kidney-Transplanted Patients Treated with Calcineurin Inhibitors.* **International Journal of Molecular Sciences**. 2020 Oct, 21(20), 7569. Doi: 10.3390/ijms21207569.

1.1 PATIENTS AND SAMPLES COLLECTION

In this study, size-exclusion chromatography (SEC)-isolated uEV samples from three groups of kidney-transplanted patients (NKF, IFTA and CNIT) were used. Table 3 summarizes the clinical data of each patient when urine sample was collected. As expected, patients in the NKF group presented significantly lower serum creatinine levels than IFTA (p=0.012) and CNIT (p=0.012), but no other significant differences were found. Patient DC15, the unique patient affected by chronic CNIT, presented the highest serum creatinine level. Table 4 summarizes the induction treatment at kidney transplantation, immunosuppression regime at sample's collection and the diagnosis based on renal biopsy and clinical parameters. Figure 10 shows histological images of transplanted kidneys representative of each group. All patients were receiving an immunosuppressive regime consisting of prednisone and a calcineurin inhibitor (in most cases tacrolimus, only one patient in each group was

receiving cyclosporine A), with or without mycophenolate mofetil. The histopathological results of the Banff scoring are summarized in Annex Table 1. Acute CNIT was diagnosed in four out of five cases by the presence of isometric vacuolization of the tubular epithelium and the preservation of the microvilli on the apical border. The other CNIT patient was diagnosed with chronic CNIT because of the presence of grade 3 arteriolar hyalinosis and circumferential hyalinosis with peripheric nodules. The diagnosis of CNIT was further supported by the high blood levels of tacrolimus, determined according to the study by Cosio et *al*. [265] or high levels of cyclosporine A based on the Symphony study [61]. Patients in the IFTA group presented different grades of fibrosis in the renal biopsy with no other signs of pathology. The determination of IFTA grade was based on the mean values of the Banff parameters chronic interstitial and tubular lesions (ci and ct). Also, IFTA patients showed lower blood levels of tacrolimus and cyclosporine A compared to CNIT patients, and similar to NFK patients. Patient DI8 suffered a previous episode of acute cellular rejection and one episode of acute humoral rejection 21 and 9 months before urine collection, respectively. This patient showed no histopathological signs of rejection at sample collection and was therefore included in the study.

Table 3. Clinical parameters of the study patients at urine collection time.

Id.	Age	Sex	DM	HT	Crea.	Prot.	Time RT	LD	D. age
DN1	64	F	-	-	0.86	99	137.9	-	53
DN2	65	M	-	+	0.86	110	186.6	-	37
DN3	45	F	-	+	0.82	30	113.6	-	43
DN4	42	M	-	+	0.89	187	186.6	-	30
DN5	57	M	-	+	0.9	92	166.4	-	45
DN6	65	F	-	-	0.85	55	70.0	+	37
DN7	69	F	-	+	1.14	86	57.8	+	58
DI8	50	F	-	-	2	62	21.7	+	48
DI9	64	M	-	+	1.6	1600	84.6	-	71
DI10	68	M	-	+	2.49	94	25.8	-	67
DI11	68	M	+	+	2.62	800	15.1	-	38
DI12	53	F	-	+	2.3	806	252.3	-	35
DC13	55	M	+	+	2.29	506	0.5	+	62
DC14	33	M	-	-	1.93	232	2.8	+	59
DC15	49	F	-	+	3.08	427	238.8	-	45
DC16	50	F	-	-	2.49	207	5.5	-	60
DC17	41	F	-	+	1.80	76	25.7	-	34
Sig.	ns	ns	ns	ns	***	ns	ns	ns	ns
p-value	0.064[a]	0.784[b]	0.452[b]	0.784[b]	<0.001[a]	0.093[a]	0.113[a]	0.784[b]	0.387[a]

[a] Kruskall-Wallis test or [b] Chi-squared test were performed to determine statistical differences between groups.

Id., sample identification; DM, diabetes mellitus type 2; HT, arterial hypertension; Crea., serum creatinine (mg/dL); Prot., proteinuria (mg/g creatinine); Time RT., months from renal transplantation until sample collection; LD, living donor; D. age, donor's age; N, NKF, C, CNIT; I, IFTA; F, female; M, male.

Table 4. Immunosuppression regime of patients of the NKF, CNIT and IFTA groups.

Id.	Induction treatment	IS at urine collection	High CNI	Diagnosis
DN1	IL2RA	PR, CSA	-	NKF
DN2	rATG	PR, TAC, MMF	-	NKF
DN3	IL2RA	PR, TAC	-	NKF
DN4	IL2RA	PR, TAC	-	NKF
DN5	IL2RA	PR, TAC	-	NKF
DN6	IL2RA	PR, TAC, MMF	-	NKF
DN7	IL2RA	PR, TAC, MMF	-	NKF
DI8	IL2RA	PR, TAC, MMF	-	IFTA (G2)
DI9	IL2RA	PR, TAC, MMF	-	IFTA (G1)
DI10	IL2RA	PR, TAC, MMF	-	IFTA (G2)
DI11	IL2RA	PR, TAC, MMF	-	IFTA (G2)
DI12	IL2RA	PR, CSA	-	IFTA (G2)
DC13	IL2RA	PR, TAC, MMF	+	aCNIT
DC14	IL2RA	PR, TAC, MMF	+	aCNIT
DC15	IL2RA	PR, CSA, MMF	+	cCNIT
DC16	IL2RA	PR, TAC, MMF	+	aCNIT
DC17	IL2RA	PR, TAC, MMF	+	aCNIT

Id. sample identification; IS, immunosuppressive treatment; CNI, calcineurin inhibitors; D, discovery; N, NKF, C, CNIT; I, IFTA; IL2RA, interleukin 2 receptor antagonists; rATG, rabbit anti-thymocyte globulin; PR, prednisone; CSA, cyclosporine A; TAC, tacrolimus; MMF, mycophenolate mofetil; NKF, normal kidney function; aCNIT, acute CNI toxicity; cCNIT, chronic CNI toxicity; IFTA (G), interstitial fibrosis and tubular atrophy (grade).

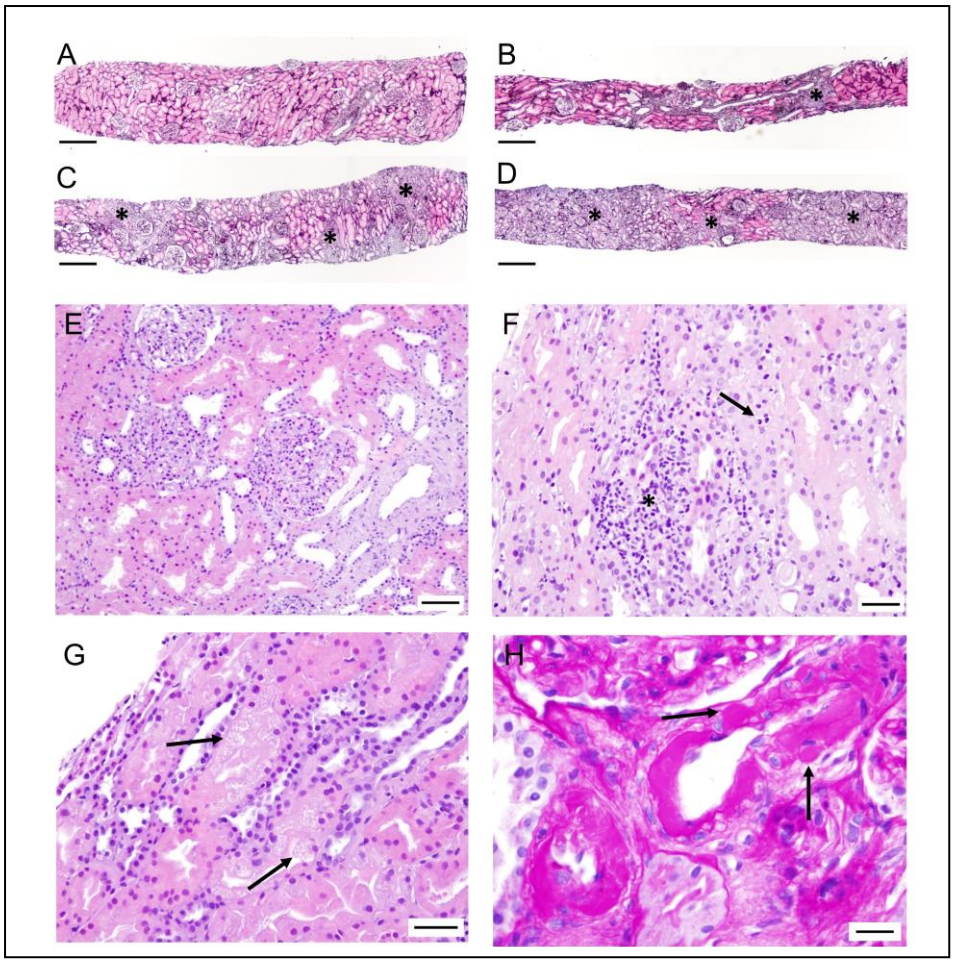

Figure 10. Representative histological photographs of kidney biopsies from transplanted kidneys showing different alterations. **(A-D)** Silver methenamine (Jones)-stained biopsies with grades 0, 1, 2 and 3 of IFTA, respectively. Asterisks indicate fibrin and collagen deposits. (200x, scale bars represent 500 µm). **(E-F)** Hematoxilin/eosin staining of a biopsy with **(E)** minimal histological alterations (100x, scale bar represents 100 µm) and **(F)** interstitial infiltrate typical of acute cellular rejection, where arrows point at tubulitis with infiltrating immune cells and the asterisk indicates interstitial inflammation in non-scared areas of the cortex (200x, scale bar represents 50 µm). **(G)** Hematoxilin/eosin stained biopsy showing acute tubular CNIT with isometric vacuolization of the proximal tubular epithelial cells' cytoplasm (indicated with arrows) (200x, scale bar represents 50 µm). **(H)** Periodic acid-Schiff staining of a kidney with chronic vascular CNIT showing severe arteriolar hyalinosis with circumferential involvement. Arrows indicate adventitial hyaline deposits (pearl-like pattern) (Banff score ah3) (400x, scale bar represents 20 µm).

1.2 GLOBAL ANALYSIS OF THE UEV PROTEOME

A total of 730 proteins were confidently identified after processing mass spectrometry data. Confirming previous results, and as expected by the enrichment technique used, the FunRich analysis of the identified proteins revealed that the most significantly enriched terms were those related to the secretion of EV such as "vesicle mediated transport" or "extracellular region" according to Gene Ontology (GO) - Biological Process (BP) and Cellular Component (CC) enrichment analysis, respectively (Annex table 2 and Annex table 3). The number of identified proteins in CNIT samples (mean±sd, 369±73.9) was significantly higher compared to NKF samples (168.6±65.1) and higher than IFTA samples (246.8±47.0) (Figure 11a). We then assessed the homogeneity of the samples within each group. First, the number of shared proteins among the samples in each group with respect to the total number of proteins identified in the group was analysed. The seven NKF samples shared up to 28 proteins of a total of the 394 in the group (7.1%). Five CNIT patients shared up to 143 of 621 proteins (23.0%), and five IFTA patients shared 64 of 512 proteins (12.5%). In total, 17 proteins were shared among all samples analysed (Figure 11b).

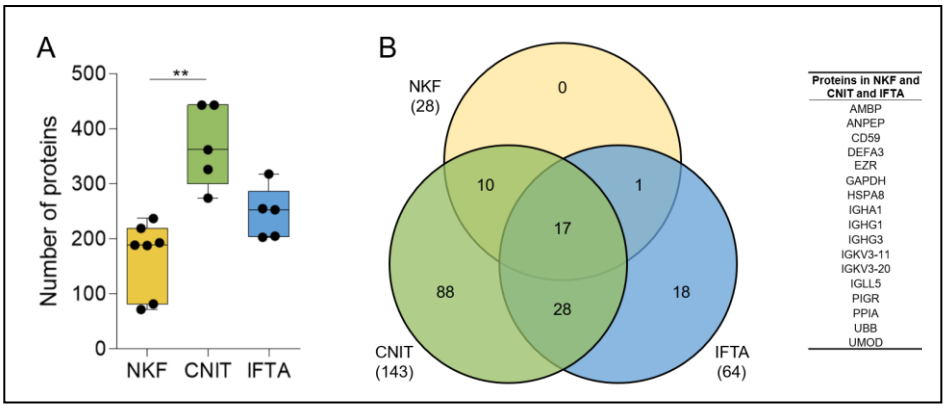

Figure 11. **(A)** Number of proteins found by mass-spectrometry in uEV samples in each group. Whiskers represent minimum to maximum; horizontal line represents the mean (**p<0.01). **(B)** Venn diagram showing the number of coinciding proteins between the samples of each group (in brackets) and between the all the samples in the study (number in the corresponding circles). On the right, list of the 17 proteins found in all samples

Second, we performed a multiple correlation analysis among samples included in each group as a measure of intragroup homogeneity. Each sample's protein expression was compared with every other sample in the same group to obtain the mean of all Pearson correlation coefficient. NKF and CNIT groups were the most homogeneous (mean Pearson coefficient > 0.6) (Figure 12a and Figure 12b). Conversely, the IFTA group showed a lower level of internal homogeneity (barely > 0.5) (Figure 12c). In this group, sample DI8 presented a low Pearson coefficient when individually tested with every other IFTA sample (Pearson coefficients < 0.400), suggesting a particular behaviour, as observed later. Of note, if I13 sample was not considered in this assay, the mean Pearson coefficient of IFTA samples increased to 0.654, a value similar to that obtained in the CNIT group.

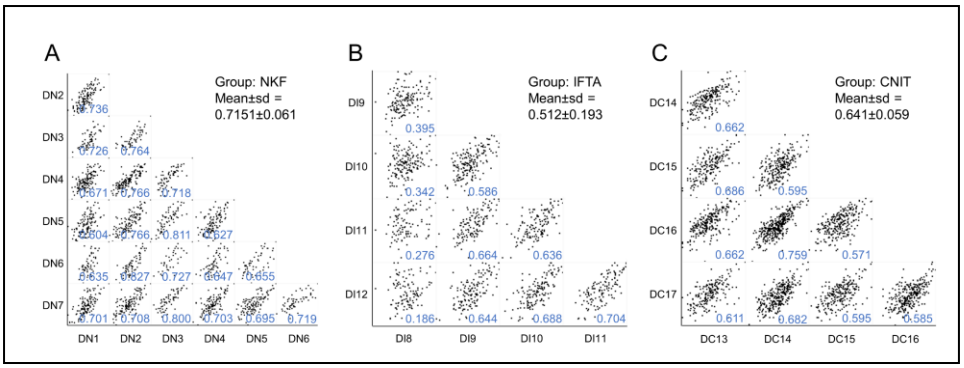

Figure 12. Multi-scatter plots showing correlations of samples within each group (**(A)**, NKF; **(B)**, CNIT; and **(C)**, IFTA). In each individual plot the Pearson correlation coefficients are shown in blue and the corresponding mean±sd for each group is shown in black.

1.3 DIFFERENTIALLY EXPRESSED PROTEINS

A principal component analysis (PCA) was performed in order to get more insight onto the global protein variation in the two renal alterations (CNIT and IFTA) and the NKF groups (Figure 13a). CNIT patients were clearly segregated from IFTA and NKF patients by Component 1, which accounted for a 23.9% of the variability among samples, while Component 2, which accounted for 17.1% of the variability, permitted to segregate the three groups of samples. Only the sample of the IFTA group (DI8), which that had a low correlation with the other IFTA samples, did not cluster together with the rest of samples in its group.

Based on this observation, a more concise comparison was performed using a volcano plot to depict the proteins that were significantly overexpressed between groups. Those proteins having $p<0.01$ and fold change >10 or <-10 in each comparison were considered as more relevant. From 71 proteins found more expressed in CNIT samples compared to NKF samples (Figure 13b), three

(CTSZ, RAB8A and SERPINC1) showed a notable low *p*-value ($<10^{-8}$). On the other hand, up to 39 proteins were significantly more expressed in the CNIT group compared to IFTA patients (Figure 13c), among which five proteins (ADIRF, CAPG, STXBP2, GNAI1 and ATP1A1) presented a remarkably lower *p*-value ($<10^{-7}$) Of note, no proteins were overexpressed in the NKF group and only three proteins (HIST1H4A, HRG and IGHV4-28) were significantly more expressed in the IFTA group versus CNIT. The full list of significant proteins from the volcano plots can be seen in Annex table 4 and Annex table 5.

Figure 13. **(A)** Principal component analysis (PCA) biplot shows distribution of samples according to Components 1 and 2. Each circle represents a sample, which are labelled and coloured according to their group. Volcano plots depict the differentially expressed proteins **(B)** between CNIT and NKF, and **(C)** between CNIT and IFTA. Each circle represents a protein. On y-axis -log(*p*-value) from a t-test is represented, with a dashed line at $p<0.01$ to indicate significance, over which proteins are coloured in orange. The expression fold change is represented on the x-axis, with dashed lines at >10 and <-10.

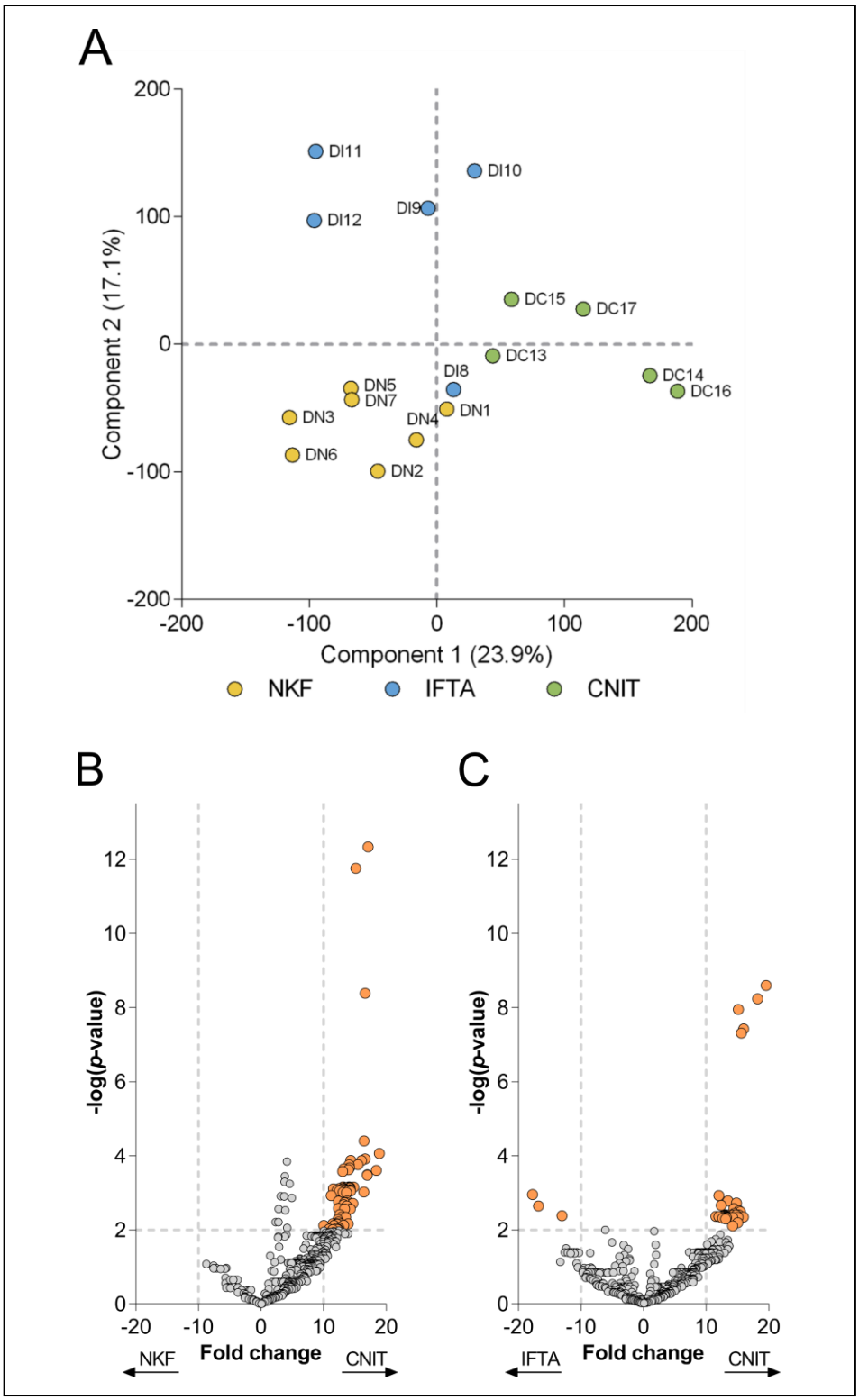
A
200
100
0
-100
-200
Component 2 (17.1%)
DI11
DI10
DI9
DI12
DC15
DC17
DC13
DI8
DC14
DC16
DN5
DN7
DN3
DN4
DN1
DN6
DN2
-200
-100
0
100
200
Component 1 (23.9%)
NKF
IFTA
CNIT
B
C
-log(p-value)
12
10
8
6
4
2
0
-20
-10
0
10
20
Fold change
NKF
CNIT
IFTA

1.4 BIOLOGICAL PROCESSES ENRICHMENT ANALYSIS

After identifying significant proteins differentially expressed in CNIT, the GSEA software was used to reveal the GO biological processes that were up- or downregulated in this group compared to the other groups (each gene being equivalent to a protein). A total of 45 gene sets were significantly enriched (nominal p-value<0.05) in CNIT compared to NKF. None of them reached the minimal significant FDR of 0.25, probably because of the dimension of the difference in protein numbers and level of expression. Nevertheless, the most overexpressed gene set was "negative regulation of immune response" (Annex table 6 and Annex table 7).

When comparing CNIT and IFTA, up to 128 gene sets were significantly upregulated (FDR<0.25) in CNIT patients (Annex table 8). The most overexpressed gene sets were "epithelial cell differentiation" and "regulation of actin filament length" (Figure 14a). In addition, CNIT presented overexpression of vesicle-related gene sets such as "Vesicle organization" or "multivesicular body organization". Other gene sets more expressed in CNIT than in IFTA were "cell cycle" and "intracellular protein transport". On the reverse comparison, 59 gene sets were upregulated in IFTA compared to CNIT (Annex table 9), "protein activation cascade" and "humoral immune response" being two of the most significant ones (Figure 14b). Other gene sets related to inflammatory response and complement activation were also upregulated.

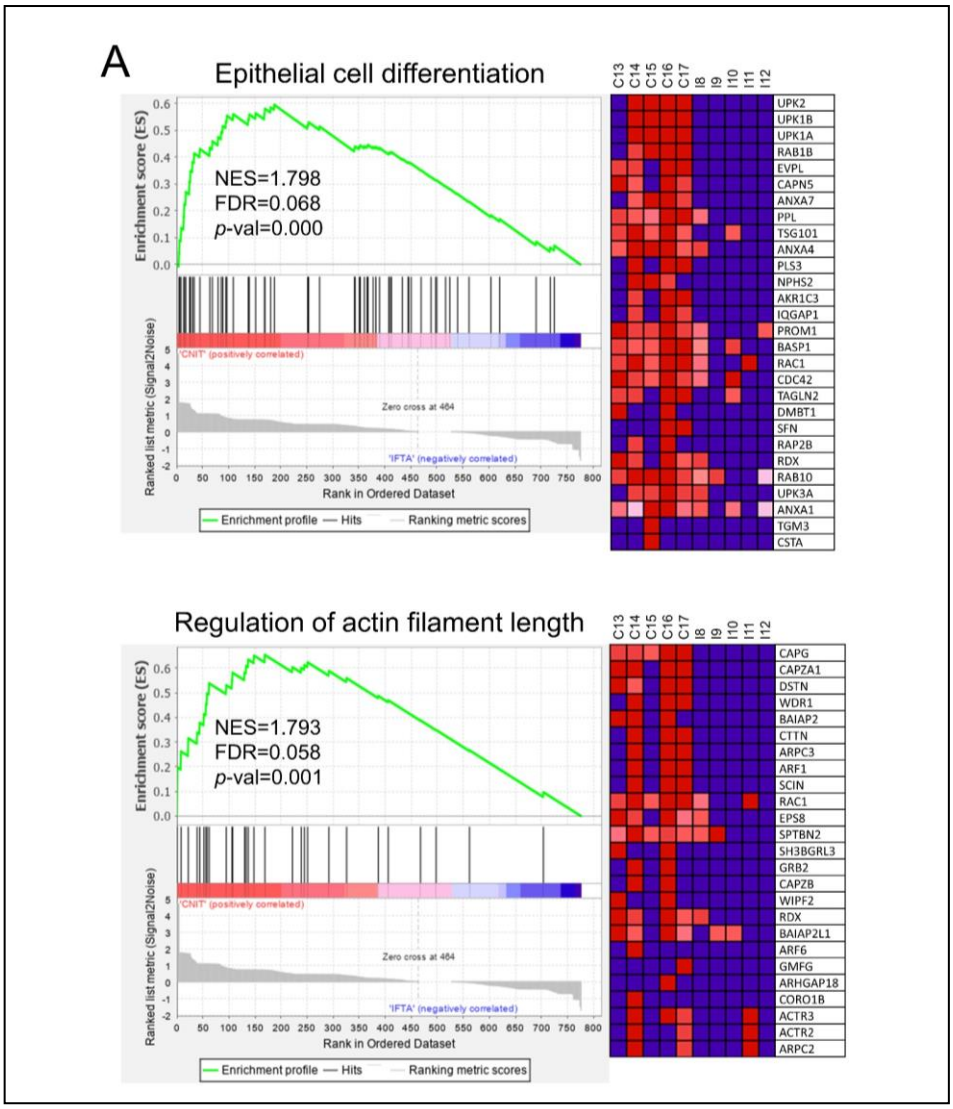
A
Epithelial cell differentiation
NES=1.798
FDR=0.068
p-val=0.000
Enrichment score (ES)
Ranked list metric (Signal2Noise)
'CNIT' (positively correlated)
'IFTA' (negatively correlated)
Zero cross at 464
Rank in Ordered Dataset
Enrichment profile
Hits
Ranking metric scores
C13 C14 C15 C16 C17 I8 I9 I10 I11 I12
UPK2
UPK1B
UPK1A
RAB1B
EVPL
CAPN5
ANXA7
PPL
TSG101
ANXA4
PLS3
NPHS2
AKR1C3
IQGAP1
PROM1
BASP1
RAC1
CDC42
TAGLN2
DMBT1
SFN
RAP2B
RDX
RAB10
UPK3A
ANXA1
TGM3
CSTA
Regulation of actin filament length
NES=1.793
FDR=0.058
p-val=0.001
CAPG
CAPZA1
DSTN
WDR1
BAIAP2
CTTN
ARPC3
ARF1
SCIN
RAC1
EPS8
SPTBN2
SH3BGRL3
GRB2
CAPZB
WIPF2
RDX
BAIAP2L1
ARF6
GMFG
ARHGAP18
CORO1B
ACTR3
ACTR2
ARPC2

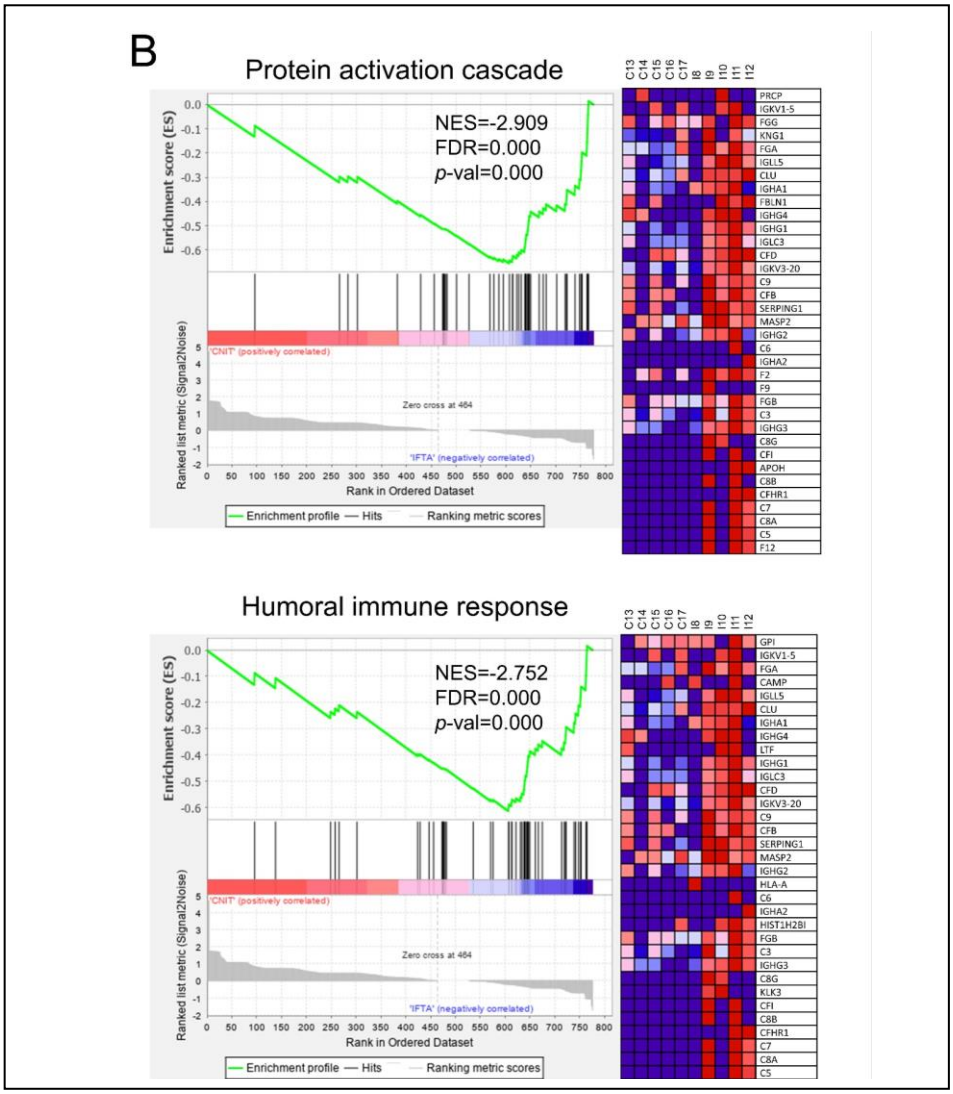

Figure 14. Enrichment plots from GSEA conducted with GO-BP gene sets, each gene accounting for one protein. Statistically significant up-regulation of **(A)** "epithelial cell differentiation" and "regulation of actin filament length" was found in CNIT when compared with IFTA (to the left of the x-axis, positive running enrichment score (ES)), and **(B)** "protein activation cascade" and "humoral immune response" was found in IFTA compared to CNIT (to the right of the x-axis, negative ES). Vertical black lines indicate the position of individual genes of the gene set in the ranked list. The heatmap on the right shows the relative expression level of the most up-regulated genes of the gene set (red = high, blue = low). NES, normalized enrichment score; FDR, false discovery rate; *p*-val, *p*-value.

1.5 UROPLAKIN EXPRESSION

Interestingly, several proteins of the uroplakin family (UPK1A, UPK1B, UPK2 and UPK3A), as well as envoplakin (EVPL) and periplakin (PPL) (citolinker proteins) were significantly upregulated in CNIT compared to IFTA and NKF (Figure 15). These proteins are members of the "epithelial cell differentiation" gene set.

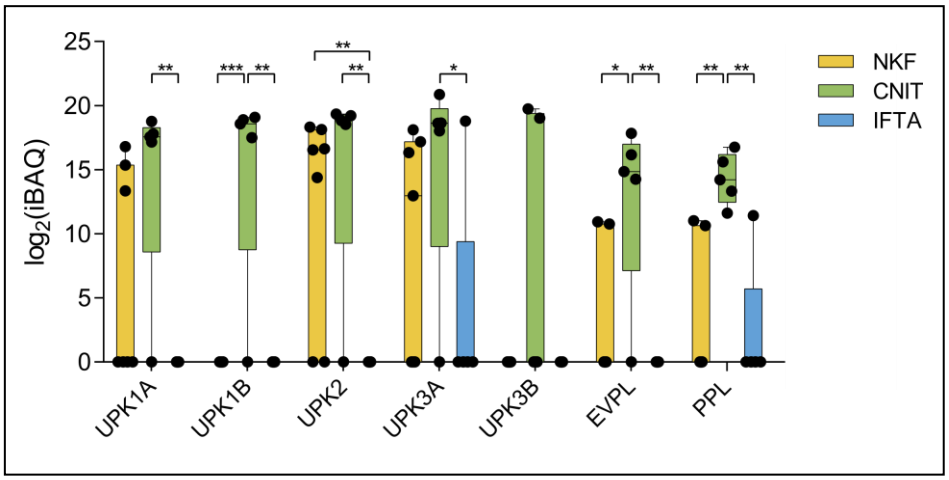

Figure 15. Expression profile of seven proteins of the uroplakin and plakin family. Whiskers represent minimum to maximum, the line in the middle represents the mean.

2 PART II: URINARY VITRONECTIN IDENTIFIES PATIENTS WITH HIGH LEVELS OF FIBROSIS IN KIDNEY GRAFTS

The text in this section has been accepted for publication in:

Carreras-Planella L, Cucchiari D, Cañas L, Juega J, Franquesa M, Bonet J, Revuelta I, Diekmann F, Taco O, Lauzurica R, Borràs FE. *Urinary Vitronectin identifies patients with high levels of fibrosis in kidney grafts.* **Journal of Nephrology**.

2.1 PATIENTS AND SAMPLES COLLECTION

Two cohorts of patients (n=23 and n=41) participated in this study, as detailed in the Methods section. The patients were classified into 4 groups according to the biopsy result and analytical parameters: normal kidney function (NKF), interstitial fibrosis and tubular atrophy (IFTA), acute cellular rejection (ACR) and calcineurin inhibitors toxicity (CNIT). Clinical data from the two cohorts included in the study are summarized in Annex table 10 and Annex table 11. As expected, serum creatinine levels and proteinuria were higher or significantly higher in pathologic groups compared to the NKF group. The histopathological results annotated using the Banff scoring system are shown in Annex table 1 and Annex table 12. In six cases in the verification cohort, a detailed Banff scoring could not be carried out because of insufficient material, but a diagnosis could be established. Figure 10 shows histological images of transplanted kidneys representative of each group.

2.2 CHARACTERIZATION OF UEV-ENRICHED FRACTIONS PROTEOME

Urinary EV-enriched fractions were analyzed by their proteomic content. In the discovery phase, a total of 1,121 proteins were identified among all samples. After strict filtering of these sequences, up to 777 proteins were confidently identified, including EV-specific proteins such as ezrin, CD9 and CD81 tetraspanins and the Annexin and 14-3-3 families in almost all samples. FunRich analysis reported that the most enriched Gene Ontology - Cellular Component (GOCC) was "Exosomes", followed by "Extracellular", "Extracellular region" and "Lysosome", all with a *p*-value<0.001 (Figure 16a). ACR and CNIT presented a significantly higher number of proteins than the NKF group (Figure 16b). There were 15 proteins shared by all the 23 samples, which are related to "Exosomes" according to the GO-CC analysis (Table 5 and Figure 17).

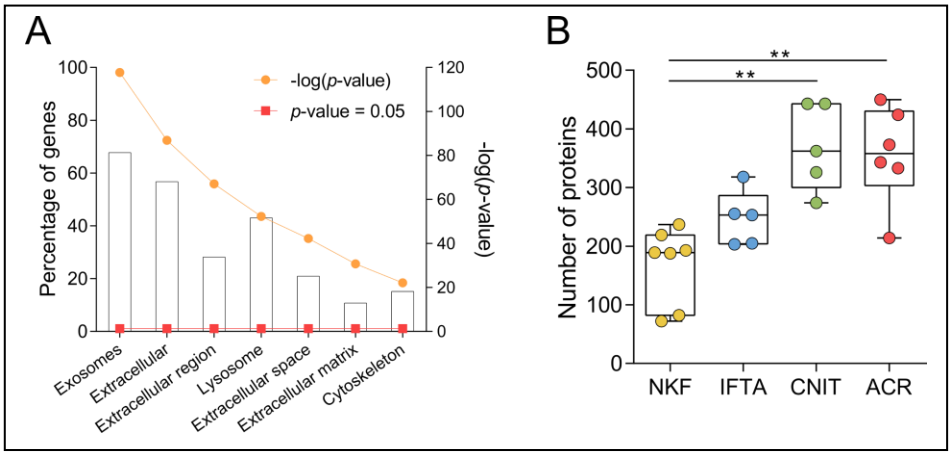

Figure 16. **(A)** Gene Ontology – Cellular Component (GOCC) analysis of proteins found in all uEV samples. Bars represent the percentage of proteins related to that GOCC in the samples. Orange circles show the -log10(*p*-value) of the enrichment, while red squares signal the significance reference *p*-value=0.05. **(B)** Number of proteins found in uEV samples of each study group. NKF, normal kidney function; IFTA, interstitial fibrosis and tubular atrophy; ACR, acute cellular rejection; CNIT, calcineurin inhibitor toxicity (** *p*<0.001).

Table 5 . List of the 15 proteins shared by all samples.

Gene names	Protein names
EZR	Ezrin
IGHG1	Ig gamma-1 chain C region
IGHG3	Ig gamma-3 chain C region
IGLL5	Immunoglobulin lambda-like polypeptide 5
IGKC	Ig kappa chain C region
UBB	Ubiquitin-60S ribosomal protein L40
CD59	CD59 glycoprotein
IGHA1	Ig alpha-1 chain C region
AMBP	Alpha-1-microglobulin
GAPDH	Glyceraldehyde-3-phosphate dehydrogenase
UMOD	Uromodulin
HSPA8	Heat shock cognate 71 kDa protein
ANPEP	Aminopeptidase N
DEFA3	Neutrophil defensin 3
PPIA	Peptidyl-prolyl cis-trans isomerase A

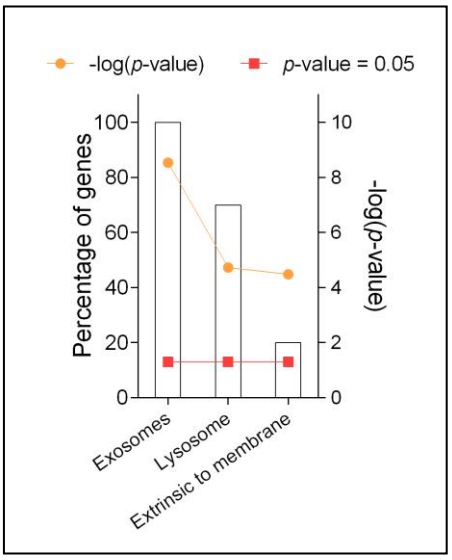

Figure 17. Gene Ontology – Cellular Component (GOCC) analysis of the 15 proteins shared by all uEV samples. Bars represent the percentage of proteins related to that GOCC in the samples. Orange circles show the -log10(*p*-value) of the enrichment, while red squares signal the significance reference *p*-value=0.05.

2.3 ALTERATIONS IN GRAFTED KIDNEYS ARE REFLECTED IN UEV PROTEOME

A volcano plot was performed to visualize differentially expressed proteins between the pathological groups and the NKF group (Figure 18a). Only proteins with *p*-value<0.01 and fold change >5 or <-5 were considered as significantly different. Seven proteins were over-expressed in the NKF group, while a total of 48 proteins were over-expressed in the pathological group. These included cathepsin D (CTSD), retinol binding protein 4 (RBP4), antithrombin (SERPINC1, previously known as antithrombin III), vitronectin (VTN) and cystatin-C (CST3) (the full list of differentially expressed proteins is shown in Annex table 13). Then, a principal component analysis (PCA) was performed to reveal clustering of samples according to their proteomic profile (Figure 18b). Most NKF samples (5 out of 7) were clearly segregated from the rest of the samples. Interestingly, most IFTA samples (4 out of 5) were also segregated from ACR and CNIT, which constituted the third cluster. Protein expression data, statistical analyses and other protein characteristics (see section "4.2.1 Selection criteria of candidate proteins for the validation phase" in Materials and methods) were used to select the 23 candidate proteins for the verification phase. The expression of each protein is shown in Figure 19.

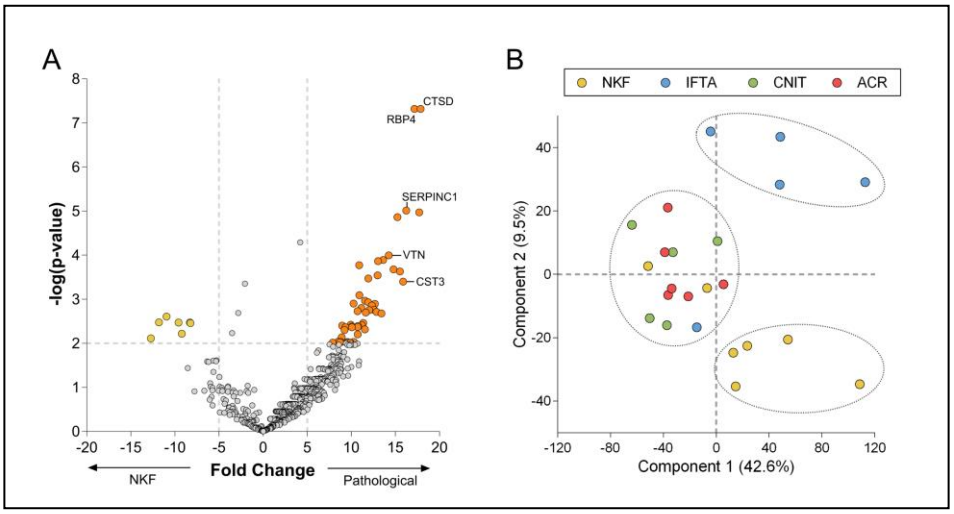

Figure 18. Differentially expressed proteins between pathological and NKF groups. **(A)** Volcano plot showing proteins significantly more expressed in pathological (IFTA, ACR and CNIT; to the right) or in NKF (to the left) groups. Each dot represents a protein. Y-axis represents –log(*p*-value), where significant *p*-value=0.01 is indicated by a horizontal dashed grey line. Significant proteins with a fold change >5 or <-5 (indicated by vertical dashed grey lines on the x-axis) are shown with bigger darker circles. The proteins investigated later on are labelled with their gene name. **(B)** Principal component analysis (PCA) that shows the distribution of samples according to Components 1 (which explains 42.6% of the variability among samples, x-axis) and 2 (which explains 9.5% of the variability among samples, y-axis). Samples were coloured according to their group. Dashed lines circle samples clustering. CTSD, Cathepsin D; RBP4, retinol binding protein 4; VTN, vitronectin; CST3, cystatin C; SERPINC1, antithrombin.

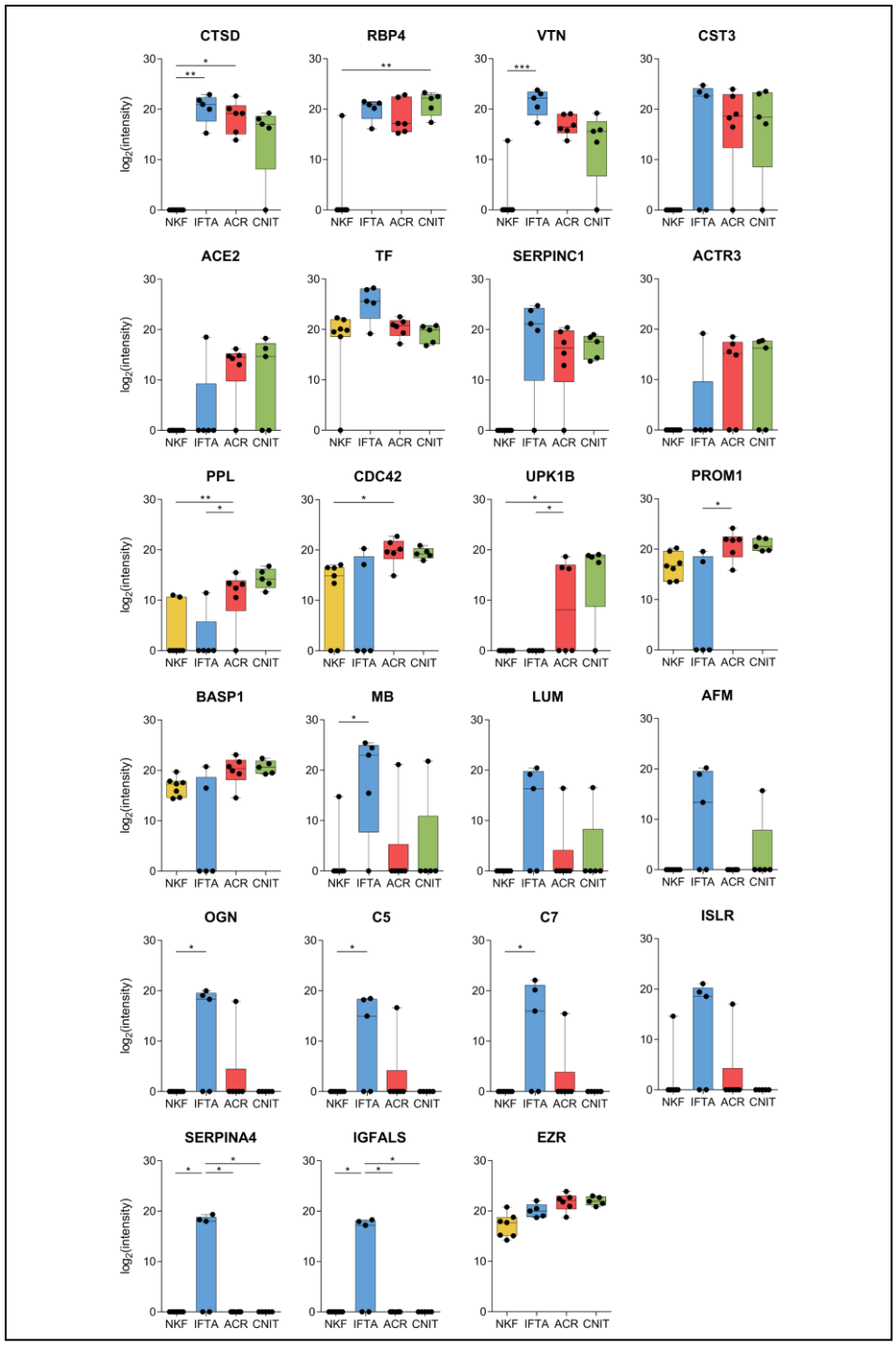

Figure 19. Intensity of the 23 selected proteins from the discovery phase. Ezrin expression before normalization is shown. Box plots show the mean and minimum to maximum (*, p<0.05; **, p<0.01; ***, p<0.001).

2.4 GENE SET ENRICHMENT ANALYSIS IN IFTA

Given the results of the PCA, we further focused on the differences between NKF and IFTA groups. According to GSEA results, 46 gene sets were significantly enriched (nominal *p*-value<0.01) in IFTA group and 26 gene sets in the NKF group (Figure 20a). The most enriched Biological Process term according to Gene Ontology in IFTA compared to NKF was Regulation of protein activation cascade (Figure 20b). This gene set is composed of 35 genes, 22 of which were found in IFTA samples. Importantly, the three most expressed genes of this gene set were vitronectin (VTN), fibrinogen alpha chain (FGA) and SERPINC1 and other proteins related to the Complement system (Figure 20c). A volcano plot was also performed to visualize the proteins with significantly different expression between NKF and IFTA groups, where CTSD and RBP4 were amongst the significantly different proteins, as well as VTN and SERPINC1 (Figure 20d).

A

Gene ontology – Biological process term	NES	FDR q-val
Regulation of protein activation cascade	1.783	0.093
Negative regulation of response to wounding	1.749	0.082
Negative regulation of coagulation	1.737	0.068
Regulation of response to wounding	1.730	0.058
Regulation of protein maturation	1.730	0.047
Regulation of coagulation	1.718	0.046
Regulation of wound healing	1.704	0.050
Negative regulation of wound healing	1.690	0.054
Positive regulation of response to wounding	1.678	0.059
Regulation of inflammatory response	1.676	0.055

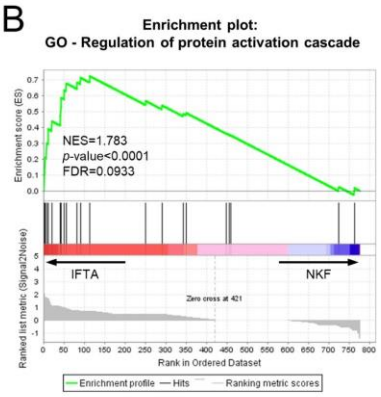

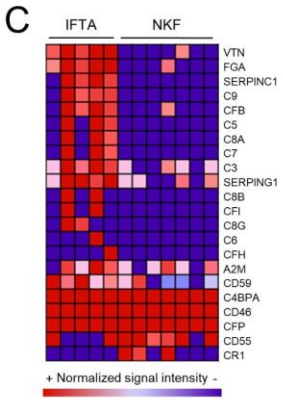

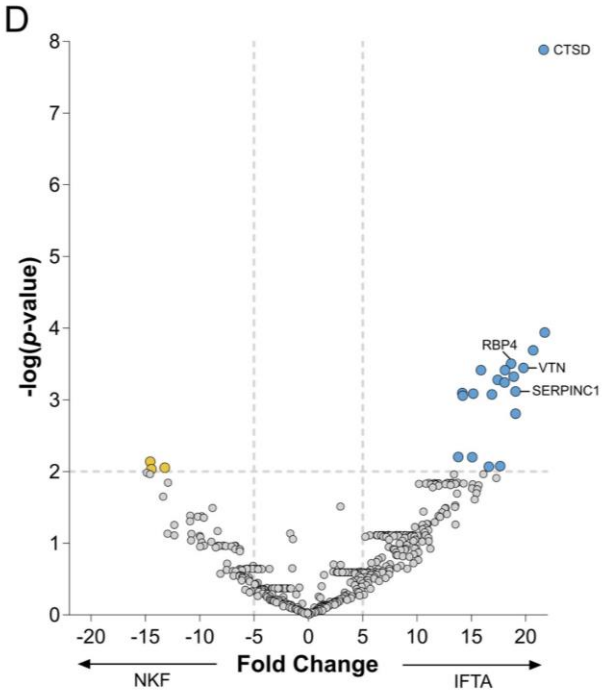

Figure 20. The uEV proteome shows significant differences between IFTA and NKF. **(A-B)** The differences between IFTA and NKF were investigated using the Gene Set Enrichment Analysis (GSEA) software, under the conception that each gene corresponds to a protein. **(A)** List of the ten most enriched Gene Ontology – Biological Process (GO-BP) gene set in IFTA compared to NKF group. **(B)** GSEA Enrichment plot of the GO-BP "Regulation of protein activation cascade". Shown on the x-axis is the rank order of the IFTA genes from the most upregulated (position 1) to the most down-regulated (position 777) compared to NKF. The "barcode" indicates the position of the genes of the mentioned gene set in this rank. The y-axis shows the enrichment score (ES) which is higher when genes found in that pathway are upregulated in IFTA. NES, normalized enrichment score. **(C)** Heat map of the expression of proteins of the GO-BP "Regulation of protein activation cascade" in IFTA and NKF uEV. **(D)** Volcano plot showing proteins significantly more expressed in IFTA (to the right) and NKF (to the left) uEV samples by targeted mass-spectrometry. The proteins investigated later on are labelled with their gene name. CTSD, Cathepsin D; RBP4, retinol binding protein 4; VTN, vitronectin; SERPINC1, antithrombin.

2.5 DIFFERENTIALLY EXPRESSED PROTEINS IN PATHOLOGICAL GROUPS

In a second cohort of patients, twenty-three proteins selected as candidates for verification were analyzed by targeted proteomics. From a total of 41 samples of the second cohort, four samples were discarded from the analysis either because of technical error or lack of peptide signal detection in the targeted proteomics analysis (final n=37). Only peptides that were detected in at least 90% of the samples were considered, resulting in 15 proteins. From these, in 5 cases the mean of the two peptides was used (mean±sd Pearson R correlation score was 91.2±0.1). Up to five proteins that showed a higher expression in pathological samples compared to NKF samples in the discovery phase were confirmed by targeted proteomics: CTSD, RBP4, VTN, CST3 and SERPINC1. When analyzing the results in each particular pathological condition,

ACR samples showed statistically significant differences with the NKF group for the expression of CTSD, RBP4 and SERPINC1. The IFTA and CNIT groups did not show significant differences either with the NKF group or the other pathological groups. Uroplakin-1B (UPK1B) and periplakin (PPL) were among the selected proteins for the verification phase because they showed a significantly higher expression in the CNIT group. Nevertheless, UPK1B concentration in uEV did now show differences between groups and PPL had to be excluded from the analysis because it was only present in 51.3% of the samples (the exclusion cut-off was 90%) (Figure 21).

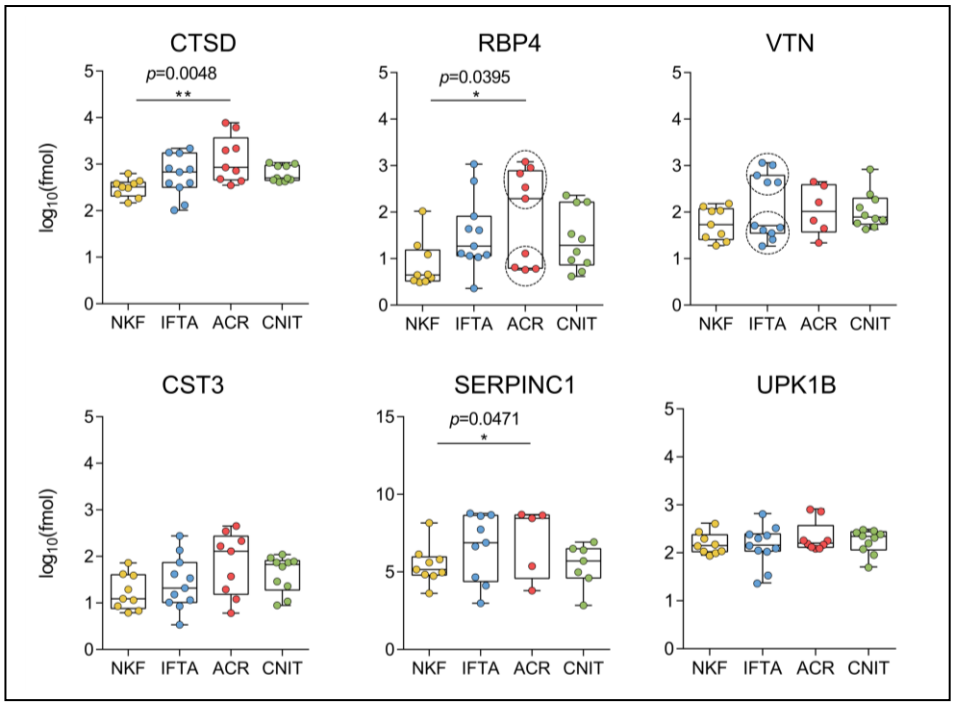

Figure 21. Protein expression in uEV of each group of the verification cohort. Protein levels were measured by targeted mass-spectrometry. In RBP4 and VTN, dashed circles were used to highlight the binomial distribution of individual samples in ACR and IFTA, respectively. Boxplots show the mean of each group and whiskers show minimum to maximum. CTSD, Cathepsin D; RBP4, retinol binding protein 4; VTN, vitronectin; CST3, cystatin C; SERPINC1, antithrombin; UPK1B, uroplakin-1B.

2.6 VITRONECTIN IS SIGNIFICANTLY MORE EXPRESSED IN HIGH GRADE FIBROSIS SAMPLES

When looking closely at the expression of each protein, RBP4 in the ACR group and vitronectin in the IFTA group showed a bimodal distribution of the samples (Hartigan's dip test for unimodality *p*-value = 0.009 and 0.016, respectively). To deepen in these observations, we further analyzed 15 additional parameters of these samples, such as the origin of the organ (living or deceased donor), time from transplantation to collection of the sample, serum creatinine at the collection of the sample, graft failure or induction drugs, among others. While no significant differences could be found between the two subgroups of ACR samples regarding the expression of RBP4, we observed that samples with the highest expression of vitronectin in the IFTA group were those that presented the highest level of chronic interstitial lesions and chronic tubular lesions (ci ct) in the histopathological results. Interestingly, the expression of vitronectin was significantly higher in patients showing a ci ct score > 2 or above, regardless of the pathological group of the sample (Figure 22a). A receiver operating characteristics (ROC) curve to discriminate patients with ci ct score of ≤ 2 from > 2 presented an area under the curve (AUC) of 0.96 (Figure 22b).

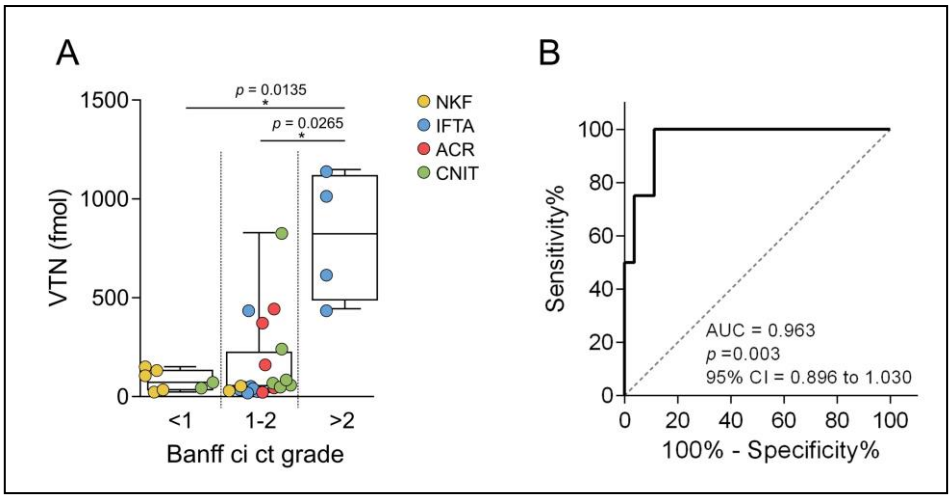

Figure 22. Vitronectin expression differences in uEV measured by targeted MS regarding kidney fibrosis grade. **(A)** Vitronectin expression in uEV by targeted MS regarding the Banff criteria of chronic interstitial and tubular lesions (ci ct) grade. The colour code indicates sample group. Boxplots show the mean of each group and whiskers show minimum to maximum. **(B)** ROC curve based on targeted proteomics levels of vitronectin as a stand-alone biomarker to differentiate Banff ci ct grades ≤ 2 (n=27) from > 2 (n=4). AUC, area under the curve; CI, confidence interval.

3 PART III: VALIDATION WITH ANTIBODY-BASED TECHNIQUES

3.1 EVALUATION OF PROTEIN BIOMARKERS OF RENAL ALTERATIONS BY WB

Since a diagnosis based on mass-spectrometry for the detection of biomarkers would not be suitable for the clinics, we evaluated western blot as a validation technique for differentially expressed proteins. One of the advantages offered by this technique is the possibility of hybridizing one membrane containing different samples with several antibodies, thus allowing the identification of pathology-associated profiles. However, a limitation inherent to SEC-isolated uEV samples is the low quantity of recovered protein. Thus, the maximum amount available was used in each case (typically between 3 and 20 µm). Initially, up to twenty proteins were selected from the discovery phase to be evaluated by western blot including some EV markers such as ezrin, LGALS3BP and TSG101. Ezrin and TSG101 were detected in most uEV samples and were used as positive controls and to normalize the intensity of each evaluated protein. In contrast, a common control protein such as GAPDH could not be detected in several samples. Mesenchymal stem/stromal cells lysates (used as positive control of the technique) were positive for ezrin and GAPDH but were negative for LGALS3BP and TSG101 (Figure 23). LGALS3BP showed a single band (at 115 kDa) or a double band (at 85 and 115 kDa) in some of the samples. The lowest quantity of uEV at which ezrin could be detected was approximately 1 µg/well, although the actual quantity was highly variable among samples. Usually, the expression of other proteins required higher quantities of loaded protein. Despite these limitations, we set up a series of WB analysis with the aim to validate the proteomic results.

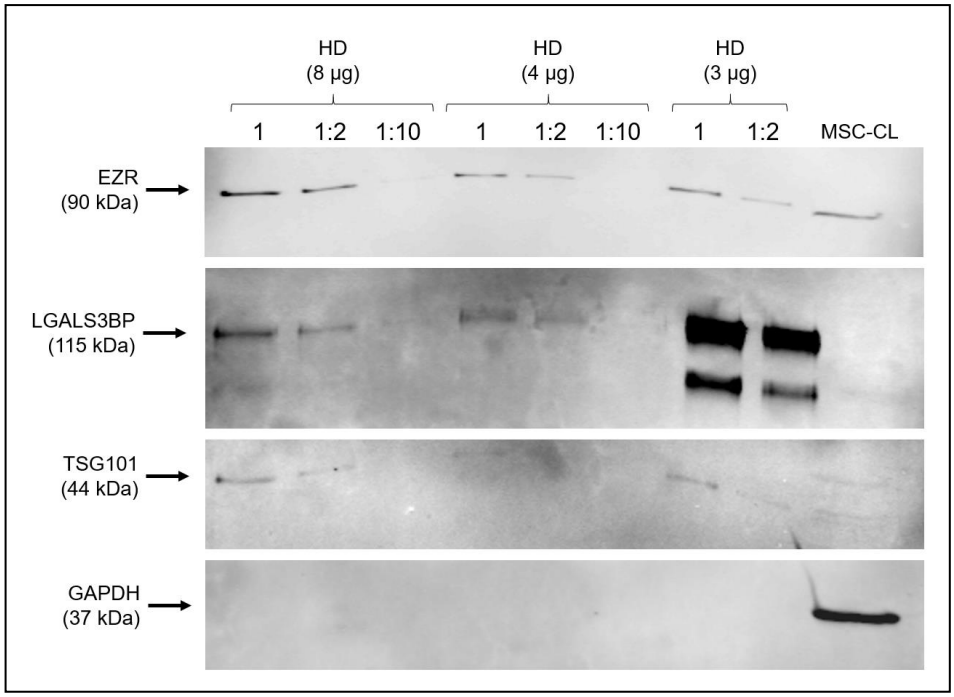

Figure 23. Western blot membrane showing ezrin, LGALS3BP, TSG101 and GAPDH expression in uEV samples at decreasing dilutions and MSC-CL (mesenchymal stem/stromal cells cell lysate, control.

From the 17 proteins that showed significantly different expression between pathologies in the discovery phase of the proteomic analysis, only 3 (DSTN, RBP4 and CTSD) could be found in some uEV samples (Figure 24). Moreover, proteins were often non-detected in samples from pathological groups where they were expected (e.g. compare three IFTA samples in Figure 24a). Although the mean expression of these proteins was higher in pathological groups compared to NKF, the differences were not significant (Figure 25). Given all these inconsistencies, we finally decided not to deepen in validating the proteomic results using WB.

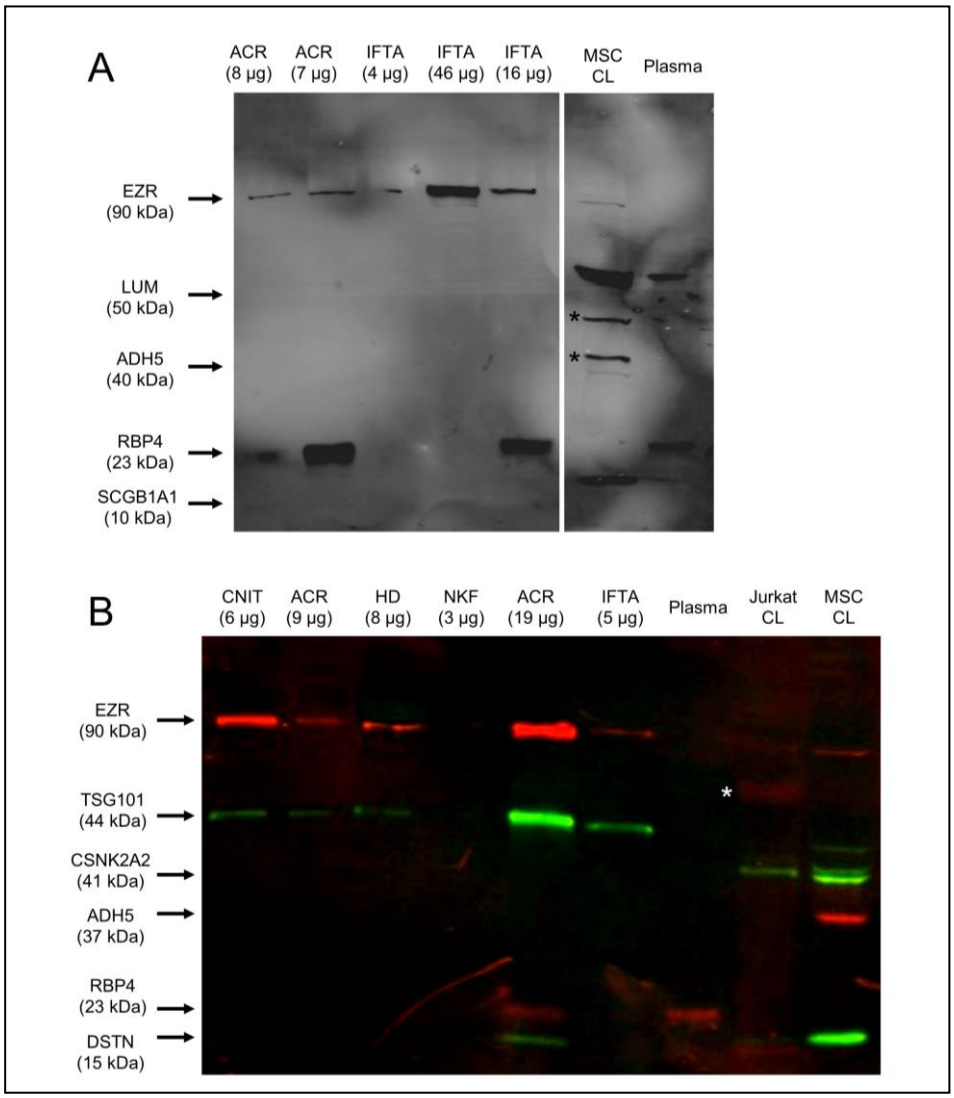

Figure 24. Representative western blot membranes showing the expression of different proteins in various samples. Membranes were hybridized 5 **(A)** and 4 **(B)** times. Cell lysates and plasma were used as positive controls. Asterisks (*) indicate unspecificaly hybridized bands. EZR, ezrin; LUM, lumican; ADH5, alcohol dehydrogenase 5; RBP4, retinol binding protein 4; SCGB1A1, uteroglobin; TSG101, tumour susceptibility gene; CSNK2A2, casein kinase 2 alpha 2; DSTN, destrin; HD, healthy donor; CL, cell lysate.

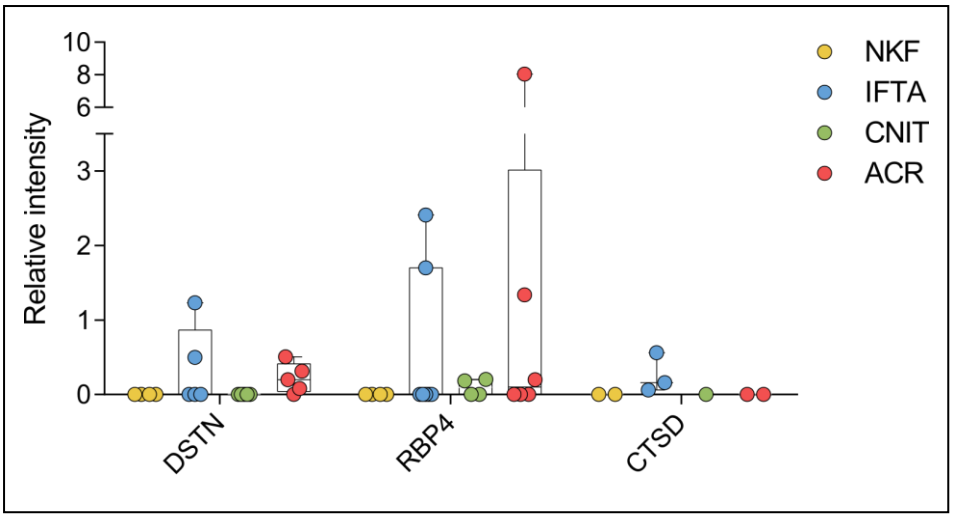

Figure 25. Relative intensity of the proteins destrin (DSTN), retinol binding protein 4 (RBP4) and Cathepsin D (CTSD). Box plots demonstrate the mean and minimum to maximum. No statistically significant differences were found (2 way-ANOVA with Tukey's multiple comparisons test).

3.2 VALIDATION OF VITRONECTIN AS BIOMARKER OF FIBROSIS WITH ELISA

Having observed the difficult to define pathological protein profiles by WB, we moved to more sensitive techniques and focused on specific proteins. Vitronectin attracted our attention because of the bimodal distribution found in patients and its apparent relation with the fibrosis grade. Thus, the results related to vitronectin were further validated first with a preliminary ELISA. First, urine samples from a limited number of kidney-transplanted patients with different grades of fibrosis were used in order to optimize the sample processing and ELISA protocol. a) Whole urine, b) urine concentrated through a 100 kDa cut-off filter unit, c) urine concentrated through a 50 kDa cut-off filter unit, d) uEV isolated by SEC or e) uEV isolated with ExoGAG method were

tested. The method that rendered the best results (i.e. measurable concentration of vitronectin and patients with higher ci ct score showing significantly higher concentration) was c) urine concentrated through a 50 kDa cut-off filter to concentrate urine the sample 10 times (data not shown). The two samples with ci ct score of 0, presented a negligible vitronectin concentration (Figure 26a). Similarly to the targeted proteomics results, a ROC curve of the ELISA results showed an AUC of 0.87 (Figure 26b).

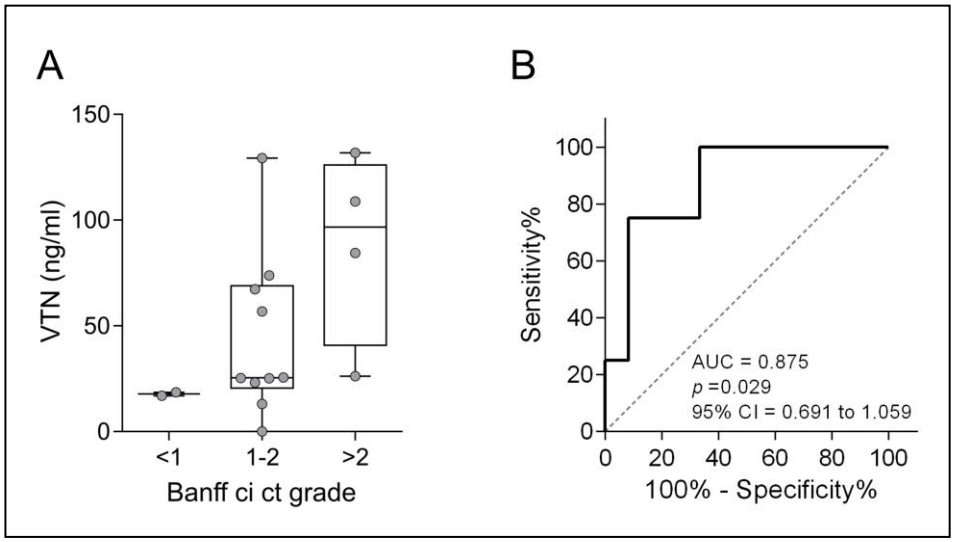

Figure 26. Vitronectin levels in concentrated urine measured by ELISA regarding kidney fibrosis grade. **(A)** Vitronectin concentration in urine was measured by ELISA and the values were stratified regarding the Banff criteria of chronic interstitial and tubular lesions (ci ct) grade. Boxplots show the mean of each group and whiskers show minimum to maximum. **(B)** ROC curve based on ELISA of vitronectin as a stand-alone biomarker to differentiate Banff ci ct grades ≤ 2 (n=12) from > 2 (n=4). AUC, area under the curve; CI, confidence interval.

DISCUSSION

> *Si la gente pensara una cuarta parte de lo que habla, este mundo sería un paraíso.*

— Carlos Ruiz Zafón, Marina

1 PART I: PROTEOMIC CHARACTERIZATION OF URINARY EXTRACELLULAR VESICLES FROM KIDNEY-TRANSPLANTED PATIENTS TREATED WITH CALCINEURIN INHIBITORS

CNIT in kidney-transplantation is controversial. In this study, the uEV proteome of kidney-transplanted patients diagnosed with CNIT was analysed and compared to either kidney-transplanted patients with clinically normal kidney function or diagnosed of IFTA, all of them receiving a similar immunosuppressive regime including CNI. Expectedly, both CNIT and IFTA patients presented a significantly higher serum creatinine than NKF patients.

A first characterization of all the proteins found by MS showed that there was an enrichment of proteins related to the secretion of EV, which denotes the efficacy of uEV enrichment performed using SEC. An efficient EV purification is key to greatly diminish the interference of abundant soluble proteins (especially uromodulin) for a mass-spectrometry analysis, contributing to the detection of lower abundance proteins that may be potential biomarkers [229], [289], [290].

The PCA-based comparison of the proteomic results could clearly separate the three groups of samples, indicating that the uEV proteome has different patterns in NKF, CNIT and IFTA. Only sample DI8, which showed a low correlation coefficient with the other samples in its group, did not cluster as the other IFTA samples did. A possible explanation for this observation might be the two previous episodes of rejection that DI8 patient had suffered within 2 years before sample collection. Although these differences were not

observed in the biopsy performed at the time of urine sample collection, they do seem to be still reflected in the uEV proteome. Also interestingly, although chronic CNIT can present lesions compatible with an IFTA diagnosis at the histological level [291], sample C10 did not cluster with IFTA samples. In fact, despite being the unique CNIT sample diagnosed of a chronic CNIT instead of acute CNIT, there was no apparent segregation of C10 from the other CNIT samples in the PCA, pointing to the resemblance of the pathological process in both chronic and acute cases, at least at the uEV proteomic level. Yet, as this study has been performed on a limited number of samples, these results have to be cautiously interpreted.

Gene sets significantly overexpressed in the CNIT group included vesicle-related gene sets. Some studies described that acute CNIT can cause tubular epithelial cell cytoplasmic small vacuoles and abundant lysosomes because of dilatations of the smooth endoplasmic reticulum by aqueous fluid [177]–[179]. Moreover, it has been shown that a pathological process, like CNIT, increases the secretion activity of kidney cells [292]. Hypothetically, some of these vesicles may be released into the lumen of the proximal tubules, and then be found in urine and captured as extracellular vesicles, thus increasing the number of proteins found in the proteomic analysis in CNIT samples, as we report here.

In renal biopsies, CNIT often show features shared with IFTA lesions. Both cyclosporin-A and tacrolimus are directly responsible of the increase of TGF-β1 [154], a factor that promotes interstitial fibrosis by increasing synthesis of proteins of the extracellular matrix and decreasing their degradation [293], [294]. Moreover, TGF-β1 induces epithelium-to-mesenchymal transition at the

tubular level leading to fibrosis by the generation of myofibroblasts [295], [296]. Also, it has been shown that CNI drugs induce apoptosis on tubular and interstitial cells *in vitro* [297], [298]. The GSEA analysis show overexpression of different gene sets in CNIT compared to IFTA as well as NKF, suggesting the activation of specific mechanisms in CNIT. Specifically, the proteome of CNIT was significantly enriched in gene sets related to epithelial cell differentiation, probably due to the death of tubular epithelial cells that forces their regeneration. Members of the uroplakin family (UPK1A, UPK1B, UPK2 and UPK3A) were also overexpressed in CNIT compared to IFTA. Uroplakins are transmembrane proteins that bind to each other to form a plaque on the surface of the urothelium, which covers the renal pelvis, ureters, urinary bladder and prostatic urethra, to prevent influx of urine from the lumen [299]. The molecular weight of uroplakins ranges from 15 to 47 kDa, what suggests their intravesicular location [300]. Periplakin and envoplakin, two other members of the plakin family that function as cell-linker proteins, were also found enriched in CNIT [301]. These two proteins present a larger molecular weight of around 200 kDa and would possibly elute in the uEV-enriched fractions of SEC as free proteins instead of being carried by uEV [302], [303]. Salih et *al.* described that patients in advanced stages of autosomal dominant polycystic kidney disease (ADPKD) presented increased levels of periplakin and envoplakin in their uEV [304]. In our study, only one patient in the CNIT group (C11) was diagnosed with ADPKD, but all the other CNIT samples also presented high levels of periplakin and envoplakin. The higher abundance of plakins in CNIT uEV suggests that the toxic effect of CNI on the urothelium may increase citolinker proteins' activity and this would be reflected in a higher

presence in their uEV. Therefore, plakin family members could represent promising biomarkers for CNIT in uEV.

Conversely, the CNIT uEV proteome did not reflect genes related to protein activation cascade and humoral response as well as other inflammatory processes when compared to IFTA. The reason could be that patients in the CNIT group had higher serum levels of CNI [265] which could be responsible for an increased capacity of suppressing the inflammatory response.

Only a few studies using proteomic approaches have defined the effect of CNIT on the kidney. Sidgel et *al.* [305] investigated the urinary proteome of kidney-transplanted paediatric patients with different pathologies including CNIT. They found a panel of ten proteins that potentially differentiated CNIT from chronic allograft nephropathy, although none of them coincided with our results, most probably because of the differences between whole urine and uEV. Other groups studied the effect of CNI on renal cell lines *in vitro* [306], [307]. They found that CNIT caused an increase in endoplasmic reticulum stress, mitochondrial apoptosis and involvement of the phosphatidylinositol 3-kinases (PI3K), metalloproteinases (MMP), protein kinase C (PKC) and glycogen synthase kinase 3 (GSK3) pathways. To our best knowledge, our study is the first analysis of the effect of CNIT on kidney-transplanted patients on uEV proteome.

There is a lack of knowledge on how CNIT develops in renal transplanted patients despite the wide use of CNI and their contribution to kidney graft loss. Thus, a better knowledge of the effect of CNI at the renal level is of utmost importance for the detection and management in patients undertaking

kidney transplantation. Although no conclusive biomarkers can be asserted from this single pilot study, we found a higher expression of proteins from the plakin family in CNIT group, which may be envisaged as promising biomarkers and merit future investigation. This work adds further evidence to the potential of uEV as a source of non-invasive protein biomarkers for the better detection and monitoring of this renal alteration in kidney-transplanted patients.

2 PART II: URINARY VITRONECTIN IDENTIFIES PATIENTS WITH HIGH LEVELS OF FIBROSIS IN KIDNEY GRAFTS

Accurate and early diagnosis of potential alterations in renal-transplanted patients is fundamental to improve both graft and patients' survival. The current diagnostic method to determine the nature of the pathology is renal biopsy. This method is highly invasive, it cannot be performed frequently and it only analyses a small random portion of the kidney, what along with a rather subjective evaluation leads to around 20% of misdiagnosis.[185], [191] Knowing the potential of EV in the field of biomarker discovery and especially urinary EV for kidney-related pathologies,[228], [263], [308] we searched for protein biomarkers of kidney graft alterations in transplant recipients with four different diagnoses. Using a bottom-up proteomics approach in two independent cohorts, we found some EV-associated proteins differently expressed in patients with pathological kidneys compared to NKF patients. Moreover, we discovered vitronectin as a potential biomarker of kidney fibrosis.

Extracellular vesicles shuttle their bioactive cargo between cells and have a key role in many pathophysiological processes.[122], [209] Their paramount role in kidney transplantation rejection has been described in antibody mediated rejection [309] and ischemia-reperfusion injury.[310] Furthermore, some studies envisage the use of EV derived from mesenchymal stem/stromal cells (MSC) in the kidney transplant rejection setting, and report that they could inhibit tubular cell apoptosis and interstitial fibrosis, and promote proliferation of progenitor cells.[311]–[314]

Focusing on the potential of EV as biomarkers, in our study up to 777 proteins were confidently identified, which were significantly related to exosomes and extracellular-related terms. Interestingly, the NKF group had a lower number of identified proteins. In addition, we found several proteins differentially expressed in the uEV from pathological samples compared to NKF. This suggests that pathological changes occurring in the kidney are reflected in the proteomic content of uEV.[228], [263]

At the beginning of the study, patients of the two cohorts were classified exclusively based on histopathological diagnosis and clinical criteria into NKF, IFTA, ACR and CNIT groups. Although distinctive diagnosis for CNIT or IFTA is controversial, the PCA analyses of proteomic data clearly segregated IFTA from CNIT samples, pointing to a different proteomic pattern between these two entities. One of the most interesting proteins identified in our study was vitronectin, which was significantly more expressed in patients with a high degree of kidney fibrosis – determined by ci ct Banff score – in the verification phase. Vitronectin is a protein with multiple roles found in the serum and in the extracellular matrix. In the lower urinary tract, vitronectin can originate from plasma extravasation and from synthesis by the urothelium,[315] but it is difficult to determine the precedence of the uEV-related vitronectin we found in our samples. One of the functions of vitronectin is to inhibit the terminal complement pathway and the membrane attach complex (MAC).[316] Vitronectin is found in sclerotic glomerulus in immune deposits containing C5b-9,[317] and one study suggests the it plays a protective in the glomeruli in membranous nephropathy.[318] Conversely, it binds with high affinity to plasminogen activator inhibitor-1 (PAI-1), a potent profibrotic glycoprotein

and their binding plays a key role in fibrosis in several tissues, although the exact mechanisms are controversial. In the kidney, it has been described to increase PAI-1 activity and hamper fibrinolysis leading to an aggravation of renal failure.[319] Moreover, in the event of vascular injury, PAI-1 and vitronectin promote neointima formation after vascular injury.[320] Contrarily, in another study with a mouse cardiac fibrosis model the results showed that binding of vitronectin with PAI-1 could be protective against fibrosis.[316] Other studies also support that vitronectin inhibits fibrogenesis by interacting with PAI-1,[321], [322] while others state that it has no effect.[323], [324] In either case, vitronectin promises to be not only an interesting diagnosis biomarker but also a therapeutic target for kidney fibrosis that merits further investigation.

Vitronectin also participates in blood coagulation by interacting with SERPINC1.[325] Both proteins were found more expressed in pathological samples and the GO term "Regulation of protein activation cascade", which includes 49 proteins more found in our samples, was also enriched in pathological groups. Conversely to that observed with vitronectin, we did not find a direct association between SERPINC1 and high level of fibrosis.

Changes in the levels of urinary vitronectin have been reported before. In a study by Takahashi et *al.*,[326] vitronectin was investigated by ELISA in the urine of paediatric kidney patients. The protein was significantly increased when mesangial sclerosis changes were occurring. Also, in a murine model, kidney vitronectin mRNA and protein expression was higher in mice with chronic kidney disease than controls,[323] yet the same authors also found

that vitronectin did not have an implication in fibrogenesis in a Vtn knock-out mice model.

With regard to the fibrotic level of kidneys, Mohammed-Ali Zahraa et *al.* [327] recently reported six angiotensin II-related proteins that were increased in patients diagnosed with mild fibrosis compared with absence of fibrosis. However, they could not distinguish between moderate or severe fibrosis. Noticeably, moderate to severe fibrosis has been associated to poorer prognosis regarding renal functional and graft survival,[137], [140]–[147], [168] therefore stressing the importance of a biomarker for such stages. While our results showed that vitronectin values in targeted proteomics clearly discriminate between low (< 1) and severe (> 2) levels of fibrosis, we also detected some overlapping in the expression of vitronectin between patients with low-moderate (1-2) and severe (> 2) grade of fibrosis. This overlapping may be due to several reasons, including a possible misclassification of the samples due to the sampling and the evaluation of the renal biopsy – which is estimated to be around 20%.[185], [191] Of note, 20% (4 out of 20) samples in the low-moderate fibrosis group (1-2) were those contributing to higher deviation. Although vitronectin was among the significant proteins found in the discovery phase, none of the patients in this phase presented degree 3 of fibrosis, and therefore a limitation of the study may be that the relation of vitronectin with degree 3 of fibrosis could only be observed in the second phase. Yet, as targeted mass spectrometry is still far from being applicable to the clinical setting, we also investigated whether our results were similar in a conventional ELISA, a cost-efficient, fast, simple and sensitive method for the detection of proteins. In a pilot study, with a still limited number of patients,

ELISA revealed similar results to targeted proteomics data, thus validating the observation and confirming the translationality of the assay. Since the number of samples is still limited, further validation analyses on bigger cohorts of patients with different degrees of fibrosis will be performed to fully confirm these observations.

In urine, protein concentration variation caused by differences in water intake and renal function represents an additional challenge for the search of biomarkers. Several studies about urinary protein biomarker opted for the normalization by urinary creatinine [255], [326]. Yet, creatinine excretion suffers large individuals variations and is affected by renal pathologies [328], [329]. Moreover, the uEV secretion rate in relation to urine production is still unknown, so in this study vitronectin concentration was not normalized to creatinine.

Moreover, another limitation of our study was that most of the biopsies were performed before the newest Banff classification introduced the i-IFTA item.[112] Inflammation within areas of fibrosis is associated with cellular rejection, either acute or chronic, and worse outcomes (DeKAF cohort study).[330] In the future, it would be interesting to analyze if inflammation within areas of fibrosis has any effect on urinary proteomics.

For what we think is the first time, we report vitronectin as a potential non-invasive biomarker of severe kidney fibrosis in kidney-transplanted patients. When further validated in a larger cohort of patients, this observation may allow 1) a more frequent monitoring of kidney transplanted patients, 2) sparing kidney biopsies and its associated complications, 3) an earlier

diagnosis and 4) the possibility to apply the optimal treatment to regulate the progression of fibrosis. In this sense, severe fibrosis can only be slowed down and is still not reversible. However, anti-fibrotic therapies are under the spotlight of researchers, with currently more than 20 clinical studies on anti-fibrotic interventions in kidney (reviewed in [137]). All these would directly impact graft and patients' survival, as well as improving their quality of life.

3 GLOBAL DISCUSSION

Our study followed the commonly used bottom-up pipeline for protein biomarker search and was structured in three phases: discovery phase, verification phase and validation phase. In agreement with other studies [331]–[333], results of the discovery phase showed different uEV proteome patterns in each group. Encouraged by these findings, we selected a list of candidate biomarker proteins for further validation and identification of pathology-associated protein patterns. As we envision the use of urinary biomarkers in the clinical laboratory, a cost- and time-effective method such as antibody-based techniques was considered.

In a study by Wang et *al.*, they identified proteins that were upregulated in prostate cancer patients compared to controls with high specificity using shotgun MS. However, several of the promising biomarkers could not be validated later using ELISA or WB due to excessively low quantity in uEV and/or lack of proper antibodies [331], [334]. In fact, literature is full of studies searching for biomarkers of renal alterations which demonstrate that changes happening in the kidney are reflected in the urinary proteome. However, only a few report having validated those results, denoting the complexity of this step [199].

Thus, we first decided to evaluate uEV samples of kidney-transplanted patients using WB. Several EV markers (TSG101, GAPDH and ezrin) could be detected in the samples, demonstrating the presence of uEV [209], [335]. Nevertheless, most of the above mentioned target proteins were not detected in any of the samples or, in other cases, they did not appear when expected. There may be

several reasons that explain those results. First, the quantity of target protein loaded into the gel may have been below the antibodies' detection threshold. Second, MS may be more sensitive for the detection of determined proteins than WB. Also, the possibility that MS analysis - a technique based on statistical probability of detecting peptides - was not reflecting the reality cannot be ruled out [334]. In addition, commercially available antibodies for WB are optimized for cell or tissue lysates samples, not for EV. In EV, the protein content is always very low (at least, if isolated by SEC [229] as in our case) and may have changed its conformation during the normal cellular packaging of EV. An additional limitation of the WB experiments was the low number of available samples, that made it not possible to optimize the sample processing or to test other antibodies.

In our study, to partially overcome this problem, we conducted a verification phase with targeted MS before focusing on an antibody-based technique for further validation and pointing to the clinical setting. Up to twenty-three proteins were evaluated in a new cohort of patients. Results of the verification phase showed that CTSD, RBP4, CTS3 and SERPINC1, among others, were consistently overexpressed in all pathological groups compared to the NKF group.

Considering that none of these proteins (CTSD, RBP4, CTS3 and SERPINC1) were specifically pointing to a given type of pathology, and together with all the limitations encountered during the validation with WB, we decided to change our focus to the particular behaviour of vitronectin, as discussed in the previous section.

Another issue concerning the development of a diagnosis test is the processing of the sample, which has to be optimized to reduce time and costs. Sometimes, antibody-based techniques are more sensitive to detect single proteins than MS techniques, so whole urine instead of uEV can be used. In a study about acute TCMR diagnosis, the proteome of uEV from kidney-transplanted patients with this alteration was compared with equivalent patients with stable kidney function. UC was used to isolate uEV for the MS analysis, but, for the validation by WB of five candidate proteins, urine was concentrated with an ultrafiltration device (after cells and debris depletion). That protocol enabled an efficient concentration of uEV that proved to be useful for antibody-based detection of some of the candidate proteins, but not for others [336]. A very similar protocol was used in this thesis for the ELISA validation of vitronectin.

Initially, vitronectin was found by MS in uEV, but later experiments demonstrated the feasibility of detecting this protein by ELISA, a technique easily applicable to the clinical setting due to its time- and cost-effectiveness. Moreover, the sample processing has been shortened from isolating uEV by SEC to just concentrating the sample to be detected by ELISA, what would also contribute to an easier translationality. The first ELISA pilot study showed that patients with high-grade of IFTA presented significantly higher urinary vitronectin expression, confirming the results of the verification phase. While still a larger number of samples needs to be tested, the results are indeed encouraging.

Besides, in the discovery phase the CNIT group showed upregulation of the gene set "epithelial development" and, particularly, of proteins from the

uroplakin and plakin families. Unfortunately, this result could not be validated or verified. In the WB experiments, anti-UPK1B and UPK3B antibodies did not show detection of their respective antigens in uEV (the possible causes are stated above). In the verification phase, the proteins that adjusted to the selection criteria for targeted proteomics were uroplakin-1B and periplakin, and finally only uroplakin-1B could be analysed (the expression of periplakin among samples was too low to be evaluated). However, the expression of uroplakin-1B was not significantly different between groups. Further experiments testing other proteins should be conducted to state solid conclusions.

A short mention should be made in this discussion to a specific category of patients that was firstly included in the study. Patients were classified in four groups according to their histopathological diagnosis and clinical parameters. Three of the groups presented pathological renal alterations (IFTA, CNIT and ACR), while NKFs served as control group. Not surprisingly, previous proteomics studies about ACR in renal transplantation showed a higher regulation of inflammatory urinary proteins compared to chronic renal processes [199]. In the verification phase of our study, a significantly higher expression of several proteins was found in the ACR group, despite some intragroup heterogeneity observed. These results suggest that ACR also present a singular uEV proteome pattern. Anyhow, in the current clinical scenario ACR is successfully handled in most cases using available diagnostic tools and treatment. Thus, we decided to focus on IFTA and CNIT for a better characterization and definition of biomarkers able to segregate both pathological situations.

In summary, with this work we have shown 1) that the uEV proteome changes accordingly to specific renal alterations in kidney-transplanted patients; 2) that some proteins, if further validated, could become biomarkers of CNIT; 3) and found a potential biomarker of severe kidney fibrosis for kidney-transplanted patients that can be measured non-invasively and repeatedly.

The results of this study led to the application of a European patent (currently under second revision in the European Patent Office). In this line, the next steps in this project will be to perform further validation analyses in order to:

- Determine a threshold in the assay that enables an objective and precise diagnosis of fibrosis grade.

- Optimize sample processing (for example, to determine the effect of freezing/thawing the sample, optimal sample volume).

- Optimize ELISA antibodies and kits.

- Determine the effect of other concomitant pathologies and the feasibility of application for CKD non-transplanted patients.

Overall, we are confident that vitronectin will represent a novel and precise biomarker kidney fibrosis. Since chronic graft rejection in kidney transplantation is the main cause of graft failure, the inclusion of this test into the clinics, along with new developments in the control of fibrotic lesions, would contribute largely to the improvement of patients' quality of life and survival.

CONCLUSIONS

It seems to me that the natural world is the greatest source of excitement; the greatest source of visual beauty; the greatest source of intellectual interest. It is the greatest source of so much in life that makes life worth living.

— David Attenborough, naturalist and broadcaster

CONCLUSIONS

1. The analyses of the uEV proteome from kidney-transplanted patients shows changes that may be specifically related to the ongoing alteration. Among other observations, we stated that:

    1.1. The uEV proteome from patients diagnosed with CNIT shows overexpression of proteins related to epithelium development.

    1.2. Up to 48 proteins were found to be significantly overexpressed in samples from transplanted patients affected of a pathological alteration in the graft.

2. CTSD, RBP4, CST3, SERPINC1 and VTN are significantly overexpressed in pathological groups compared to NKF patients, as verified in a new cohort. Focussing in specific pathological situations we may conclude that:

    2.1. From the twenty-three selected proteins for the verification phase, only CTSD, RBP4, CST3, SERPINC1 and VTN showed an expression consistent with the results from the discovery phase, as they were significantly overexpressed in pathological groups as a whole when compared to NKF patients.

    2.2. Uroplakin-1B could not be verified by targeted proteomics as a marker of CNIT. Other members of the uroplakin and plakin families still need further verification.

    2.3. VTN presents a higher expression in transplanted patients with high degree of kidney fibrosis.

3. This higher expression of vitronectin in kidney-transplanted patients affected of high degree of fibrosis can also be observed by ELISA. This fact opens the possibility of monitoring these patients in a non-invasive, cost- and time-effective manner.

ANNEXES

Annex table 1. Banff scoring of kidney biopsies from the discovery cohort.

Group	Sample	i	t	v	g	ah	ci	ct	cv	cg	mm	ptc	ti
IFTA	DI8	0	0	0	0	0	1	1	1	0	0	0	2
	DI9	0	0	0	0	3	1	1	1	0	0	0	1
	DI10	0	0	0	1	1	1	1	0	0	1	0	1
	DI11	0	0	0	0	3	2	2	3	0	1	0	1
	DI12	0	0	0	0	3	2	2	1	0	1	0	1
CNIT	DC13	0	0	0	0	0	0	0	2	0	0	0	1
	DC14	0	0	0	0	0	1	1	0	0	0	0	1
	DC15	0	0	0	0	3	2	2	1	0	0	0	3
	DC16	0	0	0	0	0	1	1	1	0	1	0	0
	DC17	0	0	0	0	0	0	0	1	0	0	0	0
ACR	DA18	0	0	0	0	3	2	2	3	0	0	0	2
	DA19	1	1	0	0	2	1	1	2	0	0	0	1
	DA20	3	2	1	1	0	0	0	0	0	0	3	3
	DA21	3	3	2	0	1	0	0	2	0	0	0	3
	DA22	2	2	2	0	3	1	1	2	0	1	0	2
	DA23	2	2	0	0	0	0	0	1	0	0	0	2

i, interstitial infiltrate; t, tubulitis; v, vasculitis; g, glomerulitis; ah, arteriolar hyalinosis; ci, chronic interstitial lesions; ct, chronic tubular lesions; cv, chronic vascular lesions; cg, chronic glomerular lesions; mm, mesangial matrix; ptc, peritubular capillaritis; ti, total interstitial inflammation.

Annex table 2. Gene Ontology – Biological Process most significantly enriched terms in the 730 proteins found in the mass-spectrometry analysis in NKF, IFTA and CNIT groups.

Term description	Observed gene count	Background gene count	FDR
Vesicle-mediated transport	261	1699	3.12e-91
Regulated exocytosis	178	691	4.79e-89
Exocytosis	184	774	1.53e-87
Secretion by cell	192	959	1.05e-80
Secretion	198	1070	2.14e-78
Leukocyte mediated immunity	156	632	4.94e-75
Neutrophil mediated immunity	140	498	7.63e-73
Neutrophil activation involved in immune response	138	489	6.03e-72
Myeloid leukocyte mediated immunity	141	519	7.00e-72
Neutrophil degranulation	137	485	1.61e-71
Leukocyte degranulation	139	507	2.53e-71
Myeloid cell activation involved in immune response	140	519	3.81e-71
Myeloid leukocyte activation	144	574	7.13e-70
Immune effector process	174	927	6.09e-69
Transport	355	4130	2.66e-67
Cell activation involved in immune response	144	620	3.51e-66
Establishment of localization	358	4248	5.63e-66
Leukocyte activation involved in immune response	143	616	1.06e-65
Cell activation	173	1024	1.66e-62
Localization	392	5233	2.37e-61

Annex table 3. Gene Ontology – Cellular Component most significantly enriched terms in the 730 proteins found in the mass-spectrometry analysis.

Term description	Observed gene count	Background gene count	FDR
Vesicle	311	2318	2.46e-100
Extracellular region	312	2505	3.40e-93
Cytoplasmic vesicle	291	2226	5.22e-90
Secretory granule	190	828	1.23e-89
Cytoplasmic vesicle part	234	1447	1.44e-85
Secretory vesicle	195	948	3.94e-85
Cytoplasmic vesicle lumen	115	340	5.28e-67
Secretory granule lumen	111	323	3.13e-65
Extracellular region part	197	1375	2.27e-62
Endomembrane system	349	4347	4.70e-59
Extracellular space	175	1134	8.46e-59
Cytoplasmic part	524	9377	4.96e-54
Cytoplasm	560	11238	7.03e-44
Cell periphery	355	5254	1.07e-42
Plasma membrane	347	5159	8.21e-41
Lysosome	106	582	8.55e-40
Vacuole	112	682	1.92e-38
Whole membrane	166	1554	2.56e-36
Vacuolar lumen	61	172	6.27e-36
Azurophil granule	58	155	3.53e-35

Annex table 4. List of the proteins significantly differently expressed shown in the volcano plot of CNIT vs. NKF (Figure 13b).

Gene name	Fold change	-log(*p*-value)
CTSZ	17.09682	12.33218
RAB8A	15.14346	11.75521
SERPINC1	16.64265	8.38317
NAPSA	16.46061	4.400914
TTR	18.90059	4.059741
GSTP1	16.6204	3.910614
YWHAQ	14.32559	3.870245
CAPG	16.03821	3.866636
FGA	15.49457	3.755747
GNAI1	14.04115	3.753342
PTGR1	14.11435	3.673125
STXBP2	13.22334	3.640962
CNP	13.96733	3.619861
RBP4	18.42533	3.606263
SLC3A2	13.04238	3.57344
CA1	16.96889	3.483952
ADIRF	16.96444	3.473245
CAPZA1	13.09425	3.159562
EIF5A2	14.04444	3.157831
CRABP2	14.17305	3.153388
UPK1B	14.80527	3.151623
TUBB	14.20602	3.147056
CBR1	13.52186	3.140921
CTSD	14.12	3.129715
FBP1	13.27951	3.11967
RAB1B	12.49896	3.11859
FLOT1	13.09407	3.11681
RAB8B	11.55652	3.106566
CAPN5	13.2108	3.091306
GNA13	12.91073	3.089945
ARHGDIB	14.245	3.083094
DSTN	13.25582	3.074183
PTPN13	12.15206	3.070595
PLSCR1	14.0724	3.06606
RAP1A	13.99524	3.059056
BAIAP2L1	12.53215	3.050912

EPS8	14.28895	3.04115
CST3	16.441	3.021803
SLC34A2	13.1171	3.016683
IDH1	13.63968	3.001035
PPL	11.21278	2.922073
PKM	13.76167	2.77458
HSPG2	12.35273	2.769925
HSP90AA1	13.65436	2.73587
ACTN4	13.33733	2.727924
EPS8L2	14.65043	2.710358
PGK1	13.20971	2.676922
EFEMP1	13.67455	2.644454
VPS37B	12.34922	2.578884
TPI1	14.26845	2.563448
PRDX6	13.34694	2.562729
ASAH1	12.58008	2.409175
EHD1	12.88952	2.345764
LMAN2	13.51137	2.339659
YWHAG	12.26183	2.272777
CALB1	12.37555	2.209791
ANXA6	11.45126	2.165348
AGT	13.93267	2.164472
DPP4	12.11966	2.163453
ITIH4	12.73345	2.159698
ASS1	12.16517	2.152552
PGAM1	13.19666	2.124046
MYH9	10.01056	2.117177
MARCKS	11.63666	2.115895
CA2	12.35211	2.061382
PRDX1	12.44137	2.051854
SNAP23	12.01325	2.035146
RAB7A	10.90947	2.022379
RHOA	12.33847	2.016213
MSN	12.20578	2.010916
AKR1A1	11.45235	2.003496

Annex table 5. List of the proteins significantly differently expressed shown in the volcano plot of CNIT vs. IFTA (Figure 13c). A negative fold change indicates more expression in the IFTA group.

Gene name	Fold Change	-log(*p*-value)
ADIRF	19.57731	8.591249
CAPG	18.2191	8.235004
STXBP2	15.14143	7.948807
GNAI1	15.98835	7.419415
ATP1A1	15.60777	7.307434
PPL	12.02056	2.922208
VPS37B	13.47743	2.781843
SNCG	14.83107	2.723545
RAB8A	12.38739	2.662239
TSG101	14.43177	2.572905
EHD4	15.24505	2.515646
VPS28	15.43811	2.490042
ANXA4	14.45527	2.440012
CAPZA1	13.09425	2.402834
UPK2	15.1833	2.401713
CRABP2	14.17305	2.398072
CD47	13.33802	2.39788
UPK1A	14.25236	2.39681
UPK1B	14.80527	2.396711
ANXA6	13.10347	2.388609
CD2AP	12.67408	2.375768
RAB1B	12.49896	2.37124
FLOT1	13.09407	2.369867
RAB8B	11.55652	2.361971
EVPL	12.62046	2.358555
PPP2R1A	12.01373	2.358262
CAPN5	13.2108	2.350211
THY1	15.95974	2.346988
VPS4A	13.51522	2.343438
S100A11	15.07003	2.337983
DSTN	13.25582	2.337018
CALB1	13.51569	2.336079
FABP5	14.20961	2.333802
CLIC6	13.24979	2.330843
MYO1C	12.86527	2.315403
ANXA7	12.63252	2.313072
SLC34A2	13.1171	2.292739
RHOA	15.02891	2.192228
DPP4	14.22212	2.1078
HIST1H4A	-17.75791	2.951101
IGHV4-28	-13.0448	2.379408
HRG	-16.79686	2.64356

Annex table 6. Top 20 most enriched Gene Ontology - Biological Process terms in CNIT compared to NKF from GSEA.

Gene ontology – Biological process term	Size	NES	NOM p-val	FDR q-val
Regulation of protein serine threonine kinase activity	34	1.515	0.019	0.542
Cellular component morphogenesis	47	1.520	0.007	0.548
Regulation of peptide transport	17	1.489	0.035	0.567
Regulation of organelle organization	82	1.483	0.005	0.569
Golgi vesicle transport	22	1.478	0.028	0.571
Regulation of actin filament length	26	1.559	0.014	0.572
Response to nutrient	17	1.473	0.049	0.573
Localization within membrane	15	1.521	0.030	0.582
Regulation of hormone levels	33	1.567	0.008	0.582
Positive regulation of cellular component biogenesis	39	1.527	0.015	0.582
Small gtpase mediated signal transduction	38	1.490	0.014	0.588
Cell cycle phase transition	15	1.652	0.008	0.588
Cell projection assembly	20	1.495	0.026	0.592
Regulation of ras protein signal transduction	17	1.538	0.024	0.596
Positive regulation of protein serine threonine kinase activity	19	1.371	0.096	0.601
Actin filament organization	29	1.498	0.022	0.602
Neuron projection morphogenesis	25	1.545	0.012	0.603
Negative regulation of response to wounding	24	1.368	0.079	0.605
Gliogenesis	16	1.372	0.080	0.607
Regulation of blood pressure	16	1.528	0.038	0.614

NES, Normalized enrichment score; NOM p-val, nominal *p*-value; FDR q-val, false discovery rate *q*-value.

Annex table 7. Enriched Gene Ontology - Biological Process terms in NKF compared to CNIT from GSEA.

Gene ontology – Biological process term	Size	NES	NOM p-val	FDR q-val
Negative regulation of immune response	16	-1.224	0.174	0.871
Aminoglycan metabolic process	17	-0.631	0.951	0.966
Response to radiation	16	-1.26	0.162	1
B cell mediated immunity	18	-0.741	0.8	1
Carbohydrate derivative catabolic process	17	-0.814	0.806	1
Cellular response to cytokine stimulus	19	-0.843	0.821	1
Complement activation	21	-0.785	0.84	1
Adaptive immune response based on somatic recombination of immune receptors built from immunoglobulin superfamily domains	19	-0.772	0.853	1
Humoral immune response mediated by circulating immunoglobulin	18	-0.803	0.906	1
Ammonium ion metabolic process	15	-0.676	0.914	1

NES, Normalized enrichment score; NOM p-val, nominal *p*-value; FDR q-val, false discovery rate *q*-value.

Annex table 8. Top 20 most enriched Gene Ontology - Biological Process terms in CNIT compared to IFTA from GSEA.

Gene ontology – Biological process term	**Size**	**NES**	**NOM p-val**	**FDR q-val**
Regulation of actin filament length	29	1.793	0.001	0.058
Epithelial cell differentiation	59	1.798	0.000	0.068
Regulation of protein complex disassembly	29	1.801	0.000	0.083
Cell cycle	57	1.757	0.001	0.087
Actin filament organization	32	1.641	0.009	0.091
Regulation of actin filament based process	47	1.712	0.000	0.092
Regulation of cell cycle process	28	1.642	0.002	0.093
Modulation of synaptic transmission	25	1.644	0.013	0.095
Vesicle organization	41	1.741	0.001	0.096
Intracellular protein transport	61	1.645	0.002	0.097
Multivesicular body organization	20	1.633	0.007	0.098
Regulation of cell cycle	38	1.630	0.007	0.098
Endomembrane system organization	54	1.714	0.000	0.098
Regulation of cellular component biogenesis	80	1.611	0.001	0.099
Regulation of protein polymerization	27	1.655	0.003	0.099
Regulation of cellular component size	46	1.647	0.002	0.099
Membrane budding	27	1.694	0.002	0.099
Multi organism membrane organization	19	1.650	0.014	0.100
Negative regulation of protein complex disassembly	17	1.683	0.009	0.101
Virion assembly	22	1.612	0.012	0.101

NES, Normalized enrichment score; NOM p-val, nominal *p*-value; FDR q-val, false discovery rate *q*-value.

Annex table 9. Top 20 most enriched Gene Ontology - Biological Process terms in IFTA compared to CNIT from GSEA.

Gene ontology – Biological process term	Size	NES	NOM p-val	FDR q-val
Protein activation cascade	51	-2.909	0.000	0.000
Complement activation	37	-2.852	0.000	0.000
Humoral immune response mediated by circulating immunoglobulin	32	-2.754	0.000	0.000
Humoral immune response	51	-2.752	0.000	0.000
B cell mediated immunity	32	-2.682	0.000	0.000
Adaptive immune response based on somatic recombination of immune receptors built from immunoglobulin superfamily domains	35	-2.671	0.000	0.000
Lymphocyte mediated immunity	39	-2.491	0.000	0.000
Aminoglycan metabolic process	23	-2.448	0.000	0.000
Mucopolysaccharide metabolic process	15	-2.416	0.000	0.000
Regulation of protein maturation	25	-2.367	0.000	0.001
Regulation of acute inflammatory response	23	-2.315	0.000	0.001
Regulation of humoral immune response	21	-2.316	0.000	0.001
Regulation of protein activation cascade	22	-2.280	0.000	0.002
Carbohydrate derivative catabolic process	26	-2.171	0.000	0.003
Negative regulation of coagulation	17	-2.142	0.000	0.004
Negative regulation of wound healing	17	-2.122	0.000	0.005
Adaptive immune response	42	-2.110	0.000	0.005
Defense response to bacterium	36	-2.086	0.000	0.005
Platelet degranulation	47	-2.070	0.000	0.006
Blood coagulation fibrin clot formation	15	-2.055	0.006	0.006

NES, Normalized enrichment score; NOM p-val, nominal *p*-value; FDR q-val, false discovery rate *q*-value.

Annex table 10. Clinical parameters of the patients in the discovery cohort.

Clinical parameter	NKF (n=7)	IFTA (n=5)	ACR (n=6)	CNIT (n=5)	*p*-value	Sig.
Age (years) (mean±sd)	58.1± 10.6	60.6± 8.5	49.8± 17.8	45.6± 8.6	0.147[a]	ns
Female (n (%))	4 (57.1%)	2 (40.0%)	0 (0.0%)	3 (60.0%)	0.126[b]	ns
DM (n (%))	0 (0.0%)	1 (20.0%)	1 (16.7%)	1 (20.0%)	0.672[b]	ns
Hypertension (n (%))	5 (71.4%)	5 (100.0%)	3 (50.0%)	3 (60.0%)	0.321[b]	ns
Living donor (n (%))	2 (28.6%)	1 (20.0%)	2 (33.3%)	2 (40.0%)	0.917[b]	ns
Previously transplanted (n (%))	1 (14.3%)	0 (0.0%)	1 (16.7%)	0 (0.0%)	0.635[b]	ns
Baseline immunosuppression						
TAC-MPA	6	2	5	4	0.699 [b]	ns
TAC-mTORi	0	0	0	0		
Other	1	3	1	1		
Donor age (years) (mean±sd)	43.3± 9.7	51.8± 16.5	60.5± 14.3	52± 12.1	0.217[a]	ns
Donor sex (female, n (%))	4 (57.1%)	4 (80.0%)	3 (50.0%)	4 (80.0%)	0.620[b]	ns
Serum creatinine (mg/dL)	0.90± 0.11	2.20± 0.41	3.23± 1.73	2.32± 0.51	0.003[a]	*
Proteinuria (mg/g creatinine)	94.1± 49.3	672.4± 632.8	328.3± 206.6	289.6± 174.3	0.081[a]	ns
Months from transplantation (mean (range))	131.3 (57.8-186.6)	79.9 (15.1-252.3)	8.5 (1.1-25.2)	54.7 (0.5-238.8)	0.009[a]	*

[a] Kruskall-Wallis test was performed.

[b] Chi-squared test was performed.

DM, diabetes mellitus type 2; months from transplantation, months elapsed from transplantation until collection of the urine sample; Sig., significance; ns, non-significant (*p*-value>0.01); **p*-value<0.01.

Annex table 11. Clinical parameters of the patients in the verification cohort.

Clinical parameter	NKF (n=10)	IFTA (n=11)	ACR (n=10)	CNIT (n=10)	*p*-value	Sig.
Age (years) (mean±sd)	46.4± 13.7	54.4± 5.9	49.5± 11.1	53.3± 15.6	0.412[a]	ns
Female (n (%))	4 (40.0%)	5 (45.5%)	3 (30.0%)	1 (10.0%)	0.325[b]	ns
DM (n (%))	7 (70.0%)	6 (54.5%)	3 (30.0%)	1 (10.0%)	0.033[b]	*
Hypertension (n (%))	9 (90.0%)	7 (63.6%)	7 (70.0%)	7 (70.0%)	0.561[b]	ns
Living donor (n (%))	3 (30.0%)	2 (18.2%)	2 (20.0%)	10 (100.0%)	<0.001[b]	***
Previously transplanted (n (%))	0 (0.0%)	3 (27.3%)	0 (0.0%)	1 (10.0%)	0.112[b]	ns
Baseline immunosuppression						
TAC-MPA	7	3	5	6	0.545[b]	ns
TAC-mTORi	3	7	4	3		
Other	0	1	1	1		
Donor age (years) (mean±sd)	37.8± 21.6	49.6± 9.4	48.5± 11.4	59.4± 9.1	0.010[a]	*
Donor sex (female, n (%))	7 (70.0%)	2 (18.2%)	5 (50.0%)	9 (90.0%)	0.007[b]	**
Serum creatinine (mg/dL)	1.11± 0.60	1.79± 0.75	1.86± 0.52	1.95± 0.94	0.007[a]	**
Proteinuria (mg/g creatinine)	114± 148	634± 1511	646± 740	156± 115	0.004[a]	**
Months from transplantation (mean (range))	11.5 (4.2-20.3)	27.0 (3.6-172.1)	39.7 (0.5-188.9)	47.2 (1.57-251.1)	0.246[a]	ns

[a] Kruskall-Wallis test was performed.

[b] Chi-squared test was performed.

DM, diabetes mellitus type 2; months from transplantation, months elapsed from transplantation until collection of the urine sample; Sig., significance; ns, non-significant (*p*-value>0.01); **p*-value<0.01; ***p*-value<0.001.

Annex table 12. Banff scoring of kidney biopsies from the verification cohort.

Group	Sample	i	t	v	g	ah	ci	ct	cv	cg	mm	ptc	ti
NKF	VN1	0	0	0	0	0	0	1	0	0	0	0	0
	VN2	0	0	0	0	0	1	1	0	0	0	0	0
	VN3	0	0	0	0	0	0	0	0	0	0	0	0
	VN4	0	0	0	0	0	0	0	0	0	0	0	0
	VN5	/	/	/	/	/	/	/	/	/	/	/	/
	VN6	0	0	0	0	0	0	0	1	0	0	0	0
	VN7	0	0	0	0	1	1	1	0	0	0	0	1
	VN8	0	0	0	0	0	0	1	0	0	0	0	0
	VN9	0	0	0	0	0	0	0	0	0	0	0	0
	VN10	/	/	/	/	/	/	/	/	/	/	/	/
IFTA	VI11	0	0	0	0	0	3	3	1	0	0	0	1
	VI12	0	0	0	0	2	3	3	1	0	2	0	1
	VI13	1	0	0	0	0	3	3	0	0	0	0	1
	VI14	0	0	0	0	0	3	2	2	0	0	0	1
	VI15	0	0	0	0	0	2	2	1	0	0	1	0
	VI16	0	0	0	0	0	2	2	1	0	0	2	1
	VI17	0	0	0	0	0	1	1	1	0	0	0	1
	VI18	0	0	0	0	1	2	2	1	0	0	0	0
	VI19	1	0	0	1	1	2	2	2	0	0	1	2
	VI20	0	0	0	0	1	2	2	2	0	0	0	1
	VI21	0	0	0	0	0	2	2	1	0	0	0	1
CNIT	VC22	0	0	0	0	3	2	2	2	0	1	0	1
	VC23	0	0	0	1	3	2	2	2	0	0	0	1
	VC24	0	0	0	0	0	1	0	1	0	0	0	0
	VC25	0	0	0	0	2	2	2	1	0	0	0	0
	VC26	/	/	/	/	/	/	/	/	/	/	/	/
	VC27	0	0	0	0	0	0	1	1	0	0	0	0
	VC28	0	0	0	0	1	1	1	0	0	0	0	1
	VC29	/	/	/	/	/	/	/	/	/	/	/	/
	VC30	0	0	0	0	0	2	2	2	0	0	0	1
	VC31	0	0	0	0	1	1	1	0	0	0	0	1
ACR	VA32	/	/	/	/	/	/	/	/	/	/	/	/
	VA33	2	2	0	0	0	1	1	1	0	0	0	2
	VA34	3	3	0	0	1	1	1	2	0	0	0	0
	VA35	2	2	0	0	0	1	1	0	0	0	0	0
	VA36	2	3	0	0	0	2	1	1	0	0	1	2
	VA37	1	3	0	0	0	1	1	1	0	0	1	1
	VA38	1	1	0	0	0	0	0	0	0	0	0	1
	VA39	/	/	/	/	/	/	/	/	/	/	/	/
	VA40	3	3	0	0	1	1	1	1	0	0	1	3
	VA41	2	2	0	0	0	1	1	0	0	0	0	2

i, interstitial infiltrate; t, tubulitis; v, vasculitis; g, glomerulitis; ah, arteriolar hyalinosis; ci, chronic interstitial lesions; ct, chronic tubular lesions; cv, chronic vascular lesions; cg, chronic glomerular lesions; mm, mesangial matrix; ptc, peritubular capillaritis; ti, total interstitial inflammation; /, not evaluable.

Annex table 13. Full list of significant proteins from the volcano plot (Figure 18A) in the discovery phase. Proteins more expressed in the Pathological groups (IFTA, CNIT and ACR) have a positive fold change, whereas proteins more expressed in the NKF group have a negative fold change (last seven proteins).

p-value	Fold Change	Majority protein IDs	Protein names	Gene names
4.80E-08	17.157	Q5VY30; A0A0C4DGV7; P02753	Retinol-binding protein 4; Plasma retinol-binding protein(1-182); Plasma retinol-binding protein(1-181); Plasma retinol-binding protein(1-179); Plasma retinol-binding protein(1-176)	RBP4
4.83E-08	17.861	P07339; C9JH19; H7C469; F8WD96	Cathepsin D; Cathepsin D light chain; Cathepsin D heavy chain	CTSD
9.75E-06	16.235	P01008; Q8TCE1	Antithrombin-III	SERPINC1
1.07E-05	17.709	P02766; A0A087WT59; A0A087WV45	Transthyretin	TTR
1.38E-05	15.238	P02671	Fibrinogen alpha chain; Fibrinopeptide A; Fibrinogen alpha chain	FGA
1.01E-04	14.252	P04004	Vitronectin; Vitronectin V65 subunit; Vitronectin V10 subunit; Somatomedin-B	VTN
1.29E-04	13.613	P18669; P15259	Phosphoglycerate mutase 1; Phosphoglycerate mutase 2	PGAM1; PGAM2
1.37E-04	13.024	P06744; K7EQ48; A0A0A0MTS2; A0A0J9YXP8; A0A0J9YYH3; A0A0J9YX90	Glucose-6-phosphate isomerase	GPI
1.70E-04	10.905	P26038	Moesin	MSN
2.10E-04	14.795	P14174	Macrophage migration inhibitory factor	MIF
2.35E-04	15.513	P00915; E5RHP7; E5RH81; E5RFE7; E5RIF9; E5RG43; H0YBE2	Carbonic anhydrase 1	CA1
2.87E-04	12.983	P16152; E9PQ63; A8MTM1	Carbonyl reductase [NADPH] 1	CBR1

3.39E-04	11.930	P14618; B4DNK4; H3BTN5; H3BR70; H3BQ34	Pyruvate kinase PKM; Pyruvate kinase	PKM
4.00E-04	15.883	P01034	Cystatin-C	CST3
8.13E-04	10.923	Q96IU4; F8W9U3; B4DQI4	Alpha/beta hydrolase domain-containing protein 14B	ABHD14B
1.09E-03	11.564	B7ZKJ8; Q14624; H7C0L5	Inter-alpha-trypsin inhibitor heavy chain H4; 70 kDa inter-alpha-trypsin inhibitor heavy chain H4; 35 kDa inter-alpha-trypsin inhibitor heavy chain H4	ITIH4
1.17E-03	11.906	B4E1Z4; E7ETN3; P00751	Complement factor B; Complement factor B Ba fragment; Complement factor B Bb fragment	CFB
1.26E-03	10.247	P61006	Ras-related protein Rab-8A	RAB8A
1.27E-03	12.670	P09211; A8MX94	Glutathione S-transferase P	GSTP1
1.39E-03	12.335	P62834; A0A075B6Q0	Ras-related protein Rap-1A	RAP1A
1.58E-03	11.140	P27348; E9PG15	14-3-3 protein theta	YWHAQ
1.75E-03	12.589	O14773; A0A0C4DGZ9	Tripeptidyl-peptidase 1	TPP1
1.77E-03	12.035	P60174	Triosephosphate isomerase	TPI1
1.87E-03	10.708	O43707	Alpha-actinin-4	ACTN4
1.94E-03	12.870	O96009; M0QXC5	Napsin-A	NAPSA
2.00E-03	11.651	Q9Y696	Chloride intracellular channel protein 4	CLIC4
2.10E-03	13.422	P01019	Angiotensinogen; Angiotensin-1; Angiotensin-2; Angiotensin-3; Angiotensin-4; Angiotensin 1-9; Angiotensin 1-7; Angiotensin 1-5; Angiotensin 1-4	AGT
3.45E-03	11.347	P40925; B9A041; B8ZZ51; C9JF79	Malate dehydrogenase, cytoplasmic;Malate dehydrogenase	MDH1
3.79E-03	9.934	Q14344	Guanine nucleotide-binding protein subunit alpha-13	GNA13

3.90E-03	11.205	Q5JP53; P07437; Q5ST81; Q9BVA1; Q13885	Tubulin beta chain; Tubulin beta-2B chain; Tubulin beta-2A chain	TUBB; TUBB2B; TUBB2A
4.00E-03	8.969	Q9UHR4	Brain-specific angiogenesis inhibitor 1-associated protein 2-like protein 1	BAIAP2L1
4.06E-03	10.758	Q9UBR2	Cathepsin Z	CTSZ
4.16E-03	10.090	Q12929	Epidermal growth factor receptor kinase substrate 8	EPS8
4.26E-03	10.721	Q9UHL4	Dipeptidyl peptidase 2	DPP7
4.33E-03	9.331	A0A087WUL0; Q3LXA3; H0YCY6	Bifunctional ATP-dependent dihydroxyacetone kinase/FAD-AMP lyase (cyclizing); ATP-dependent dihydroxyacetone kinase; FAD-AMP lyase (cyclizing)	TKFC; DAK
4.35E-03	10.073	Q14914; Q5JVP2	Prostaglandin reductase 1	PTGR1
4.85E-03	11.540	P02748	Complement component C9; Complement component C9a; Complement component C9b	C9
4.99E-03	9.234	A0A0G2JIW1; P0DMV9; P0DMV8; V9GZ37	Heat shock 70 kDa protein 1B; Heat shock 70 kDa protein 1A	HSPA1B; HSPA1A
6.27E-03	10.736	Q5T2W1; A8MUH7	Na(+)/H(+) exchange regulatory cofactor NHE-RF3;Putative PDZ domain-containing protein 1P	PDZK1; PDZK1P1
7.32E-03	8.916	P01024	Complement C3; Complement C3 beta chain; C3-beta-c; Complement C3 alpha chain; C3a anaphylatoxin; Acylation stimulating protein; Complement C3b alpha chain; Complement C3c alpha chain fragment 1; Complement C3dg fragment; Complement C3g fragment; Complement C3d fragment; Complement C3f fragment; Complement C3c alpha chain fragment 2	C3

9.16E-03	8.514	P10909; H0YC35; H0YLK8	Clusterin; Clusterin beta chain; Clusterin alpha chain; Clusterin	CLU
9.35E-03	10.289	J3KRE2; J3KTF8; J3QQX2; P52565; J3KS60; J3KRY1	Rho GDP-dissociation inhibitor 1	ARHGDIA
9.36E-03	8.810	A0A087X0K1; Q9Y376	Calcium-binding protein 39	CAB39
9.39E-03	9.579	P00558	Phosphoglycerate kinase 1	PGK1
9.52E-03	9.659	C9J7K9; O15162; H7C5I5; C9J9P4	Phospholipid scramblase 1	PLSCR1
9.53E-03	8.721	O75955; A2AB09	Flotillin-1	FLOT1
9.67E-03	9.900	B5MC82; P30046; A6NHG4; J3KQ18	D-dopachrome decarboxylase; D-dopachrome decarboxylase-like protein	DDT; DDTL
9.73E-03	7.884	Q08257; A6NP24	Quinone oxidoreductase	CRYZ
2.47E-03	-10.947	Q02413	Desmoglein-1	DSG1
3.36E-03	-11.812	P31431	Syndecan-4	SDC4
3.38E-03	-9.594	Q96FE7; C9JMK5	Phosphoinositide-3-kinase-interacting protein 1	PIK3IP1
3.39E-03	-8.301	Q5T749	Keratinocyte proline-rich protein	KPRP
3.48E-03	-8.234	P09603; E9PJA2	Macrophage colony-stimulating factor 1; Processed macrophage colony-stimulating factor 1	CSF1
6.06E-03	-9.222	Q08554	Desmocollin-1	DSC1
7.76E-03	-12.723	P81605	Dermcidin; Survival-promoting peptide; DCD-1	DCD

International Journal of
Molecular Sciences

MDPI

Article

Proteomic Characterization of Urinary Extracellular Vesicles from Kidney-Transplanted Patients Treated with Calcineurin Inhibitors

Laura Carreras-Planella [1,2], Javier Juega [1,3,4], Omar Taco [3,4], Laura Cañas [1,3,4], Marcella Franquesa [1,4], Ricardo Lauzurica [1,4,5] and Francesc Enric Borràs [1,2,3,5,*]

1 REMAR-IVECAT Group, Can Ruti Campus, Germans Trias i Pujol Health Science Research Institute, 08916 Badalona, Spain; lcarreras@igtp.cat (L.C.-P.); juega.javier@gmail.com (J.J.); laucanyas78@hotmail.com (L.C.); mfranquesa@igtp.cat (M.F.); rlauzurica.germanstrias@gencat.cat (R.L.)
2 Department of Cell Biology, Physiology and Immunology, Autonomous University of Barcelona, Bellaterra, 08193 Cerdanyola del Vallès, Spain
3 Autonomous University of Barcelona, Bellaterra, 08193 Cerdanyola del Vallès, Spain; oetaco.germanstrias@gencat.cat
4 Nephrology Department, Can Ruti Campus, Germans Trias i Pujol University Hospital, 08916 Badalona, Spain
5 Instituto de Salud Carlos III, Red de Investigación Renal (ISCIII-REDinREN RD16/0009 Feder Funds), 28029 Madrid, Spain
* Correspondence: feborras@igtp.cat

Received: 10 September 2020; Accepted: 12 October 2020; Published: 14 October 2020

Abstract: Use of immunosuppressive drugs is still unavoidable in kidney-transplanted patients. Since their discovery, calcineurin inhibitors (CNI) have been considered the first-line immunosuppressive agents, in spite of their known nephrotoxicity. Chronic CNI toxicity (CNIT) may lead to kidney fibrosis, a threatening scenario for graft survival. However, there is still controversy regarding CNIT diagnosis, monitoring and therapeutic management, and their specific effects at the molecular level are not fully known. Aiming to better characterize CNIT patients, in the present study, we collected urine from kidney-transplanted patients treated with CNI who (i) had a normal kidney function, (ii) suffered CNIT, or (iii) presented interstitial fibrosis and tubular atrophy (IFTA). Urinary extracellular vesicles (uEV) were enriched and the proteome was analyzed to get insight into changes happening during CNI. Members of the uroplakin and plakin families were significantly upregulated in the CNIT group, suggesting an important role in CNIT processes. Although biomarkers cannot be asserted from this single pilot study, our results evidence the potential of uEV as a source of non-invasive protein biomarkers for a better detection and monitoring of this renal alteration in kidney-transplanted patients.

Keywords: exosomes; renal transplantation; tacrolimus; cyclosporine A; proteomics

1. Introduction

The calcineurin inhibitors (CNI) cyclosporine A [1,2] and tacrolimus have become the current first-line immunosuppressive agents in kidney transplantation [3–5] for more than 30 years. Their main mechanism of action is based on the disruption of T-cell activation and proliferation by inhibiting calcineurin, the enzyme responsible of the dephosphorylation and activation of NFATc that triggers the transcription of interleukin (IL)-2. Hampering IL-2/IL2R interaction reduces T-cell activation and proliferation, a crucial step in graft rejection [6]. About 94% of renal-transplanted patients receive a CNI-based immunosuppressive regime [7], yet it is well-known that CNI treatment can produce nephrotoxicity, commonly referred to as CNI toxicity (CNIT) [8]. There is still controversy

in the diagnosis, monitoring, and therapeutic management of CNIT (reviewed in [9]). Acute CNIT (aCNIT) is histologically associated with the appearance of isometric vacuolization of the tubular epithelium [10–12], while chronic CNI (cCNIT) produces chronic renal lesions such as interstitial fibrosis, tubular atrophy, arteriolar hyalinosis, and glomerulosclerosis [13,14], all contributing to the progressive and irreversible deterioration of the renal function and graft-loss [15,16]. To avoid this scenario, CNI levels in patients should be maintained within a narrow therapeutic window, a big challenge due to the high inter- and intraindividual pharmacokinetic variability of these drugs [17,18]. There are currently no specific markers of CNIT, and tacrolimus or cyclosporine A trough levels not always correlate with CNIT [19].

Urinary extracellular vesicles (uEV) have been shown to carry proteins that reflect the pathophysiological state of cells in the urinary system [20]. Thus, the analysis of uEV can shed light on the pathophysiological processes occurring in the kidney and as well as providing a source of non-invasive biomarkers of renal alterations. With the aim of characterizing CNIT in renal transplantation, we collected urine samples and isolated uEV from kidney-transplanted patients (all treated with CNI) that were classified into: (i) normal kidney function (NKF), (ii) CNIT, or (iii) interstitial fibrosis and tubular atrophy (IFTA). The uEV proteome was characterized by mass-spectrometry.

2. Results

2.1. Patients and Samples

In this study, size-exclusion chromatography (SEC)-isolated uEV samples from three groups of kidney-transplanted patients (NKF, IFTA, and CNIT) were used. Table 1 summarizes the clinical data of each patient when urine sample was collected. As expected, patients in the NKF group presented significantly lower serum creatinine levels than IFTA ($p = 0.012$) and CNIT ($p = 0.012$), but no other significant differences were found. Patient C10, the unique patient affected by chronic CNIT, presented the highest serum creatinine level. Table 2 summarizes the induction treatment at kidney transplantation, immunosuppression regime at sample's collection and the diagnosis based on renal biopsy and clinical parameters. All patients were receiving an immunosuppressive regime consisting of prednisone and a calcineurin inhibitor (in most cases tacrolimus, only one patient in each group was receiving cyclosporine A), with or without mycophenolate mofetil. The histopathological results of the Banff scoring are summarized in Supplementary Table S1 and representative histological photographs are displayed in Supplementary Figure S1. Acute CNIT was diagnosed in four out of five cases by the presence of isometric vacuolization of the tubular epithelium and the preservation of the microvilli on the apical border. The other CNIT patient was diagnosed with chronic CNIT because of the presence of grade 3 arteriolar hyalinosis and circumferential hyalinosis with peripheric nodules. The diagnosis of CNIT was further supported by the high blood levels of tacrolimus, determined according to the study by Cosio et al. [21] or high blood levels of cyclosporine A based on the Symphony study [22]. Patients in the IFTA group presented different grades of fibrosis in the renal biopsy with no other signs of pathology. The determination of IFTA grade was based on the mean values of the Banff parameters chronic interstitial and tubular lesions (ci and ct). Also, IFTA patients showed lower blood levels of tacrolimus and cyclosporine A compared to CNIT patients, and similar to NFK patients. Patient I13 suffered a previous episode of acute cellular rejection and one episode of acute humoral rejection 21 and 9 months before urine collection, respectively. This patient showed no histopathological signs of rejection at sample collection and was therefore included in the study.

Table 1. Clinical parameters of the study patients at urine collection.

Group, Sample	Age	Gender	DM	HT	Crea.	Prot.	Months from RT	LD	Donor Age
N1	64	F	−	−	0.86	99	137.9	−	53
N2	65	M	−	+	0.86	110	186.6	−	37
N3	45	F	−	+	0.82	30	113.6	−	43
N4	42	M	−	+	0.89	187	186.6	−	30
N5	57	M	−	+	0.9	92	166.4	−	45
N6	65	F	−	−	0.85	55	70.0	+	37
N7	69	F	−	+	1.14	86	57.8	+	58
C8	55	M	+	+	2.29	506	0.5	+	62
C9	33	M	−	−	1.93	232	2.8	+	59
C10	49	F	−	+	3.08	427	238.8	−	45
C11	50	F	−	−	2.49	207	5.5	−	60
C12	41	F	−	+	1.80	76	25.7	−	34
I13	50	F	−	−	2.00	62	21.7	+	48
I14	64	M	−	+	1.60	1600	84.6	−	71
I15	68	M	−	+	2.49	94	25.8	−	67
I16	68	M	+	+	2.62	800	15.1	−	38
I17	53	F	−	+	2.30	806	252.3	−	35
Sig.	ns	ns	ns	ns	***	ns	ns	ns	ns
p-value	0.064 [a]	0.784 [b]	0.452 [b]	0.784 [b]	<0.001 [a]	0.093 [a]	0.113 [a]	0.784 [b]	0.387 [a]

[a] Kruskall–Wallis test or [b] Chi-squared test were performed to determine statistical differences between groups. N, NKF, C, CNIT; I, IFTA; DM, diabetes mellitus type 2; HT, arterial hypertension; Crea., serum creatinine (mg/dL); Prot., proteinuria (mg/g creatinine); Months from RT., months from renal transplantation until sample collection; LD, living donor; F, female; M, male.

Table 2. Immunosuppression regime at urine collection.

Group, Sample	Induction Treatment	IS at Urine Collection	High CNI	Diagnosis
N1	IL2RA	PR, CSA	−	NKF
N2	rATG	PR, TAC, MMF	−	NKF
N3	IL2RA	PR, TAC	−	NKF
N4	IL2RA	PR, TAC	−	NKF
N5	IL2RA	PR, TAC	−	NKF
N6	IL2RA	PR, TAC, MMF	−	NKF
N7	IL2RA	PR, TAC, MMF	−	NKF
C8	IL2RA	PR, TAC, MMF	+	aCNIT
C9	IL2RA	PR, TAC, MMF	+	aCNIT
C10	IL2RA	PR, CSA, MMF	+	cCNIT
C11	IL2RA	PR, TAC, MMF	+	aCNIT
C12	IL2RA	PR, TAC, MMF	+	aCNIT
I13	IL2RA	PR, TAC, MMF	−	IFTA (G2)
I14	IL2RA	PR, TAC, MMF	−	IFTA (G1)
I15	IL2RA	PR, TAC, MMF	−	IFTA (G2)
I16	IL2RA	PR, TAC, MMF	−	IFTA (G2)
I17	IL2RA	PR, CSA	−	IFTA (G2)

IS, immunosuppressive treatment; CNI, calcineurin inhibitors; N, NKF, C, CNIT; I, IFTA; IL2RA, interleukin 2 receptor antagonists; rATG, rabbit anti-thymocyte globulin; PR, prednisone; CSA, cyclosporine A; TAC, tacrolimus; MMF, mycophenolate mofetil; NKF, normal kidney function; aCNIT, acute CNI toxicity; cCNIT, chronic CNI toxicity; IFTA (G), interstitial fibrosis and tubular atrophy (grade).

2.2. Global Analysis of the uEV Proteome

A total of 730 proteins were confidently identified after processing mass spectrometry data. Confirming previous results, and as expected by the enrichment technique used, the FunRich analysis of the identified proteins revealed that the most significantly enriched terms were those related to the secretion of EV such as "vesicle mediated transport" or "extracellular region" according to Gene Ontology (GO)—Biological Process (BP) and Cellular Component (CC) enrichment analysis, respectively (Supplementary Tables S2 and S3).

The number of identified proteins in CNIT samples (mean ± sd, 369 ± 73.9) was significantly higher compared to NKF samples (168.6 ± 65.1) and higher than IFTA samples (246.8 ± 47.0) (Figure 1A).

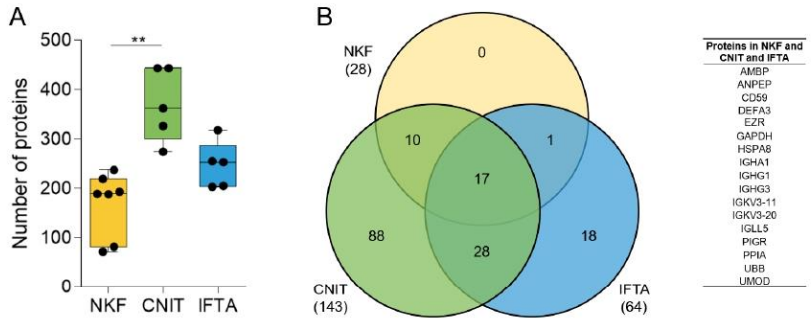

Figure 1. (**A**) Number of proteins found by mass-spectrometry in uEV samples in each group. Whiskers represent minimum to maximum; horizontal line represents the mean (** $p < 0.01$). (**B**) Venn diagram showing the number of coinciding proteins between the samples of each group (in brackets) and between the all the samples in the study (number in the corresponding circles). On the right, list of the 17 proteins found in all samples.

We then assessed the homogeneity of the samples within each group. First, the number of shared proteins among the samples in each group with respect to the total number of proteins identified in the group was analyzed. The seven NKF samples shared up to 28 proteins of a total of the 394 in the group (7.1%). Five CNIT patients shared up to 143 of 621 proteins (23.0%), and five IFTA patients shared 64 of 512 proteins (12.5%). In total, 17 proteins were shared among all samples analyzed (Figure 1B).

Second, we performed a multiple correlation analysis among samples included in each group as a measure of intragroup homogeneity. Each sample's protein expression was compared with every other sample in the same group to obtain the mean of all Pearson correlation coefficient. NKF and CNIT groups were the most homogeneous (mean Pearson coefficient > 0.6) (Figure 2A,B). Conversely, the IFTA group showed a lower level of internal homogeneity (barely > 0.5) (Figure 2C). In this group, sample I13 presented a low Pearson coefficient when individually tested with every other IFTA sample (Pearson coefficients < 0.400), suggesting a particular behavior, as observed later. Of note, if I13 sample was not considered in this assay, the mean Pearson coefficient of IFTA samples increased to 0.654, a value similar to that obtained in the CNIT group.

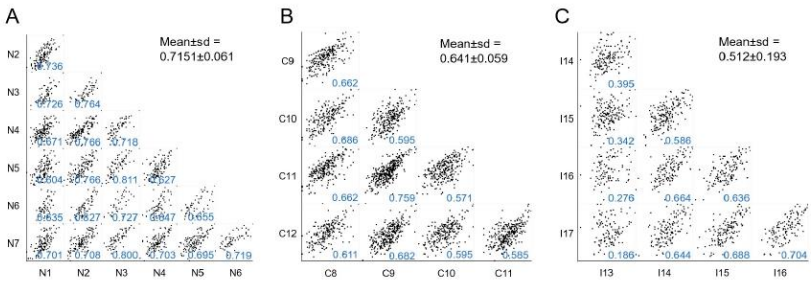

Figure 2. Multi-scatter plots showing correlations of samples within each group: (**A**), NKF; (**B**), CNIT; and (**C**), IFTA. In each individual plot the Pearson correlation coefficients are shown in blue and the corresponding mean ± sd for each group is shown in black.

2.3. Differentially Expressed Proteins

A principal component analysis (PCA) was performed in order to get more insight onto the global protein variation in the two renal alterations (CNIT and IFTA) and the NKF groups (Figure 3A). CNIT patients were clearly segregated from IFTA and NKF patients by Component 1, which accounted for a 23.9% of the variability among samples, while Component 2, which accounted for 17.1% of the variability, permitted to segregate the three groups of samples. Only the sample of the IFTA group (I13), which had a low correlation with the other IFTA samples, did not cluster together with the rest of samples in its group.

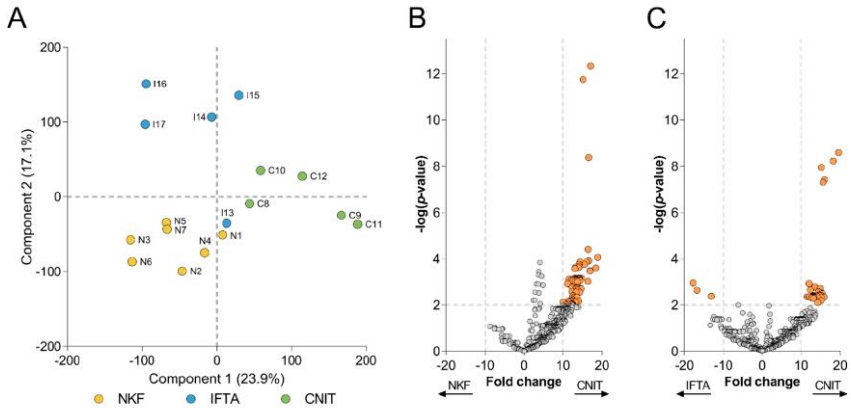

Figure 3. (**A**) Principal component analysis (PCA) biplot that shows distribution of samples according to Components 1 and 2. Each circle represents a sample, which are labelled and colored according to their group. Volcano plots depict the differentially expressed proteins (**B**) between CNIT and NKF, and (**C**) between CNIT and IFTA. Each circle represents a protein. On y-axis −log(*p*-value) from a t-test is represented, with a dashed line at $p < 0.01$ to indicate significance, over which proteins are colored in orange. The expression fold change is represented on the x-axis, with dashed lines at >10 and <−10.

Based on this observation, a more concise comparison was performed using a volcano plot to depict the proteins that were significantly overexpressed between groups. Those proteins having $p < 0.01$ and fold change >10 or <−10 in each comparison were considered as more relevant. From 71 proteins found more expressed in CNIT samples compared to NKF samples (Figure 3B), three (CTSZ, RAB8A and SERPINC1) showed a notable low *p*-value ($<10^{-8}$). On the other hand, up to 39 proteins were significantly more expressed in the CNIT group compared to IFTA patients (Figure 3C), among which five proteins (ADIRF, CAPG, STXBP2, GNAI1, and ATP1A1) presented a remarkably lower p-value ($<10^{-7}$) Of note, no proteins were overexpressed in the NKF group and only three proteins (HIST1H4A, HRG, and IGHV4-28) were significantly more expressed in the IFTA group versus CNIT. The full list of significant proteins from the volcano plots can be seen in Supplementary Tables S4 and S5.

2.4. Biological Processes Enrichment Analysis

After identifying significant proteins differentially expressed in CNIT, the GSEA software was used to reveal the GO biological processes that were up- or downregulated in this group compared to the other groups (each gene being equivalent to a protein). A total of 45 gene sets were significantly enriched (nominal *p*-value < 0.05) in CNIT compared to NKF. None of them reached the minimal significant false discovery rate (FDR) of 0.25, probably because of the dimension of the difference in

protein numbers and level of expression. Nevertheless, the most overexpressed gene set was "Negative regulation of immune response" (Supplementary Tables S6 and S7).

When comparing CNIT and IFTA, up to 128 gene sets were significantly upregulated (FDR < 0.25) in CNIT patients (Supplementary Table S8). The most overexpressed gene sets were "epithelial cell differentiation" and "regulation of actin filament length" (Figure 4A). In addition, CNIT presented overexpression of vesicle-related gene sets such as "vesicle organization" or "multivesicular body organization." Other gene sets more expressed in CNIT than in IFTA were "cell cycle" and "intracellular protein transport."

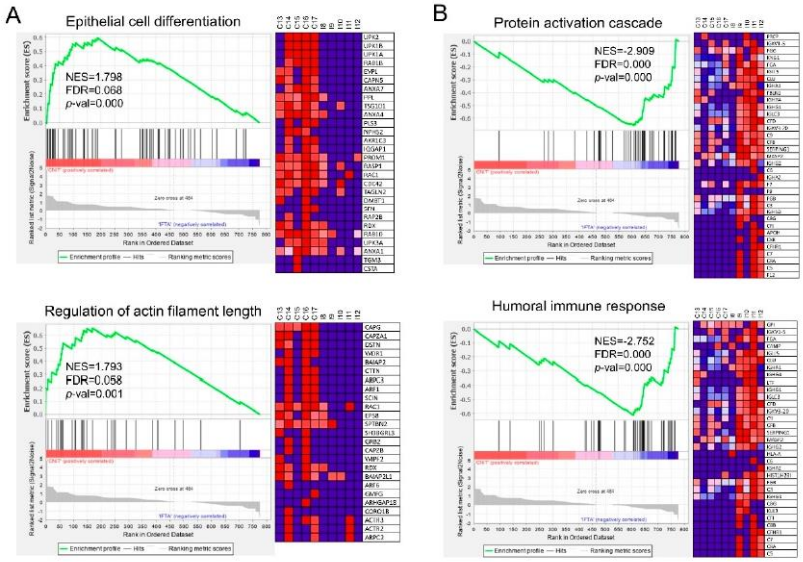

Figure 4. Enrichment plots from GSEA conducted with GO-BP gene sets, each gene accounting for one protein. Statistically significant up-regulation of (**A**) "epithelial cell differentiation" and "regulation of actin filament length" was found in CNIT when compared with IFTA (to the left of the x-axis, positive running enrichment score (ES)). (**B**) "Protein activation cascade" and "humoral immune response" were found up-regulated in IFTA compared to CNIT (to the right of the x-axis, negative ES). Vertical black lines indicate the position of individual genes of the gene set in the ranked list. Heatmap on the right of each plot show the relative expression level of the most up-regulated genes of the gene set (red = high, blue = low). NES, normalized enrichment score; FDR, false discovery rate; *p*-val, *p*-value.

On the reverse comparison, 59 gene sets were upregulated in IFTA compared to CNIT (Supplementary Table S9), "protein activation cascade" and "humoral immune response" (Figure 4B) being two of the most significant ones. Other gene sets related to inflammatory response and complement activation were also upregulated.

Interestingly, several proteins of the uroplakin family (UPK1A, UPK1B, UPK2, and UPK3A), as well as envoplakin (EVPL) and periplakin (PPL) (citolinker proteins) were significantly upregulated in CNIT compared to IFTA and NKF (Figure 5). These proteins are members of the "epithelial cell differentiation" gene set.

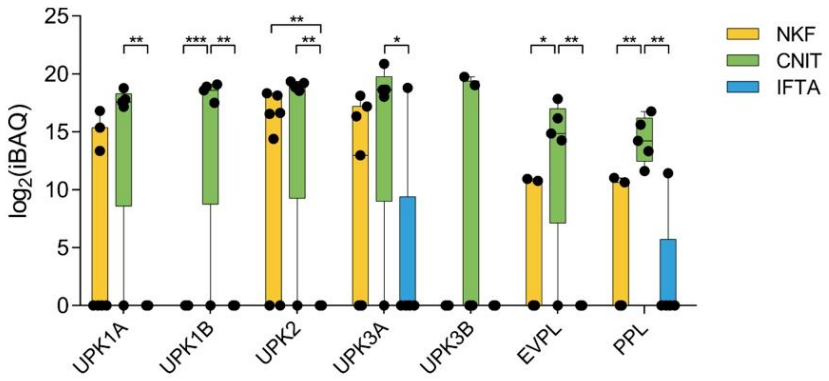

Figure 5. Expression profile of seven proteins of the uroplakin and plakin families. Whiskers represent minimum to maximum; horizontal line represents the mean. UPK1A, uroplakin 1A; UPK1B, uroplakin 1B; UPK2, uroplakin 2; UPK3A, uroplakin 3A; UPK3B, uroplakin 3B; EVPL, envoplakin; PPL, periplakin. * $p < 0.05$; ** $p < 0.01$; *** $p < 0.001$.

3. Discussion

CNIT in kidney-transplantation is controversial. In this study, the uEV proteome of kidney-transplanted patients diagnosed with CNIT was analyzed and compared to either kidney-transplanted patients with clinically normal kidney function or diagnosed with IFTA without CNIT, all of them receiving a similar immunosuppressive regime including CNI. Expectedly, both CNIT and IFTA patients presented a significantly higher serum creatinine than NKF patients.

A first characterization of all the proteins found by mass-spectrometry showed that there was an enrichment of proteins related to the secretion of EV, which denotes the efficacy of uEV enrichment performed using SEC. An efficient EV purification is key to greatly diminish the interference of abundant soluble proteins (especially uromodulin) for a mass-spectrometry analysis, contributing to the detection of lower abundance proteins that may be potential biomarkers [23–25].

The PCA-based comparison of the proteomic results could clearly separate the three groups of samples, indicating that the uEV proteome follows different patterns in NKF, CNIT, and IFTA. Only sample I13, which showed a low correlation coefficient with the other samples within its group, did not cluster as the other IFTA samples did. A possible explanation for this observation could be the two previous episodes of rejection that I13 patient had suffered within 2 years before sample collection. Yet, as no signs of rejection were observed in the biopsy performed at the time of urine sample collection, the patient was finally included in the assay. Our results may suggest those rejection episodes do seem to be still reflected in the uEV proteome. Also interestingly, although chronic CNIT can present lesions compatible with an IFTA diagnosis at the histological level [26], sample C10 did not cluster with IFTA samples. In fact, despite being the unique CNIT sample diagnosed of a chronic CNIT instead of acute CNIT, there was no apparent segregation of C10 from the other CNIT samples in the PCA, pointing to the resemblance of the pathological process in both chronic and acute cases, at least at the uEV proteomic level. Yet, as this study has been performed on a limited number of samples, these results have to be cautiously interpreted.

Vesicle-related gene sets were significantly overexpressed in the CNIT group. Some studies have described that acute CNIT can cause tubular epithelial cell cytoplasmic small vacuoles and abundant lysosomes due to dilatations of the smooth endoplasmic reticulum by aqueous fluid [10–12]. Moreover, it has been shown that a pathological process, like CNIT, increases the secretion activity of kidney cells [27]. Hypothetically, some of these vesicles may be released into the lumen of the proximal tubules and then in urine, so they would be captured as extracellular vesicles, thus increasing the number of proteins found in the proteomic analysis in CNIT samples, as we report here.

In renal biopsies, CNIT often show features shared with IFTA lesions. Both cyclosporin-A and tacrolimus are directly responsible of the increase of TGF-β1 [28], a factor that promotes interstitial fibrosis by increasing synthesis of proteins of the extracellular matrix and decreasing their degradation [29,30]. Moreover, TGF-β1 induces epithelium-to-mesenchymal transition at the tubular level leading to fibrosis by the generation of myofibroblasts [31,32]. Also, it has been shown that CNI drugs induce apoptosis on tubular and interstitial cells in vitro [33,34]. The GSEA analysis show overexpression of different gene sets in CNIT compared to IFTA as well as NKF, suggesting the activation of specific mechanisms in CNIT. Specifically, the proteome of CNIT was significantly enriched in gene sets related to epithelial cell differentiation, probably because of the death of tubular epithelial cells that force their regeneration. Members of the uroplakin family (UPK1A, UPK1B, UPK2, and UPK3A) were also overexpressed in CNIT compared to IFTA. Uroplakins are transmembrane proteins that bind to each other to form a plaque on the surface of the urothelium to prevent influx of urine from the lumen, which covers the renal pelvis, ureters, urinary bladder, and prostatic urethra [35]. The molecular weight of uroplakins ranges from 15 to 47 kDa, suggesting their intravesicular location [36]. Periplakin and envoplakin, two other members of the plakin family that function as cell-linker proteins, were also found enriched in CNIT [37]. These two proteins present a larger molecular weight of around 200 kDa and would possibly elute in the uEV-enriched fractions of SEC as free proteins instead of being carried by uEV [38,39]. Salih et al. described that patients in advanced stages of autosomal dominant polycystic kidney disease (ADPKD) presented increased levels of periplakin and envoplakin in their uEV [40]. In our study, only one patient in the CNIT group (C11) was diagnosed with ADPKD, but all the other CNIT samples also presented high levels of periplakin and envoplakin. The higher abundance of plakins in CNIT uEV suggests that the toxic effect of CNI on the urothelium may increase citolinker proteins' activity and this would be reflected in a higher presence in their uEV. Therefore, plakin family members could represent promising biomarkers for CNIT in uEV.

Conversely, the CNIT uEV proteome did not reflect genes related to protein activation cascade and humoral response as well as other inflammatory processes when compared to IFTA. The reason behind could be that patients in the CNIT group had higher serum levels of CNI [21] which could be responsible for an increased capacity to suppress the inflammatory response.

Only a few studies using proteomic approaches have defined the effect of CNIT on kidneys. Sidgel et al. [41] investigated the urinary proteome of kidney-transplanted pediatric patients with different pathologies, including CNIT. They found a panel of ten proteins that potentially differentiated CNIT from chronic allograft nephropathy, although none of them coincided with our results, most probably because of the differences between using whole urine or uEV. Other groups studied the effect of CNI on renal cell lines in vitro [42,43]. They found that CNIT caused an increase in endoplasmic reticulum stress, mitochondrial apoptosis, and involvement of the phosphatidylinositol 3-kinases (PI3K), metalloproteinases (MMP), protein kinase C (PKC), and glycogen synthase kinase 3 (GSK3) pathways. To our best knowledge, our study is the first to analyze the uEV proteome of kidney-transplanted patients diagnosed of CNIT.

There is a lack of knowledge on how CNIT develops in renal transplanted patients despite the wide use of CNI and their contribution to kidney graft loss. Thus, a better knowledge of the effect of CNI at the renal level is of utmost importance for the detection and management in patients undertaking kidney transplantation. Although no conclusive biomarkers can be asserted from this single pilot study, we found a higher expression of proteins from the plakin family in the CNIT group, which may be envisaged as promising biomarkers and merit future investigation. This work adds further evidence to the potential of uEV as a source of non-invasive protein biomarkers for the better detection and monitoring of this renal alteration in kidney-transplanted patients.

4. Materials and Methods

4.1. Patients and Pre-Processing of Samples

Urine samples were collected from kidney-transplanted patients classified into three groups: normal kidney function (NKF) (n = 7) as determined by analytical parameters (creatinemia and proteinuria), CNIT (n = 5), and interstitial fibrosis tubular atrophy (IFTA) (n = 5), both diagnosed by analytical parameters and by per-cause renal biopsy. Patients classified in the IFTA group had a biopsy diagnosis of IFTA in the absence of any other cause. None of the patients presented C4d deposits in the renal biopsy. Morning mid-stream urine was collected immediately before per-cause renal biopsy (in the case of alteration of serum creatinine and proteinuria). Inclusion criteria were male or female patients older than 18 years of age and ability to give informed consent. Exclusion criteria were hematuria or urinary tract infection demonstrated by the presence of leukocyturia and/or bacteriuria and a previous kidney transplantation. All patients were receiving a similar immunosuppressive regime including CNI. This study was performed in line with the principles of the Declaration of Helsinki [44]. Approval was granted by the Ethics Committee "Comitè d'Ètica de la investigació clínica de l'Hospital Universitari Germans Trias i Pujol" and in accordance with its recommendations of the Guideline for Good Clinical Practice. Informed consent was obtained from all individual participants included in the study. An arbitrary number was used to label samples to protect patients' identity.

4.2. Samples Processing and uEV Isolation

Urine samples were centrifuged (600× g 15 min) to eliminate cells and debris and stored at −80 °C with protease inhibitor (AEBSF, 0.138 mg/mL; Roche, Basel, Switzerland). Urinary EV (uEV) were isolated following the procedure described by Monguió-Tortajada et al. [45]. In brief, urine samples (140 mL) were thawed overnight at 4 °C and centrifuged at 17,000× g for 10 min. The pellet was treated with 1,4-dithiothreitol (200 mg/mL; Sigma-Aldrich, St. Louis, MO, USA) to disrupt Tamm-horse fall protein polymers before mixing it with the initial supernatant and centrifuging again at 17,000× g for 10 min. Then, the supernatant was concentrated through a Centricon filter unit of 100 kDa cut-off (Millipore, Bedford, MA, USA) down to 1–2 mL. One mL of the concentrate was loaded onto a SEC column with 12 mL of sepharose CL-2B (Sigma-Aldrich) and 20 fractions of 500 µL were collected using phosphate-buffered saline (PBS; Sigma-Aldrich) as elution agent. Protein elution of SEC fractions was determined by reading absorbance at 280 nm with Nanodrop ND-1000 (Thermo Scientific, Waltham, MA, USA). In addition, SEC fractions were analyzed for their CD9 and CD63 content (typical tetraspanin EV markers) using beads-based assay flow cytometry. The three fractions with the highest CD9 and CD63 mean fluorescence intensity (MFI) intensity were pooled together rendering a volume of approximately 1.5 mL of uEV-enriched samples.

4.3. Mass-Spectrometry

Five hundred µL of uEV-enriched samples were used for the mass-spectrometry analysis (LC-MS/MS) on an Orbitrap XL (Thermo Scientific). Proteins were digested using LysC and Trypsin (Promega, Madison, WI, USA) and BSA (Sigma-Aldrich) solutions were included as quality controls. Data were analyzed using the Proteome Discoverer software (v2.0; Thermo Scientific) and proteins were identified using Mascot (Matrix Science, London, UK) against the SwissProt human database (UniProt, April 2015; https://www.uniprot.org/) [46] with an FDR of 0.05. The resulting raw data files were processed using the MaxQuant software [47] (version 1.5.3.30) against the SwissProt human database (UniProt, December 2015) applying a maximum FDR of 1%. Intensity-based absolute quantification (iBAQ) values normalized with the EV marker ezrin were used for subsequent analyses.

4.4. Proteomics and Statistical Analysis

The FunRich software (http://www.funrich.org, Melbourne, Australia) [48,49] was used to perform some of the GO enrichment analyses. Overlapping proteins were calculated and visualized with

the online tool InteractiVenn (http://www.interactivenn.net/) [50]. The Perseus software [51] (v1.5.6.0; http://www.perseus-framework.org, Max Planck Institute of Biochemistry, Martinsried, Germany) and GraphPad Prism software (v6.0 GraphPad Software, San Diego, CA, USA) were used for the creation of plots and the statistical analysis. After testing for normality, two-sided unpaired *t*-test (parametric) or Mann-Whitney test (non-parametric) were used for the comparison of two groups of samples; in the case of multiple-groups comparison, one way ANOVA with Holm-Sidak's multiple comparison test (parametric) or Kruskall-Wallis with Dunn's multiple comparison test (non-parametric) were performed. Finally, the Gene Set Enrichment Analysis software (GSEA v3.0, Broad Institute, Cambridge, MA, USA) [52] was used to compare the enrichment of gene sets, which were downloaded from the GSEA Molecular Signatures Database (MSigDB v6.2, Broad Institute, Cambridge, MA, USA) [53]. The normalized enrichment score (NES) accounts for differences between gene sets to allow comparisons between them. The FDR represents the nominal *p*-value adjusted for gene set size and multiple hypothesis testing. It is the estimated probability that a gene set with a given NES represents a false positive finding (significant FDR < 0.25, as recommended by the GSEA software).

5. Patents

LCP, RL and FEB have a European Patent Application pending for the present work.

Supplementary Materials: Supplementary materials can be found at http://www.mdpi.com/1422-0067/21/20/7569/s1.

Author Contributions: Conceptualization, R.L. and F.E.B.; samples acquisition, O.T., L.C., and J.J.; software, L.C.-P.; formal analysis, L.C.-P. and F.E.B.; writing—original draft preparation, L.C.-P.; writing—review and editing, O.T., L.C., J.J., M.F., R.L., and F.E.B.; project administration, R.L. and F.E.B.; funding acquisition, F.E.B. All authors have read and agreed to the published version of the manuscript.

Funding: This work was supported in part by grants from project PI13/00050 integrated in the National R+D+I and funded by the ISCIII and the European Regional Development Fund (http://www.isciii.es), the SGR program of Generalitat de Catalunya (2017-SGR-301 REMAR Group), the ISCIII-REDinREN (RD16/0009 Feder Funds), and Fundació Cellex. The project leading to these results has also received funding from "la Caixa" Foundation (ID 100010434), under agreement LCF/TR/CI19/52460021. This activity has received funding from the European Institute of Innovation and Technology (EIT). This body of the European Union receives support from the European Union's Horizon 2020 research and innovation program. LCP is sponsored by the Spanish Government FPU grant ("Formación de Personal Universitario", FPU17/01444). MF is supported by ISCIII (MS19/00018), co-funded by ERDF/ESF, "Investing in your future". FEB is a researcher from Fundació Institut de Recerca en Ciències de la Salut Germans Trias i Pujol, supported by the Health Department of the Catalan Government (Direcció General de Recerca i Innovació, Dept. Salut, Generalitat de Catalunya).

Acknowledgments: We are indebted to Miriam Morón-Font for her valuable technical help. Paula Rodríguez Martínez from the Histopathology Department of the Germans Trias i Pujol University Hospital for the biopsy histological images. The authors would also like to thank Yáñez-Mó (Unidad de Investigación, Hospital Sta Cristina, IIS-IP; Departamento Biología Molecular/CBM-SO, UAM) and Francisco Sáchez-Madrid (Servicio de Inmunología, Hospital Universitario de la Princesa, IIS-IP, UAM; Cell-cell Communication Laboratory, CNIC) for the anti-CD9 and anti-CD63 antibodies. Also, thanks to Marco A. Fernández from the Flow Cytometry Platform, IGTP.

Conflicts of Interest: LCP, RL, and FEB have a European Patent Application pending for the present work. The other authors declare no conflict of interest.

Abbreviations

aCNIT	acute calcineurin inhibitors toxicity
ANOVA	Analysis of variance
BP	Biological Process
CC	Cellular Component
cCNIT	chronic calcineurin inhibitors toxicity
CD	cluster of differentiation
CNI	calcineurin inhibitors
CNIT	calcineurin inhibitors toxicity
CSA	cyclosporine A

DM	diabetes mellitus type 2
ES	enrichment score
F	female
FDR	false discovery rate
G	grade
GO	Gene Ontology
GSEA	Gene Set Enrichment Analysis
HT	arterial hypertension
iBAQ	Intensity-based absolute quantification
IFTA	interstitial fibrosis and tubular atrophy
IL	interleukin
IL	interleukin
IL2RA	interleukin 2 receptor antagonists
IS	immunosuppressive treatment
LC-MS/MS	liquid chromatography tandem mass-spectrometry
LD	living donor
M	male
MFI	mean fluorescence intensity
MMF	mycophenolate mofetil
MSigDB	Molecular Signatures Database
NES	normalized enrichment score
NKF	normal kidney function
PBS	phosphate-buffered saline
PCA	Principal Component Analysis
PR	prednisone
rATG	rabbit anti-thymocyte globulin
RT	Renal transplantation
SEC	size-exclusion chromatography
TAC	tacrolimus
uEV	Urinary Extracellular Vesicles

References

1. Heusler, K.; Pletscher, A. The controversial early history of cyclosporin. *Swiss Med. Wkly.* **2001**, *131*, 299–302. [CrossRef] [PubMed]
2. Calne, R. Cyclosporine as a milestone in immunosuppression. *Transplant. Proc.* **2004**, *36*, 13S–15S. [CrossRef]
3. Kino, T.; Hatanaka, H.; Hashimoto, M.; Nishiyama, M.; Goto, T.; Okuhara, M.; Kohsaka, M.; Aoki, H.; Imanaka, H. FK-506, a novel immunosuppressant isolated from a Streptomyces. I. Fermentation, isolation, and physico-chemical and biological characteristics. *J. Antibiot.* **1987**, *40*, 1249–1255. [CrossRef] [PubMed]
4. Hatanaka, H.; Iwami, M.; Kino, T.; Goto, T.; Okuhara, M. FR-900520 and FR-900523, novel immunosuppressants isolated from a Streptomyces. I. Taxonomy of the producing strain. *J. Antibiot.* **1988**, *41*, 1586–1591. [CrossRef] [PubMed]
5. Starzl, T.E.; Todo, S.; Fung, J.; Demetris, A.J.; Venkataramman, R.; Jain, A. FK 506 for liver, kidney, and pancreas transplantation. *Lancet* **1989**, *2*, 1000–1004. [CrossRef]
6. Martínez-Martínez, S.; Redondo, J.M. Inhibitors of the calcineurin/NFAT pathway. *Curr. Med. Chem.* **2004**, *11*, 997–1007. [CrossRef]
7. Andreoni, K.A.; Brayman, K.L.; Guidinger, M.K.; Sommers, C.M.; Sung, R.S. Kidney and pancreas transplantation in the United States, 1996–2005. *Am. J. Transplant.* **2007**, *7*, 1359–1375. [CrossRef]
8. Azzi, J.R.; Sayegh, M.H.; Mallat, S.G. Calcineurin inhibitors: 40 years later, can't live without . . . . *J. Immunol.* **2013**, *191*, 5785–5791. [CrossRef]
9. Issa, N.; Kukla, A.; Ibrahim, H.N. Calcineurin inhibitor nephrotoxicity: A review and perspective of the evidence. *Am. J. Nephrol.* **2013**, *37*, 602–612. [CrossRef]
10. Liptak, P.; Ivanyi, B. Primer: Histopathology of calcineurin-inhibitor toxicity in renal allografts. *Nat. Clin. Pract. Nephrol.* **2006**, *2*, 398–404. [CrossRef]

11. Charney, D.A.; Bhaskaran, M.; Molmenti, E. Calcineurin inhibitor toxicity in a renal transplant recipient. *Clin. Kidney J.* **2009**, *2*, 175–176. [CrossRef] [PubMed]
12. Fogo, A.B.; Lusco, M.A.; Najafian, B.; Alpers, C.E. AJKD Atlas of renal pathology: Osmotic tubular injury. *Am. J. Kidney Dis.* **2017**, *69*, e11–e12. [CrossRef] [PubMed]
13. Nankivell, B.J.; Fenton-Lee, C.A.; Kuypers, D.R.; Cheung, E.; Allen, R.D.; O'Connell, P.J.; Chapman, J.R. Effect of histological damage on long-term kidney transplant outcome. *Transplantation* **2001**, *71*, 515–523. [CrossRef]
14. Leal, R.; Tsapepas, D.; Crew, R.J.; Dube, G.K.; Ratner, L.; Batal, I. Pathology of calcineurin and mammalian target of rapamycin inhibitors in kidney transplantation. *Kidney Int. Rep.* **2018**, *3*, 281–290. [CrossRef] [PubMed]
15. Naesens, M.; Lerut, E.; Damme, B.V.; Vanrenterghem, Y.; Kuypers, D.R.J. Tacrolimus exposure and evolution of renal allograft histology in the first year after transplantation. *Am. J. Transplant.* **2007**, *7*, 2114–2123. [CrossRef] [PubMed]
16. Serón, D.; Moreso, F.; Fulladosa, X.; Hueso, M.; Carrera, M.; Grinyó, J.M. Reliability of chronic allograft nephropathy diagnosis in sequential protocol biopsies. *Kidney Int.* **2002**, *61*, 727–733. [CrossRef]
17. Kershner, R.P.; Fitzsimmons, W.E. Relationship of FK506 whole blood concentrations and efficacy and toxicity after liver and kidney transplantation. *Transplantation* **1996**, *62*, 920–926. [CrossRef]
18. Hesselink, D.A.; Bouamar, R.; van Gelder, T. The pharmacogenetics of calcineurin inhibitor-related nephrotoxicity. *Therap. Drug Monit.* **2010**, *32*, 387–393. [CrossRef]
19. Thölking, G.; Schütte-Nütgen, K.; Schmitz, J.; Rovas, A.; Dahmen, M.; Bautz, J.; Jehn, U.; Pavenstädt, H.; Heitplatz, B.; Van Marck, V.; et al. A low tacrolimus concentration/dose ratio increases the risk for the development of acute calcineurin inhibitor-induced nephrotoxicity. *J. Clin. Med.* **2019**, *8*, 1586. [CrossRef]
20. Yáñez-Mó, M.; Siljander, P.R.-M.; Andreu, Z.; Bedina Zavec, A.; Borràs, F.E.; Buzas, E.I.; Buzas, K.; Casal, E.; Cappello, F.; Carvalho, J.; et al. Biological properties of extracellular vesicles and their physiological functions. *J. Extracell. Vesicles* **2015**, *4*, 27066. [CrossRef]
21. Cosio, F.G.; Amer, H.; Grande, J.P.; Larson, T.S.; Stegall, M.D.; Griffin, M.D. Comparison of low versus high tacrolimus levels in kidney transplantation: Assessment of efficacy by protocol biopsies. *Transplantation* **2007**, *83*, 411–416. [CrossRef] [PubMed]
22. Ekberg, H.; Grinyó, J.; Nashan, B.; Vanrenterghem, Y.; Vincenti, F.; Voulgari, A.; Truman, M.; Nasmyth-Miller, C.; Rashford, M. Cyclosporine sparing with mycophenolate mofetil, daclizumab and corticosteroids in renal allograft recipients: The CAESAR Study. *Am. J. Transplant.* **2007**, *7*, 560–570. [CrossRef] [PubMed]
23. An, M.; Wu, J.; Zhu, J.; Lubman, D.M. Comparison of an Optimized Ultracentrifugation Method versus Size-Exclusion Chromatography for Isolation of Exosomes from Human Serum. *J. Proteome Res.* **2018**, *17*, 3599–3605. [CrossRef] [PubMed]
24. Benedikter, B.J.; Bouwman, F.G.; Vajen, T.; Heinzmann, A.C.A.; Grauls, G.; Mariman, E.C.; Wouters, E.F.M.; Savelkoul, P.H.; Lopez-Iglesias, C.; Koenen, R.R.; et al. Ultrafiltration combined with size exclusion chromatography efficiently isolates extracellular vesicles from cell culture media for compositional and functional studies. *Sci. Rep.* **2017**, *7*, 1–13. [CrossRef]
25. Gámez-Valero, A.; Monguió-Tortajada, M.; Carreras-Planella, L.; Franquesa, M.; Beyer, K.; Borràs, F.E. Size-Exclusion Chromatography-based isolation minimally alters Extracellular Vesicles' characteristics compared to precipitating agents. *Sci. Rep.* **2016**, *6*, 33641. [CrossRef]
26. Schwarz, A.; Haller, H.; Schmitt, R.; Schiffer, M.; Koenecke, C.; Strassburg, C.; Lehner, F.; Gottlieb, J.; Bara, C.; Becker, J.U.; et al. Biopsy-diagnosed renal disease in patients after transplantation of other organs and tissues. *Am. J. Transplant.* **2010**, *10*, 2017–2025. [CrossRef]
27. Wang, X.; Wilkinson, R.; Kildey, K.; Potriquet, J.; Mulvenna, J.; Lobb, R.J.; Möller, A.; Cloonan, N.; Mukhopadhyay, P.; Kassianos, A.J.; et al. Unique molecular profile of exosomes derived from primary human proximal tubular epithelial cells under diseased conditions. *J. Extracell. Vesicles* **2017**, *6*, 1314073. [CrossRef]
28. Khanna, A.; Plummer, M.; Bromberek, C.; Bresnahan, B.; Hariharan, S. Expression of TGF-beta and fibrogenic genes in transplant recipients with tacrolimus and cyclosporine nephrotoxicity. *Kidney Int.* **2002**, *62*, 2257–2263. [CrossRef]
29. Farris, A.B.; Colvin, R.B. Renal interstitial fibrosis: Mechanisms and evaluation. *Curr. Opin. Nephrol. Hypertens.* **2012**, *21*, 289–300. [CrossRef]

30. Gewin, L.; Zent, R. How does TGF-β mediate tubulointerstitial fibrosis? *Semin. Nephrol.* **2012**, *32*, 228–235. [CrossRef]
31. Grgic, I.; Duffield, J.S.; Humphreys, B.D. The origin of interstitial myofibroblasts in chronic kidney disease. *Pediatr. Nephrol.* **2012**, *27*, 183–193. [CrossRef]
32. Carew, R.M.; Wang, B.; Kantharidis, P. The role of EMT in renal fibrosis. *Cell Tissue Res.* **2012**, *347*, 103–116. [CrossRef] [PubMed]
33. Puigmulé, M.; López-Hellin, J.; Suñé, G.; Tornavaca, O.; Camaño, S.; Tejedor, A.; Meseguer, A. Differential proteomic analysis of cyclosporine A-induced toxicity in renal proximal tubule cells. *Nephrol. Dial. Transplant.* **2009**, *24*, 2672–2686. [CrossRef] [PubMed]
34. Xiao, Z.; Li, C.; Shan, J.; Luo, L.; Feng, L.; Lu, J.; Li, S.; Long, D.; Li, Y. Mechanisms of renal cell apoptosis induced by cyclosporine A: A systematic review of in vitro studies. *Am. J. Nephrol.* **2011**, *33*, 558–566. [CrossRef] [PubMed]
35. Jenkins, D.; Woolf, A.S. Uroplakins: New molecular players in the biology of urinary tract malformations. *Kidney Int.* **2007**, *71*, 195–200. [CrossRef] [PubMed]
36. Min, G.; Wang, H.; Sun, T.-T.; Kong, X.-P. Structural basis for tetraspanin functions as revealed by the cryo-EM structure of uroplakin complexes at 6-Å resolution. *J. Cell Biol.* **2006**, *173*, 975–983. [CrossRef] [PubMed]
37. Karashima, T. Interaction of periplakin and envoplakin with intermediate filaments. *J. Cell Sci.* **2002**, *115*, 5027–5037. [CrossRef] [PubMed]
38. Ruhrberg, C.; Hajibagheri, M.A.; Simon, M.; Dooley, T.P.; Watt, F.M. Envoplakin, a novel precursor of the cornified envelope that has homology to desmoplakin. *J. Cell Biol.* **1996**, *134*, 715–729. [CrossRef]
39. Ruhrberg, C.; Hajibagheri, M.A.N.; Parry, D.A.D.; Watt, F.M. Periplakin, a Novel Component of Cornified Envelopes and Desmosomes That Belongs to the Plakin Family and Forms Complexes with Envoplakin. *J. Cell Biol.* **1997**, *139*, 1835–1849. [CrossRef]
40. Salih, M.; Demmers, J.A.; Bezstarosti, K.; Leonhard, W.N.; Losekoot, M.; van Kooten, C.; Gansevoort, R.T.; Peters, D.J.M.; Zietse, R.; Hoorn, E.J. Proteomics of urinary vesicles links plakins and complement to polycystic kidney disease. *J. Am. Soc. Nephrol.* **2016**, *27*, 3079–3092. [CrossRef]
41. Sigdel, T.K.; Sarwal, M.M. Assessment of circulating protein signatures for kidney transplantation in pediatric recipients. *Front. Med.* **2017**, *4*, 80. [CrossRef] [PubMed]
42. Sarró, E.; Jacobs-Cachá, C.; Itarte, E.; Meseguer, A. A pharmacologically-based array to identify targets of cyclosporine A-induced toxicity in cultured renal proximal tubule cells. *Toxicol. Appl. Pharmacol.* **2012**, *258*, 275–287. [CrossRef] [PubMed]
43. Lamoureux, F.; Mestre, E.; Essig, M.; Sauvage, F.L.; Marquet, P.; Gastinel, L.N. Quantitative proteomic analysis of cyclosporine-induced toxicity in a human kidney cell line and comparison with tacrolimus. *J. Proteom.* **2011**, *75*, 677–694. [CrossRef] [PubMed]
44. Lynöe, N.; Sandlund, M.; Dahlqvist, G.; Jacobsson, L. Informed consent: Study of quality of information given to participants in a clinical trial. *BMJ* **1991**, *303*, 610–613. [CrossRef]
45. Monguió-Tortajada, M.; Morón-Font, M.; Gámez-Valero, A.; Carreras-Planella, L.; Borràs, F.E.; Franquesa, M. Extracellular-Vesicle Isolation from Different Biological Fluids by Size-Exclusion Chromatography. *Curr. Protoc. Stem Cell Biol.* **2019**, *49*, e82. [CrossRef] [PubMed]
46. The UniProt Consortium UniProt: A worldwide hub of protein knowledge. *Nucleic Acids Res.* **2019**, *47*, D506–D515. [CrossRef]
47. Cox, J.; Mann, M. MaxQuant enables high peptide identification rates, individualized p.p.b.-range mass accuracies and proteome-wide protein quantification. *Nat. Biotechnol.* **2008**, *26*, 1367–1372. [CrossRef]
48. Pathan, M.; Keerthikumar, S.; Ang, C.-S.; Gangoda, L.; Quek, C.Y.J.; Williamson, N.A.; Mouradov, D.; Sieber, O.M.; Simpson, R.J.; Salim, A.; et al. FunRich: An open access standalone functional enrichment and interaction network analysis tool. *Proteomics* **2015**, *15*, 2597–2601. [CrossRef]
49. Pathan, M.; Keerthikumar, S.; Chisanga, D.; Alessandro, R.; Ang, C.-S.; Askenase, P.; Batagov, A.O.; Benito-Martin, A.; Camussi, G.; Clayton, A.; et al. A novel community driven software for functional enrichment analysis of extracellular vesicles data. *J. Extracell. Vesicles* **2017**, *6*, 1321455. [CrossRef]
50. Heberle, H.; Meirelles, G.V.; da Silva, F.R.; Telles, G.P.; Minghim, R. InteractiVenn: A web-based tool for the analysis of sets through Venn diagrams. *BMC Bioinform.* **2015**, *16*, 169. [CrossRef]

51. Tyanova, S.; Temu, T.; Sinitcyn, P.; Carlson, A.; Hein, M.Y.; Geiger, T.; Mann, M.; Cox, J. The Perseus computational platform for comprehensive analysis of (prote)omics data. *Nat. Methods* **2016**, *13*, 731–740. [CrossRef] [PubMed]
52. Subramanian, A.; Tamayo, P.; Mootha, V.K.; Mukherjee, S.; Ebert, B.L.; Gillette, M.A.; Paulovich, A.; Pomeroy, S.L.; Golub, T.R.; Lander, E.S.; et al. Gene set enrichment analysis: A knowledge-based approach for interpreting genome-wide expression profiles. *Proc. Natl. Acad. Sci. USA* **2005**, *102*, 15545–15550. [CrossRef] [PubMed]
53. Liberzon, A.; Subramanian, A.; Pinchback, R.; Thorvaldsdottir, H.; Tamayo, P.; Mesirov, J.P. Molecular signatures database (MSigDB) 3.0. *Bioinformatics* **2011**, *27*, 1739–1740. [CrossRef] [PubMed]

REFERENCES

[1] M. E. Salem and G. Eknoyan, 'The kidney in ancient Egyptian medicine: where does it stand?', *Am. J. Nephrol.*, vol. 19, no. 2, pp. 140–147, 1999, doi: 10.1159/000013440.

[2] A. Vargas, M. López, C. Lillo, and M. J. Vargas, 'El papiro de Edwin Smith y su trascendencia médica y odontológica', *Revista médica de Chile*, vol. 140, no. 10, pp. 1357–1362, Oct. 2012, doi: 10.4067/S0034-98872012001000020.

[3] Taylor, John H, *Journey through the afterlife: ancient egyptian book of the dead.* Place of publication not identified: Harvard Univ Press, 2013.

[4] A. Diamandopoulos and P. Goudas, 'The Role of the Kidney as a Religious, Cultural and Sexual Symbol', *American Journal of Nephrology*, vol. 22, no. 2–3, pp. 107–111, 2002, doi: 10.1159/000063747.

[5] G. Maciocia, *The Foundations of Chinese Medicine: a Comprehensive Text.* London: Elsevier Health Sciences UK, 2015.

[6] Hippocrates and M. J. Schiefsky, *On ancient medicine*, vol. 28. Boston: Brill, 2005.

[7] D. Greydanus and M. Kadochi, 'Reflections on the Medical History of the Kidney: From Alcmaeon of Croton to Richard Bright - Standing on the Shoulders of Giants', *Journal of Integrative Nephrology and Andrology*, vol. 3, no. 4, p. 101, 2016, doi: 10.4103/2394-2916.193496.

[8] A. Diamandopoulos and P. Goudas, 'Juxtaposition of Actuarius' versus Galen's ideas on renal physiology: the impact of 12 centuries', *J. Nephrol.*, vol. 22 Suppl 14, pp. 21–32, Dec. 2009.

[9] J. Scarborough, 'Galen's investigations of the kidney', *Clio Med*, vol. 11, no. 3, pp. 171–177, Oct. 1976.

[10] D. E. Greydanus and J. Merrick, Eds., *Medical history: some perspectives*, Second edition. New York: Nova Biomedical, 2018.

[11] D. Michaēlidēs, Ed., *Medicine and healing in the ancient Mediterranean world*. Oxford: Oxbow Books, 2014.

[12] E. Poulakou-Rebelakou and S. G. Marketos, 'Kidney disease in Byzantine medical texts', *Am. J. Nephrol.*, vol. 19, no. 2, pp. 172–176, 1999, doi: 10.1159/000013446.

[13] A. C. Eftychiadis, 'Renal and glomerular circulation according to Oribasius (4th century)', *Am. J. Nephrol.*, vol. 22, no. 2–3, pp. 136–138, Jul. 2002, doi: 10.1159/000063751.

[14] L. R. Angeletti and B. Cavarra, 'Critical and historical approach to Theophilus' De Urinis. Urine as blood's percolation made by the kidney and uroscopy in the middle ages', *Am. J. Nephrol.*, vol. 14, no. 4–6, pp. 282–289, 1994, doi: 10.1159/000168786.

[15] S. G. Marketos, A. G. Eftychiadis, and A. Diamandopoulos, 'Acute renal failure according to ancient Greek and Byzantine medical writers.', *J R Soc Med*, vol. 86, no. 5, pp. 290–293, May 1993.

[16] P. Mazengenya and R. Bhikha, 'Revisiting Avicenna's (980–1037 AD) anatomy of the abdominal viscera from the Canon of Medicine', *Morphologie*, vol. 102, no. 338, pp. 225–230, Sep. 2018, doi: 10.1016/j.morpho.2018.05.002.

[17] O. C. Gruner, 'A Treatise on the Canon of Medicine of Avicenna', *Incorporating a Translation of the First Book*, 1984.

[18] M. H. Shah, *The general principles of Avicenna's Canon of Medicine*, vol. 1. Naveed Clinic, 1966.

[19] S. M. A. Madineh, 'Avicenna's Canon of Medicine and Modern Urology: part I: bladder and its diseases', *Urol J*, vol. 5, no. 4, pp. 284–293, 2008.

[20] 980-1037 Avicenna, *A treatise on the Canon of medicine of Avicenna, incorporating a translation of the first book*. London : Luzac & co., 1930., 1930.

[21] A. Vesalius 1514-1564, *De humani corporis fabrica : Basel, 1543*. Octavo edition. Palo Alto, CA : Octavo, 1998.

[22] M. Cambiaghi, 'Andreas Vesalius (1514–1564)', *Journal of Neurology*, vol. 264, no. 8, pp. 1828–1830, Aug. 2017, doi: 10.1007/s00415-017-8459-2.

[23] M. E. DeBroe, D. Sacré, E. D. Snelders, and D. L. De Weerdt, 'The Flemish Anatomist Andreas Vesalius (1514-1564) and the Kidney', *American Journal of Nephrology*, vol. 17, no. 3–4, pp. 252–260, 1997, doi: 10.1159/000169110.

[24] M. Malpighi, *De viscerum structura exercitatio anatomica*. Petrus le Grand, 1669.

[25] P. M. Motta, 'Marcello Malpighi and the foundation of microscopic anatomy', *Prog. Clin. Biol. Res.*, vol. 295, pp. 3–6, 1989.

[26] E. Kinne-Saffran and R. K. Kinne, 'Jacob Henle: the kidney and beyond', *Am. J. Nephrol.*, vol. 14, no. 4–6, pp. 355–360, 1994, doi: 10.1159/000168747.

[27] Bowman, William, 'On the structure and use of the Malpighian bodies of the kidney, with observations on the circulation through that gland', *Philosophical Transactions of the Royal Society of London*, vol. 132, pp. 57–80, Jan. 1842, doi: 10.1098/rstl.1842.0005.

[28] L. G. Fine, 'William Bowman's description of the glomerulus', *Am. J. Nephrol.*, vol. 5, no. 6, pp. 437–440, 1985, doi: 10.1159/000166979.

[29] R. M. Kark, 'A prospect of Richard Bright on the centenary of his death, December 16, 1958', *Am. J. Med.*, vol. 25, no. 6, pp. 819–824, Dec. 1958, doi: 10.1016/0002-9343(58)90055-x.

[30] R. H. Young, 'Dr Richard Bright--father of medical renal disease', *Arch. Pathol. Lab. Med.*, vol. 133, no. 9, p. 1365, Sep. 2009, doi: 10.1043/1543-2165-133.9.1365.

[31] J. S. Cameron, 'Bright's Disease Today: The Pathogenesis and Treatment of Glomerulonephritis I', *BMJ*, vol. 4, no. 5832, pp. 87–90, Oct. 1972, doi: 10.1136/bmj.4.5832.87.

[32] W. B. Cannon, *The Wisdom of the Body. New York: WW Norton & Co*. Inc, 1932.

[33] M. P. Hoenig and M. L. Zeidel, 'Homeostasis, the Milieu Intérieur, and the Wisdom of the Nephron', *Clinical Journal of the American Society of Nephrology*, vol. 9, no. 7, pp. 1272–1281, Jul. 2014, doi: 10.2215/CJN.08860813.

[34] A. R. Cushny, *The Secretion of the Urine*. Longmans, Green and Company, 1917.

[35] J. M. Sands, 'Micropuncture: unlocking the secrets of renal function', *Am. J. Physiol. Renal Physiol.*, vol. 287, no. 5, pp. F866-867, Nov. 2004, doi: 10.1152/classicessays.00019.2004.

[36] J. T. Wearn and A. N. Richards, 'Observations on the composition of glomerular urine, with particular reference to the problem of reabsorption in the renal tubules', *American Journal of Physiology-Legacy Content*, vol. 71, no. 1, pp. 209–227, 1924.

[37] A. N. Richards and A. M. Walker, 'Methods of collecting fluid from known regions of the renal tubules of amphibia and of perfusing the lumen of a single tubule', *American Journal of Physiology-Legacy Content*, vol. 118, no. 1, pp. 111–120, 1936.

[38] H. H. Ussing and K. Zerahn, 'Active transport of sodium as the source of electric current in the short-circuited isolated frog skin', *Acta Physiol. Scand.*, vol. 23, no. 2–3, pp. 110–127, Aug. 1951, doi: 10.1111/j.1748-1716.1951.tb00800.x.

[39] M. B. Burg, J. Grantham, M. Abramow, J. Orloff, and J. A. Schafer, 'Preparation and study of fragments of single rabbit nephrons', *J. Am. Soc. Nephrol.*, vol. 8, no. 4, pp. 675–683, Apr. 1997.

[40] M. B. Burg and M. A. Knepper, 'Single tubule perfusion techniques', *Kidney Int.*, vol. 30, no. 2, pp. 166–170, Aug. 1986, doi: 10.1038/ki.1986.168.

[41] R. A. Wolfe *et al.*, 'Comparison of Mortality in All Patients on Dialysis, Patients on Dialysis Awaiting Transplantation, and Recipients of a First Cadaveric Transplant', *New England Journal of Medicine*, vol. 341, no. 23, pp. 1725–1730, Dec. 1999, doi: 10.1056/NEJM199912023412303.

[42] A. K. Mathur *et al.*, 'Return on investment for financial assistance for living kidney donors in the United States', *Clinical Transplantation*, vol. 32, no. 7, p. e13277, Jul. 2018, doi: 10.1111/ctr.13277.

[43] E. L. Tucker *et al.*, 'Life and expectations post-kidney transplant: a qualitative analysis of patient responses', *BMC Nephrology*, vol. 20, no. 1, Dec. 2019, doi: 10.1186/s12882-019-1368-0.

[44] T. Schlich, *The Origins of Organ Transplantation: Surgery and Laboratory Science, 1880-1930*. University of Rochester Press, 2010.

[45] Carrel A., 'La technique operatoire des anastomoses vasculaires et la transplantation des viscères.', *Lyon Med*, vol. 98:859, 1902.

[46] S. J. Knechtle and L. P. Marson, *Kidney transplantation: principles and practice*, 8th ed. St. Louis: Elsevier, 2019.

[47] E. Matevossian *et al.*, 'Surgeon Yurii Voronoy (1895-1961) - a pioneer in the history of clinical transplantation: in memoriam at the 75th anniversary of the first human kidney transplantation', *Transpl. Int.*, vol. 22, no. 12, pp. 1132–1139, Dec. 2009, doi: 10.1111/j.1432-2277.2009.00986.x.

[48] D. Hamilton, 'Alexis Carrel and the early days of tissue transplantation', *Transplantation Reviews*, vol. 2, pp. 1–15, Jan. 1988, doi: 10.1016/S0955-470X(88)80003-X.

[49] Carrel A., 'The transplantation of organs.', *New York Times*, Apr. 14, 1914.

[50] M. G. McGeown, *Clinical Management of Renal Transplantation*. Springer Netherlands, 2013.

[51] Michon L, Hamburger J, and Oeconomos N, 'Une tentative de transplantation rénale chez l'homme.', *Presse Med*, vol. 61:1419, 1953.

[52] L. Carreras-Planella, M. Monguió-Tortajada, È. Palma, F. E. Borràs, and M. Franquesa, 'Stem Cells: Immunotherapy in Solid Organ Transplantation', in *Reference Module in Biomedical Sciences*, Elsevier, 2018.

[53] M. Hatzinger, M. Stastny, P. Grützmacher, and M. Sohn, '[The history of kidney transplantation]', *Urologe A*, vol. 55, no. 10, pp. 1353–1359, Oct. 2016, doi: 10.1007/s00120-016-0205-3.

[54] R. Marcén, 'Immunosuppressive Drugs in Kidney Transplantation: Impact on Patient Survival, and Incidence of Cardiovascular Disease, Malignancy and Infection', *Drugs*, vol. 69, no. 16, pp. 2227–2243, Nov. 2009, doi: 10.2165/11319260-000000000-00000.

[55] Starzl TE, Marchioro TL, and Waddell WR, 'The reversal of rejection in human renal homografts with subsequent development of homograft tolerance', *Surg Gynecol Obstet*, vol. 117:385, 1963.

[56] G. M. Collins, M. Bravo-Shugarman, and P. I. Terasaki, 'Kidney preservation for transportation. Initial perfusion and 30 hours' ice storage', *Lancet*, vol. 2, no. 7632, pp. 1219–1222, Dec. 1969, doi: 10.1016/s0140-6736(69)90753-3.

[57] T. E. Starzl, S. Todo, J. Fung, A. J. Demetris, R. Venkataramman, and A. Jain, 'FK 506 for liver, kidney, and pancreas transplantation', *Lancet*, vol. 2, no. 8670, pp. 1000–1004, Oct. 1989, doi: 10.1016/s0140-6736(89)91014-3.

[58] K. Heusler and A. Pletscher, 'The controversial early history of cyclosporin', *Swiss Med Wkly*, vol. 131, no. 21–22, pp. 299–302, Jun. 2001, doi: 2001/21/smw-09702.

[59] D. I. Pritchard, 'Sourcing a chemical succession for cyclosporin from parasites and human pathogens', *Drug Discovery Today*, vol. 10, no. 10, pp. 688–691, May 2005, doi: 10.1016/S1359-6446(05)03395-7.

[60] R. Calne, 'Cyclosporine as a milestone in immunosuppression', *Transplant. Proc.*, vol. 36, no. 2 Suppl, pp. 13S-15S, Mar. 2004, doi: 10.1016/j.transproceed.2004.01.042.

[61] H. Ekberg *et al.*, 'Cyclosporine sparing with mycophenolate mofetil, daclizumab and corticosteroids in renal allograft recipients: the CAESAR Study', *Am. J. Transplant.*, vol. 7, no. 3, pp. 560–570, Mar. 2007, doi: 10.1111/j.1600-6143.2006.01645.x.

[62] T. Kino *et al.*, 'FK-506, a novel immunosuppressant isolated from a Streptomyces. I. Fermentation, isolation, and physico-chemical and biological characteristics', *J. Antibiot.*, vol. 40, no. 9, pp. 1249–1255, Sep. 1987, doi: 10.7164/antibiotics.40.1249.

[63] H. Hatanaka, M. Iwami, T. Kino, T. Goto, and M. Okuhara, 'FR-900520 and FR-900523, novel immunosuppressants isolated from a Streptomyces. I. Taxonomy of the producing strain', *J. Antibiot.*, vol. 41, no. 11, pp. 1586–1591, Nov. 1988, doi: 10.7164/antibiotics.41.1586.

[64] Alsberg, C L. and Black, O. F., 'Contributions to the study of maize deteriotation.', *U. S. Dept. Agr. Plant Ind. Bull.*, vol. 270, pp. 5–48, 1913.

[65] R. E. S. Bullingham, A. J. Nicholls, and B. R. Kamm, 'Clinical Pharmacokinetics of Mycophenolate Mofetil':, *Clinical Pharmacokinetics*, vol. 34, no. 6, pp. 429–455, 1998, doi: 10.2165/00003088-199834060-00002.

[66] T. van Gelder and D. A. Hesselink, 'Mycophenolate revisited', *Transpl. Int.*, vol. 28, no. 5, pp. 508–515, May 2015, doi: 10.1111/tri.12554.

[67] J. Chung, C. J. Kuo, G. R. Crabtree, and J. Blenis, 'Rapamycin-FKBP specifically blocks growth-dependent activation of and signaling by the 70 kd S6 protein kinases', *Cell*, vol. 69, no. 7, pp. 1227–1236, Jun. 1992, doi: 10.1016/0092-8674(92)90643-Q.

[68] C. J. Kuo, J. Chung, D. F. Fiorentino, W. M. Flanagan, J. Blenis, and G. R. Crabtree, 'Rapamycin selectively inhibits interleukin-2 activation of p70 S6 kinase', *Nature*, vol. 358, no. 6381, pp. 70–73, Jul. 1992, doi: 10.1038/358070a0.

[69] D. Price, Grove, V. Calvo, J. Avruch, and B. Bierer, 'Rapamycin-induced inhibition of the 70-kilodalton S6 protein kinase', *Science*, vol. 257, no. 5072, pp. 973–977, Aug. 1992, doi: 10.1126/science.1380182.

[70] J. Heitman, 'On the Discovery of TOR As the Target of Rapamycin', *PLOS Pathogens*, vol. 11, no. 11, p. e1005245, Nov. 2015, doi: 10.1371/journal.ppat.1005245.

[71] P. Ventura-Aguiar, J. M. Campistol, and F. Diekmann, 'Safety of mTOR inhibitors in adult solid organ transplantation', *Expert Opinion on Drug Safety*, vol. 15, no. 3, pp. 303–319, Mar. 2016, doi: 10.1517/14740338.2016.1132698.

[72] The Editors of Encyclopaedia Britannica, 'Encyclopædia Britannica', *Nephron*, Sep. 04, 2019. https://www.britannica.com/science/nephron (accessed Sep. 12, 2019).

[73] S. Gurusinghe, A. Tambay, and C. B. Sethna, 'Developmental Origins and Nephron Endowment in Hypertension', *Frontiers in Pediatrics*, vol. 5, Jun. 2017, doi: 10.3389/fped.2017.00151.

[74] J. P. Arroyo and A. J. Schweickert, 'Fluid Handling by the Kidneys', in *Back to Basics in Physiology*, Elsevier, 2013, pp. 77–105.

[75] Y. L. Cheng and A. W. Yu, 'ELECTROLYTES | Water–Electrolyte Balance', in *Encyclopedia of Food Sciences and Nutrition*, Elsevier, 2003, pp. 2039–2047.

[76] J. Hou, *The paracellular channel: biology, physiology, and disease*. London: Elsevier/Academic Press, 2019.

[77] M. P. Bohrer, C. Baylis, H. D. Humes, R. J. Glassock, C. R. Robertson, and B. M. Brenner, 'Permselectivity of the Glomerular Capillary Wall', *Journal of Clinical Investigation*, vol. 61, no. 1, pp. 72–78, Jan. 1978, doi: 10.1172/JCI108927.

[78] W. D. Comper and E. F. Glasgow, 'Charge selectivity in kidney ultrafiltration', *Kidney International*, vol. 47, no. 5, pp. 1242–1251, May 1995, doi: 10.1038/ki.1995.178.

[79] N. P. Goode, M. Shires, and A. M. Davison, 'The glomerular basement membrane charge-selectivity barrier: an oversimplified concept?', *Nephrology Dialysis Transplantation*, vol. 11, no. 9, pp. 1714–1716, Sep. 1996, doi: 10.1093/ndt/11.9.1714.

[80] P. Greaves, 'Urinary Tract', in *Histopathology of Preclinical Toxicity Studies*, Elsevier, 2007, pp. 570–660.

[81] B. M. Koeppen and B. A. Stanton, 'Renal Transport Mechanisms', in *Renal Physiology*, Elsevier, 2013, pp. 45–71.

[82] N. P. Curthoys and O. W. Moe, 'Proximal Tubule Function and Response to Acidosis', *Clinical Journal of the American Society of Nephrology*, vol. 9, no. 9, pp. 1627–1638, Sep. 2014, doi: 10.2215/CJN.10391012.

[83] G. Jones, D. E. Prosser, and M. Kaufmann, '25-Hydroxyvitamin D-24-hydroxylase (CYP24A1): its important role in the degradation of vitamin D', *Arch. Biochem. Biophys.*, vol. 523, no. 1, pp. 9–18, Jul. 2012, doi: 10.1016/j.abb.2011.11.003.

[84] C. Meyer, J. M. Dostou, and J. E. Gerich, 'Role of the human kidney in glucose counterregulation', *Diabetes*, vol. 48, no. 5, pp. 943–948, May 1999, doi: 10.2337/diabetes.48.5.943.

[85] M. Alsahli and J. E. Gerich, 'Renal glucose metabolism in normal physiological conditions and in diabetes', *Diabetes Res. Clin. Pract.*, vol. 133, pp. 1–9, Nov. 2017, doi: 10.1016/j.diabres.2017.07.033.

[86] E. De Vito, R. R. Cabrera, and J. C. Fasciolo, 'Renin production and release by rat kidney slices', *Am. J. Physiol.*, vol. 219, no. 4, pp. 1042–1045, Oct. 1970, doi: 10.1152/ajplegacy.1970.219.4.1042.

[87] S. T. Koury, M. C. Bondurant, and M. J. Koury, 'Localization of erythropoietin synthesizing cells in murine kidneys by in situ hybridization', *Blood*, vol. 71, no. 2, pp. 524–527, Feb. 1988.

[88] O. W. Moe *et al.*, 'Renin expression in renal proximal tubule', *J. Clin. Invest.*, vol. 91, no. 3, pp. 774–779, Mar. 1993, doi: 10.1172/JCI116296.

[89] B. M. Koeppen and B. A. Stanton, *Renal physiology*. 2019.

[90] M. A. Breshears and A. W. Confer, 'The Urinary System1', in *Pathologic Basis of Veterinary Disease*, Elsevier, 2017, pp. 617-681.e1.

[91] National Kidney Foundation, 'K/DOQI clinical practice guidelines for chronic kidney disease: evaluation, classification, and stratification', *Am. J. Kidney Dis.*, vol. 39, no. 2 Suppl 1, pp. S1-266, Feb. 2002.

[92] T. K. Chen, D. H. Knicely, and M. E. Grams, 'Chronic Kidney Disease Diagnosis and Management: A Review', *JAMA*, vol. 322, no. 13, p. 1294, Oct. 2019, doi: 10.1001/jama.2019.14745.

[93] O. E. Ayodele and C. O. Alebiosu, 'Burden of Chronic Kidney Disease: An International Perspective', *Advances in Chronic Kidney Disease*, vol. 17, no. 3, pp. 215–224, May 2010, doi: 10.1053/j.ackd.2010.02.001.

[94] V. Jha *et al.*, 'Chronic kidney disease: global dimension and perspectives', *The Lancet*, vol. 382, no. 9888, pp. 260–272, Jul. 2013, doi: 10.1016/S0140-6736(13)60687-X.

[95] K. J. Jager, C. Kovesdy, R. Langham, M. Rosenberg, V. Jha, and C. Zoccali, 'A single number for advocacy and communication—worldwide more than 850 million individuals have kidney diseases', *Nephrology Dialysis Transplantation*, vol. 34, no. 11, pp. 1803–1805, Nov. 2019, doi: 10.1093/ndt/gfz174.

[96] J. Coresh *et al.*, 'Prevalence of Chronic Kidney Disease in the United States', *JAMA*, vol. 298, no. 17, p. 2038, Nov. 2007, doi: 10.1001/jama.298.17.2038.

[97] C. Hsu, E. Vittinghoff, F. Lin, and M. G. Shlipak, 'The Incidence of End-Stage Renal Disease Is Increasing Faster than the Prevalence of Chronic Renal Insufficiency', *Annals of Internal Medicine*, vol. 141, no. 2, p. 95, Jul. 2004, doi: 10.7326/0003-4819-141-2-200407200-00007.

[98] M. Naghavi *et al.*, 'Global, regional, and national age-sex specific mortality for 264 causes of death, 1980–2016: a systematic analysis for the Global Burden of Disease Study 2016', *The Lancet*, vol. 390, no. 10100, pp. 1151–1210, Sep. 2017, doi: 10.1016/S0140-6736(17)32152-9.

[99] K. J. Foreman *et al.*, 'Forecasting life expectancy, years of life lost, and all-cause and cause-specific mortality for 250 causes of death: reference and alternative scenarios for 2016-40 for 195 countries and territories', *Lancet*, vol. 392, no. 10159, pp. 2052–2090, 10 2018, doi: 10.1016/S0140-6736(18)31694-5.

[100] 'Annual Reports', *ERA-EDTA*. https://www.era-edta.org/en/about-era-edta/organization-governance/annual-reports/ (accessed Jan. 09, 2020).

[101] M. Abecassis *et al.*, 'Kidney Transplantation as Primary Therapy for End-Stage Renal Disease: A National Kidney Foundation/Kidney Disease Outcomes Quality Initiative (NKF/KDOQI™) Conference', *Clinical Journal of the American Society of Nephrology*, vol. 3, no. 2, pp. 471–480, Mar. 2008, doi: 10.2215/CJN.05021107.

[102] 'History', *ERA-EDTA*. https://www.era-edta.org/en/about-era-edta/who-we-are/history/ (accessed Jan. 08, 2020).

[103] W. Drukker, 'The founding of the EDTA: facts and lessons', *Nephrol. Dial. Transplant.*, vol. 4, no. 5, pp. 401–407, 1989, doi: 10.1093/oxfordjournals.ndt.a091901.

[104] D. N. Kerr, 'EDTA to ERA', *Nephrol. Dial. Transplant.*, vol. 4, no. 5, pp. 411–415, 1989, doi: 10.1093/oxfordjournals.ndt.a091903.

[105] 'Organización Nacional de Trasplantes'. http://www.ont.es/Paginas/Home.aspx (accessed Jan. 09, 2020).

[106] 'Sociedad Española de Nefrología'. https://www.senefro.org/modules.php?name=home&lang=ES (accessed Jan. 09, 2020).

[107] J. Lloveras, 'The Gold Medal of the Catalan Transplantation Society to Professors J.M. Gil-Vernet and A. Caralps', *Transplant. Proc.*, vol. 31, no. 6, pp. 2199–2200, Sep. 1999, doi: 10.1016/s0041-1345(99)00305-x.

[108] '50 anys del primer trasplantament de ronyó', *Ara.cat*, Nov. 26, 2015. https://www.ara.cat/societat/anys-del-trasplantament-ronyo_0_1372662750.html (accessed Jan. 20, 2020).

[109] M. D. Gautreaux, 'Histocompatibility Testing in the Transplant Setting', in *Kidney Transplantation, Bioengineering and Regeneration*, Elsevier, 2017, pp. 223–234.

[110] B. J. Nankivell and S. I. Alexander, 'Rejection of the Kidney Allograft', *New England Journal of Medicine*, vol. 363, no. 15, pp. 1451–1462, Oct. 2010, doi: 10.1056/NEJMra0902927.

[111] S. A. Joosten, Y. W. J. Sijpkens, C. van Kooten, and L. C. Paul, 'Chronic renal allograft rejection: Pathophysiologic considerations', *Kidney International*, vol. 68, no. 1, pp. 1–13, Jul. 2005, doi: 10.1111/j.1523-1755.2005.00376.x.

[112] M. Haas *et al.*, 'The Banff 2017 Kidney Meeting Report: Revised diagnostic criteria for chronic active T cell-mediated rejection, antibody-mediated rejection, and prospects for integrative endpoints for next-generation clinical trials', *Am. J. Transplant.*, vol. 18, no. 2, pp. 293–307, 2018, doi: 10.1111/ajt.14625.

[113] A. F. Williams, E. Manias, C. J. Gaskin, and K. Crawford, 'Medicine non-adherence in kidney transplantation: medicine non-adherence in kidney transplantation', *Journal of Renal Care*, vol. 40, no. 2, pp. 107–116, Jun. 2014, doi: 10.1111/jorc.12063.

[114] J.-P. G. Squifflet, A. C. Gruessner, and R. W. G. Gruessner, 'Pancreas transplantation, bioengineering, and regeneration', in *Transplantation, Bioengineering, and Regeneration of the Endocrine Pancreas*, Elsevier, 2020, pp. 259–276.

[115] N. Singh, J. Pirsch, and M. Samaniego, 'Antibody-mediated rejection: treatment alternatives and outcomes', *Transplantation Reviews*, vol. 23, no. 1, pp. 34–46, Jan. 2009, doi: 10.1016/j.trre.2008.08.004.

[116] H.-U. Meier-Kriesche, J. D. Schold, T. R. Srinivas, and B. Kaplan, 'Lack of improvement in renal allograft survival despite a marked decrease in acute rejection rates over the most recent era', *Am. J. Transplant.*, vol. 4, no. 3, pp. 378–383, Mar. 2004.

[117] M. Naesens *et al.*, 'The histology of kidney transplant failure: a long-term follow-up study', *Transplantation*, vol. 98, no. 4, pp. 427–435, Aug. 2014, doi: 10.1097/TP.0000000000000183.

[118] H.-U. Meier-Kriesche, J. D. Schold, and B. Kaplan, 'Long-term renal allograft survival: have we made significant progress or is it time to rethink our analytic and therapeutic strategies?', *Am. J. Transplant.*, vol. 4, no. 8, pp. 1289–1295, Aug. 2004, doi: 10.1111/j.1600-6143.2004.00515.x.

[119] J. Sellarés *et al.*, 'Understanding the Causes of Kidney Transplant Failure: The Dominant Role of Antibody-Mediated Rejection and Nonadherence: Attributing Causes of Kidney Transplant Loss', *American Journal of Transplantation*, vol. 12, no. 2, pp. 388–399, Feb. 2012, doi: 10.1111/j.1600-6143.2011.03840.x.

[120] A. Gondos, B. Döhler, H. Brenner, and G. Opelz, 'Kidney Graft Survival in Europe and the United States: Strikingly Different Long-Term Outcomes', *Transplantation Journal*, vol. 95, no. 2, pp. 267–274, Jan. 2013, doi: 10.1097/TP.0b013e3182708ea8.

[121] K. E. Lamb, S. Lodhi, and H.-U. Meier-Kriesche, 'Long-term renal allograft survival in the United States: a critical reappraisal', *Am. J. Transplant.*, vol. 11, no. 3, pp. 450–462, Mar. 2011, doi: 10.1111/j.1600-6143.2010.03283.x.

[122] M. Quaglia, G. Merlotti, G. Guglielmetti, G. Castellano, and V. Cantaluppi, 'Recent Advances on Biomarkers of Early and Late Kidney Graft Dysfunction', *International Journal of Molecular Sciences*, vol. 21, no. 15, p. 5404, Jul. 2020, doi: 10.3390/ijms21155404.

[123] G. A. Böhmig, F. Eskandary, K. Doberer, and P. F. Halloran, 'The therapeutic challenge of late antibody-mediated kidney allograft rejection', *Transplant International*, May 2019, doi: 10.1111/tri.13436.

[124] J. R. Chapman, P. J. O'Connell, and B. J. Nankivell, 'Chronic renal allograft dysfunction', *J. Am. Soc. Nephrol.*, vol. 16, no. 10, pp. 3015–3026, Oct. 2005, doi: 10.1681/ASN.2005050463.

[125] L. C. Racusen and H. Regele, 'The pathology of chronic allograft dysfunction', *Kidney International*, vol. 78, pp. S27–S32, Dec. 2010, doi: 10.1038/ki.2010.419.

[126] P. E. Morrissey, M. L. Flynn, and S. Lin, 'Medication Noncompliance and its Implications in Transplant Recipients':, *Drugs*, vol. 67, no. 10, pp. 1463–1481, 2007, doi: 10.2165/00003495-200767100-00007.

[127] E. Akalin and P. J. O'Connell, 'Genomics of chronic allograft injury', *Kidney International*, vol. 78, pp. S33–S37, Dec. 2010, doi: 10.1038/ki.2010.420.

[128] Z. M. El-Zoghby *et al.*, 'Identifying specific causes of kidney allograft loss', *Am. J. Transplant.*, vol. 9, no. 3, pp. 527–535, Mar. 2009, doi: 10.1111/j.1600-6143.2008.02519.x.

[129] D. C. Rockey, P. D. Bell, and J. A. Hill, 'Fibrosis — A Common Pathway to Organ Injury and Failure', *New England Journal of Medicine*, vol. 372, no. 12, pp. 1138–1149, Mar. 2015, doi: 10.1056/NEJMra1300575.

[130] A.-E. Declèves and K. Sharma, 'Novel targets of antifibrotic and anti-inflammatory treatment in CKD', *Nature Reviews Nephrology*, vol. 10, no. 5, pp. 257–267, May 2014, doi: 10.1038/nrneph.2014.31.

[131] H. A. M. Mutsaers, E. G. D. Stribos, G. Glorieux, R. Vanholder, and P. Olinga, 'Chronic Kidney Disease and Fibrosis: The Role of Uremic Retention Solutes', *Frontiers in Medicine*, vol. 2, Aug. 2015, doi: 10.3389/fmed.2015.00060.

[132] X. Meng, D. J. Nikolic-Paterson, and H. Y. Lan, 'TGF-β: the master regulator of fibrosis', *Nature Reviews Nephrology*, vol. 12, no. 6, pp. 325–338, Jun. 2016, doi: 10.1038/nrneph.2016.48.

[133] J. Massagué, 'TGFβ signalling in context', *Nature Reviews Molecular Cell Biology*, vol. 13, no. 10, pp. 616–630, Oct. 2012, doi: 10.1038/nrm3434.

[134] B. D. Humphreys *et al.*, 'Fate Tracing Reveals the Pericyte and Not Epithelial Origin of Myofibroblasts in Kidney Fibrosis', *The American Journal of Pathology*, vol. 176, no. 1, pp. 85–97, Jan. 2010, doi: 10.2353/ajpath.2010.090517.

[135] P. Boor, T. Ostendorf, and J. Floege, 'Renal fibrosis: novel insights into mechanisms and therapeutic targets', *Nature Reviews Nephrology*, vol. 6, no. 11, pp. 643–656, Nov. 2010, doi: 10.1038/nrneph.2010.120.

[136] C. Fligny and J. S. Duffield, 'Activation of pericytes: recent insights into kidney fibrosis and microvascular rarefaction', *Current Opinion in Rheumatology*, vol. 25, no. 1, pp. 78–86, Jan. 2013, doi: 10.1097/BOR.0b013e32835b656b.

[137] T. Vanhove, R. Goldschmeding, and D. Kuypers, 'Kidney Fibrosis: Origins and Interventions', *Transplantation*, vol. 101, no. 4, pp. 713–726, Apr. 2017, doi: 10.1097/TP.0000000000001608.

[138] Y. Wang, L. Jia, Z. Hu, M. L. Entman, W. E. Mitch, and Y. Wang, 'AMP-activated protein kinase/myocardin-related transcription factor-A signaling regulates fibroblast activation and renal fibrosis', *Kidney International*, vol. 93, no. 1, pp. 81–94, Jan. 2018, doi: 10.1016/j.kint.2017.04.033.

[139] M. J. Vitalone, P. J. O'Connell, M. Wavamunno, C. L.-S. Fung, J. R. Chapman, and B. J. Nankivell, 'Transcriptome Changes of Chronic Tubulointerstitial Damage in Early Kidney Transplantation':, *Transplantation*, vol. 89, no. 5, pp. 537–547, Mar. 2010, doi: 10.1097/TP.0b013e3181ca7389.

[140] F. G. Cosio *et al.*, 'Kidney allograft fibrosis and atrophy early after living donor transplantation', *Am. J. Transplant.*, vol. 5, no. 5, pp. 1130–1136, May 2005, doi: 10.1111/j.1600-6143.2005.00811.x.

[141] B. J. Nankivell *et al.*, 'Effect of histological damage on long-term kidney transplant outcome', *Transplantation*, vol. 71, no. 4, pp. 515–523, Feb. 2001, doi: 10.1097/00007890-200102270-00006.

[142] P. C. Grimm *et al.*, 'Computerized image analysis of Sirius Red-stained renal allograft biopsies as a surrogate marker to predict long-term allograft function', *J. Am. Soc. Nephrol.*, vol. 14, no. 6, pp. 1662–1668, Jun. 2003, doi: 10.1097/01.asn.0000066143.02832.5e.

[143] M. C. Roos-van Groningen *et al.*, 'Molecular comparison of calcineurin inhibitor-induced fibrogenic responses in protocol renal transplant biopsies', *J. Am. Soc. Nephrol.*, vol. 17, no. 3, pp. 881–888, Mar. 2006, doi: 10.1681/ASN.2005080891.

[144] A. Servais *et al.*, 'Interstitial fibrosis evolution on early sequential screening renal allograft biopsies using quantitative image analysis', *Am. J. Transplant.*, vol. 11, no. 7, pp. 1456–1463, Jul. 2011, doi: 10.1111/j.1600-6143.2011.03594.x.

[145] D. Serón, F. Moreso, X. Fulladosa, M. Hueso, M. Carrera, and J. M. Grinyó, 'Reliability of chronic allograft nephropathy diagnosis in sequential protocol biopsies', *Kidney Int.*, vol. 61, no. 2, pp. 727–733, Feb. 2002, doi: 10.1046/j.1523-1755.2002.00174.x.

[146] L. Pape *et al.*, 'Computer-assisted quantification of fibrosis in chronic allograft nephropaty by picosirius red-staining: a new tool for predicting long-term graft

function', *Transplantation*, vol. 76, no. 6, pp. 955–958, Sep. 2003, doi: 10.1097/01.TP.0000078899.62040.E5.

[147] F. G. Cosio, M. El Ters, L. D. Cornell, C. A. Schinstock, and M. D. Stegall, 'Changing Kidney Allograft Histology Early Posttransplant: Prognostic Implications of 1-Year Protocol Biopsies', *Am. J. Transplant.*, vol. 16, no. 1, pp. 194–203, Jan. 2016, doi: 10.1111/ajt.13423.

[148] A. Schwarz *et al.*, 'Risk factors for chronic allograft nephropathy after renal transplantation: a protocol biopsy study', *Kidney Int.*, vol. 67, no. 1, pp. 341–348, Jan. 2005, doi: 10.1111/j.1523-1755.2005.00087.x.

[149] R. John, A. Konvalinka, A. Tobar, S. J. Kim, H. N. Reich, and A. M. Herzenberg, 'Determinants of long-term graft outcome in transplant glomerulopathy', *Transplantation*, vol. 90, no. 7, pp. 757–764, Oct. 2010, doi: 10.1097/TP.0b013e3181efcffd.

[150] A. Djamali, 'Oxidative stress as a common pathway to chronic tubulointerstitial injury in kidney allografts', *American Journal of Physiology-Renal Physiology*, vol. 293, no. 2, pp. F445–F455, Aug. 2007, doi: 10.1152/ajprenal.00037.2007.

[151] K. A. Andreoni, K. L. Brayman, M. K. Guidinger, C. M. Sommers, and R. S. Sung, 'Kidney and pancreas transplantation in the United States, 1996-2005', *American Journal of Transplantation*, vol. 7, no. s1, pp. 1359–1375, May 2007, doi: 10.1111/j.1600-6143.2006.01781.x.

[152] P. J. Morris and S. J. Knechtle, *Kidney transplantation: principles and practice*. 2014.

[153] S. Martínez-Martínez and J. M. Redondo, 'Inhibitors of the calcineurin/NFAT pathway', *Curr. Med. Chem.*, vol. 11, no. 8, pp. 997–1007, Apr. 2004, doi: 10.2174/0929867043455576.

[154] A. Khanna, M. Plummer, C. Bromberek, B. Bresnahan, and S. Hariharan, 'Expression of TGF-beta and fibrogenic genes in transplant recipients with tacrolimus and cyclosporine nephrotoxicity', *Kidney Int.*, vol. 62, no. 6, pp. 2257–2263, Dec. 2002, doi: 10.1046/j.1523-1755.2002.00668.x.

[155] M. Naesens, D. R. J. Kuypers, and M. Sarwal, 'Calcineurin Inhibitor Nephrotoxicity', *Clinical Journal of the American Society of Nephrology*, vol. 4, no. 2, pp. 481–508, Feb. 2009, doi: 10.2215/CJN.04800908.

[156] N. Issa, A. Kukla, and H. N. Ibrahim, 'Calcineurin inhibitor nephrotoxicity: a review and perspective of the evidence', *American Journal of Nephrology*, vol. 37, no. 6, pp. 602–612, 2013, doi: 10.1159/000351648.

[157] R. P. Kershner and W. E. Fitzsimmons, 'Relationship of FK506 whole blood concentrations and efficacy and toxicity after liver and kidney transplantation', *Transplantation*, vol. 62, no. 7, pp. 920–926, Oct. 1996, doi: 10.1097/00007890-199610150-00009.

[158] D. A. Hesselink, R. Bouamar, and T. van Gelder, 'The pharmacogenetics of calcineurin inhibitor-related nephrotoxicity', *Ther Drug Monit*, vol. 32, no. 4, pp. 387–393, Aug. 2010, doi: 10.1097/FTD.0b013e3181e44244.

[159] W. W. Williams, D. Taheri, N. Tolkoff-Rubin, and R. B. Colvin, 'Clinical role of the renal transplant biopsy', *Nature Reviews Nephrology*, vol. 8, no. 2, pp. 110–121, Feb. 2012, doi: 10.1038/nrneph.2011.213.

[160] Kidney Disease: Improving Global Outcomes (KDIGO) Transplant Work Group, 'KDIGO clinical practice guideline for the care of kidney transplant recipients', *Am. J. Transplant.*, vol. 9 Suppl 3, pp. S1-155, Nov. 2009, doi: 10.1111/j.1600-6143.2009.02834.x.

[161] K. Solez, F. Vincenti, and R. S. Filo, 'Histopathologic findings from 2-year protocol biopsies from a U.S. multicenter kidney transplant trial comparing tarolimus versus cyclosporine: a report of the FK506 Kidney Transplant Study Group', *Transplantation*, vol. 66, no. 12, pp. 1736–1740, Dec. 1998, doi: 10.1097/00007890-199812270-00029.

[162] M. K. Shamseddin and G. A. Knoll, 'Posttransplantation proteinuria: an approach to diagnosis and management', *Clin J Am Soc Nephrol*, vol. 6, no. 7, pp. 1786–1793, Jul. 2011, doi: 10.2215/CJN.01310211.

[163] H. Reichel, M. Zeier, and E. Ritz, 'Proteinuria after renal transplantation: pathogenesis and management', *Nephrol. Dial. Transplant.*, vol. 19, no. 2, pp. 301–305, Feb. 2004, doi: 10.1093/ndt/gfh002.

[164] I. A. Al-Awwa, S. Hariharan, and M. R. First, 'Importance of allograft biopsy in renal transplant recipients: correlation between clinical and histological diagnosis', *Am. J. Kidney Dis.*, vol. 31, no. 6 Suppl 1, pp. S15-18, Jun. 1998, doi: 10.1053/ajkd.1998.v31.pm9631859.

[165] S. Amoueian and A. Attaranzadeh, 'Renal Biopsy Interpretation', in *Topics in Renal Biopsy and Pathology*, M. Mubarak, Ed. InTech, 2012.

[166] A. D. Kirk, L. M. Jacobson, D. M. Heisey, N. F. Radke, J. D. Pirsch, and H. W. Sollinger, 'Clinically stable human renal allografts contain histological and RNA-based findings that correlate with deteriorating graft function', *Transplantation*, vol. 68, no. 10, pp. 1578–1582, Nov. 1999, doi: 10.1097/00007890-199911270-00024.

[167] D. N. Rush, S. F. Henry, J. R. Jeffery, T. J. Schroeder, and J. Gough, 'Histological findings in early routine biopsies of stable renal allograft recipients', *Transplantation*, vol. 57, no. 2, pp. 208–211, Jan. 1994, doi: 10.1097/00007890-199401001-00009.

[168] F. G. Cosio, J. P. Grande, H. Wadei, T. S. Larson, M. D. Griffin, and M. D. Stegall, 'Predicting subsequent decline in kidney allograft function from early surveillance biopsies', *Am. J. Transplant.*, vol. 5, no. 10, pp. 2464–2472, Oct. 2005, doi: 10.1111/j.1600-6143.2005.01050.x.

[169] A. Wilkinson, 'Protocol Transplant Biopsies: Are They Really Needed?', *Clinical Journal of the American Society of Nephrology*, vol. 1, no. 1, pp. 130–137, Jan. 2006, doi: 10.2215/CJN.00350705.

[170] C. Roufosse *et al.*, 'A 2018 Reference Guide to the Banff Classification of Renal Allograft Pathology':, *Transplantation*, vol. 102, no. 11, pp. 1795–1814, Nov. 2018, doi: 10.1097/TP.0000000000002366.

[171] K. Solez *et al.*, 'International standardization of criteria for the histologic diagnosis of renal allograft rejection: the Banff working classification of kidney transplant pathology', *Kidney international*, vol. 44, no. 2, pp. 411–422, 1993.

[172] D. Bhowmik, A. Dinda, P. Mahanta, and S. Agarwal, 'The evolution of the Banff classification schema for diagnosing renal allograft rejection and its implications for clinicians', *Indian Journal of Nephrology*, vol. 20, no. 1, p. 2, 2010, doi: 10.4103/0971-4065.62086.

[173] L. C. Racusen *et al.*, 'The Banff 97 working classification of renal allograft pathology', *Kidney International*, vol. 55, no. 2, pp. 713–723, Feb. 1999, doi: 10.1046/j.1523-1755.1999.00299.x.

[174] B. Sis *et al.*, 'A New Diagnostic Algorithm for Antibody-Mediated Microcirculation Inflammation in Kidney Transplants: Microcirculation Inflammation', *American*

Journal of Transplantation, vol. 12, no. 5, pp. 1168–1179, May 2012, doi: 10.1111/j.1600-6143.2011.03931.x.

[175] Berchtold L and Friedli I, Vallée JP, Moll S, Martin PY, de Seigneux S., 'Diagnosis and assessment of renal fibrosis: the state of the art', *Swiss Medical Weekly*, vol. 147, no. 1920, May 2017, doi: 10.4414/smw.2017.14442.

[176] N. Marcussen, T. S. Olsen, H. Benediktsson, L. Racusen, and K. Solez, 'Reproducibility of the Banff classification of renal allograft pathology: inter- and intraobserver variation', *Transplantation*, vol. 60, no. 10, pp. 1083–1089, Nov. 1995, doi: 10.1097/00007890-199511270-00004.

[177] P. Liptak and B. Ivanyi, 'Primer: Histopathology of calcineurin-inhibitor toxicity in renal allografts', *Nat Clin Pract Nephrol*, vol. 2, no. 7, pp. 398–404; quiz following 404, Jul. 2006, doi: 10.1038/ncpneph0225.

[178] D. A. Charney, M. Bhaskaran, and E. Molmenti, 'Calcineurin inhibitor toxicity in a renal transplant recipient', *Clinical Kidney Journal*, vol. 2, no. 2, pp. 175–176, Apr. 2009, doi: 10.1093/ndtplus/sfp007.

[179] A. B. Fogo, M. A. Lusco, B. Najafian, and C. E. Alpers, 'AJKD Atlas of renal pathology: osmotic tubular injury', *American Journal of Kidney Diseases*, vol. 69, no. 2, pp. e11–e12, Feb. 2017, doi: 10.1053/j.ajkd.2016.12.003.

[180] E. Vazquez Martul, 'Microangiopatía trombótica/síndrome hemolítico urémico. Actualización de sus características histopatológicas', *Revista Española de Patología*, vol. 51, no. 3, pp. 170–177, Jul. 2018, doi: 10.1016/j.patol.2017.10.007.

[181] N. Kambham, S. Nagarajan, S. Shah, L. Li, O. Salvatierra, and M. M. Sarwal, 'A Novel, Semiquantitative, Clinically Correlated Calcineurin Inhibitor Toxicity Score for Renal Allograft Biopsies', *Clinical Journal of the American Society of Nephrology*, vol. 2, no. 1, pp. 135–142, Jan. 2007, doi: 10.2215/CJN.01320406.

[182] R. Leal, D. Tsapepas, R. J. Crew, G. K. Dube, L. Ratner, and I. Batal, 'Pathology of calcineurin and mammalian target of rapamycin inhibitors in kidney transplantation', *Kidney International Reports*, vol. 3, no. 2, pp. 281–290, Mar. 2018, doi: 10.1016/j.ekir.2017.10.010.

[183] J. Feehally, Ed., *Comprehensive clinical nephrology*, Sixth edition. Edinburgh ; New York: Elsevier, 2019.

[184] M. Haas, 'Donor kidney biopsies: pathology matters, and so does the pathologist', *Kidney International*, vol. 85, no. 5, pp. 1016–1019, May 2014, doi: 10.1038/ki.2013.439.

[185] Tapia-Canelas, Claudia *et al.*, 'Complicaciones asociadas a la biopsia de injertos renales en pacientes trasplantados', *Nefrología*, vol. 34(1):115–9, Diciembre 2013, doi: 10.3265/Nefrologia.pre2013.Nov.12232.

[186] J. S. Lees, E. P. McQuarrie, and B. Mackinnon, 'Renal biopsy: it is time for pragmatism and consensus', *Clin Kidney J*, vol. 11, no. 5, pp. 605–609, Oct. 2018, doi: 10.1093/ckj/sfy075.

[187] 'Clinical competence in percutaneous renal biopsy. Health and Public Policy Committee. American College of Physicians', *Ann. Intern. Med.*, vol. 108, no. 2, pp. 301–303, Feb. 1988.

[188] J. Bandari, T. W. Fuller, R. M. T. Ii, and L. A. D'Agostino, 'Renal biopsy for medical renal disease: indications and contraindications', *The Canadian Journal of Urology*, p. 6, 2016.

[189] C. M. Yuan, R. M. Jindal, and K. C. Abbott, 'Observation time after kidney biopsy: when to discharge?', *Nature Reviews Nephrology*, vol. 5, no. 10, pp. 552–554, Oct. 2009, doi: 10.1038/nrneph.2009.147.

[190] N. Dhaun, C. O. Bellamy, D. C. Cattran, and D. C. Kluth, 'Utility of renal biopsy in the clinical management of renal disease', *Kidney International*, vol. 85, no. 5, pp. 1039–1048, May 2014, doi: 10.1038/ki.2013.512.

[191] J. Reeve *et al.*, 'Diagnosing Rejection in Renal Transplants: A Comparison of Molecular- and Histopathology-Based Approaches', *American Journal of Transplantation*, vol. 9, no. 8, pp. 1802–1810, Aug. 2009, doi: 10.1111/j.1600-6143.2009.02694.x.

[192] M. Fiorentino *et al.*, 'Renal Biopsy in 2015--From Epidemiology to Evidence-Based Indications', *Am. J. Nephrol.*, vol. 43, no. 1, pp. 1–19, 2016, doi: 10.1159/000444026.

[193] D. J. Lo, B. Kaplan, and A. D. Kirk, 'Biomarkers for kidney transplant rejection', *Nature Reviews Nephrology*, vol. 10, no. 4, pp. 215–225, Apr. 2014, doi: 10.1038/nrneph.2013.281.

[194] Biomarkers Definitions Working Group, 'Biomarkers and surrogate endpoints: Preferred definitions and conceptual framework', *Clinical Pharmacology & Therapeutics*, vol. 69, no. 3, pp. 89–95, Mar. 2001, doi: 10.1067/mcp.2001.113989.

[195] B. J. Nankivell, R. J. Borrows, C. L.-S. Fung, P. J. O'Connell, R. D. M. Allen, and J. R. Chapman, 'The natural history of chronic allograft nephropathy', *N. Engl. J. Med.*, vol. 349, no. 24, pp. 2326–2333, Dec. 2003, doi: 10.1056/NEJMoa020009.

[196] D. N. Rush *et al.*, 'Factors associated with progression of interstitial fibrosis in renal transplant patients receiving tacrolimus and mycophenolate mofetil', *Transplantation*, vol. 88, no. 7, pp. 897–903, Oct. 2009, doi: 10.1097/TP.0b013e3181b723f4.

[197] H. N. Reich *et al.*, 'Molecular Markers of Injury in Kidney Biopsy Specimens of Patients with Lupus Nephritis', *The Journal of Molecular Diagnostics*, vol. 13, no. 2, pp. 143–151, Mar. 2011, doi: 10.1016/j.jmoldx.2010.10.005.

[198] P. F. Halloran, K. S. Famulski, and J. Reeve, 'Molecular assessment of disease states in kidney transplant biopsy samples', *Nature Reviews Nephrology*, vol. 12, p. 534, Jun. 2016.

[199] A. Chakraborty and M. Sarwal, 'Protein biomarkers in renal transplantation', *Expert Review of Proteomics*, vol. 15, no. 1, pp. 41–54, Jan. 2018, doi: 10.1080/14789450.2018.1396892.

[200] S. Kar, S. Paglialunga, and R. Islam, 'Cystatin C Is a More Reliable Biomarker for Determining eGFR to Support Drug Development Studies', *The Journal of Clinical Pharmacology*, vol. 58, no. 10, pp. 1239–1247, Oct. 2018, doi: 10.1002/jcph.1132.

[201] J. V. Bonventre, 'Kidney injury molecule-1 (KIM-1): a urinary biomarker and much more', *Nephrology Dialysis Transplantation*, vol. 24, no. 11, pp. 3265–3268, Nov. 2009, doi: 10.1093/ndt/gfp010.

[202] V. Au, J. Feit, J. Barasch, R. N. Sladen, and G. Wagener, 'Urinary Neutrophil Gelatinase–Associated Lipocalin (NGAL) Distinguishes Sustained From Transient Acute Kidney Injury After General Surgery', *Kidney International Reports*, vol. 1, no. 1, pp. 3–9, May 2016, doi: 10.1016/j.ekir.2016.04.003.

[203] H. M. Choi *et al.*, 'Urine Neutrophil Gelatinase-Associated Lipocalin Predicts Graft Outcome up to 1 Year After Kidney Transplantation', *Transplantation Proceedings*, vol. 45, no. 1, pp. 122–128, Jan. 2013, doi: 10.1016/j.transproceed.2012.05.080.

[204] M. A. Ferguson and S. S. Waikar, 'Established and Emerging Markers of Kidney Function', *Clinical Chemistry*, vol. 58, no. 4, pp. 680–689, Apr. 2012, doi: 10.1373/clinchem.2011.167494.

[205] J. C. Sirota *et al.*, 'Urine IL-18, NGAL, IL-8 and serum IL-8 are biomarkers of acute kidney injury following liver transplantation', *BMC Nephrology*, vol. 14, no. 1, Dec. 2013, doi: 10.1186/1471-2369-14-17.

[206] M. M. A. L. Pelsers, 'Fatty acid-binding protein as marker for renal injury', *Scandinavian Journal of Clinical and Laboratory Investigation*, vol. 68, no. sup241, pp. 73–77, Jan. 2008, doi: 10.1080/00365510802150133.

[207] A. Gámez-Valero, S. I. Lozano-Ramos, I. Bancu, R. Lauzurica-Valdemoros, and F. E. Borràs, 'Urinary Extracellular Vesicles as Source of Biomarkers in Kidney Diseases', *Frontiers in Immunology*, vol. 6, no. 6, Jan. 2015, doi: 10.3389/fimmu.2015.00006.

[208] M. Salih, R. Zietse, and E. J. Hoorn, 'Urinary extracellular vesicles and the kidney: biomarkers and beyond', *American Journal of Physiology-Renal Physiology*, vol. 306, no. 11, pp. F1251–F1259, Jun. 2014, doi: 10.1152/ajprenal.00128.2014.

[209] M. Yáñez-Mó *et al.*, 'Biological properties of extracellular vesicles and their physiological functions', *Journal of Extracellular Vesicles*, vol. 4, no. 1, p. 27066, Jan. 2015, doi: 10.3402/jev.v4.27066.

[210] J. Lötvall *et al.*, 'Minimal experimental requirements for definition of extracellular vesicles and their functions: a position statement from the International Society for Extracellular Vesicles', *Journal of Extracellular Vesicles*, vol. 3, no. 1, p. 26913, Jan. 2014, doi: 10.3402/jev.v3.26913.

[211] S. J. Gould and G. Raposo, 'As we wait: coping with an imperfect nomenclature for extracellular vesicles', *Journal of Extracellular Vesicles*, vol. 2, no. 1, p. 20389, Jan. 2013, doi: 10.3402/jev.v2i0.20389.

[212] E. Rodríguez-Suárez *et al.*, 'Quantitative proteomic analysis of hepatocyte-secreted extracellular vesicles reveals candidate markers for liver toxicity', *Journal of proteomics*, vol. 103, pp. 227–240, 2014.

[213] S. Mathivanan, C. J. Fahner, G. E. Reid, and R. J. Simpson, 'ExoCarta 2012: database of exosomal proteins, RNA and lipids', *Nucleic Acids Research*, vol. 40, no. D1, pp. D1241–D1244, Jan. 2012, doi: 10.1093/nar/gkr828.

[214] H. Kalra *et al.*, 'Vesiclepedia: A Compendium for Extracellular Vesicles with Continuous Community Annotation', *PLoS Biology*, vol. 10, no. 12, p. e1001450, Dec. 2012, doi: 10.1371/journal.pbio.1001450.

[215] D.-K. Kim *et al.*, 'EVpedia: an integrated database of high-throughput data for systemic analyses of extracellular vesicles', *Journal of Extracellular Vesicles*, vol. 2, no. 1, p. 20384, Jan. 2013, doi: 10.3402/jev.v2i0.20384.

[216] D.-K. Kim *et al.*, 'EVpedia: a community web portal for extracellular vesicles research', *Bioinformatics*, vol. 31, no. 6, pp. 933–939, Mar. 2015, doi: 10.1093/bioinformatics/btu741.

[217] V. Thongboonkerd, K. R. Mcleish, J. M. Arthur, and J. B. Klein, 'Proteomic analysis of normal human urinary proteins isolated by acetone precipitation or ultracentrifugation', *Kidney International*, vol. 62, no. 4, pp. 1461–1469, Oct. 2002, doi: 10.1111/j.1523-1755.2002.kid565.x.

[218] T. Pisitkun, R.-F. Shen, and M. A. Knepper, 'Identification and proteomic profiling of exosomes in human urine', *Proc. Natl. Acad. Sci. U.S.A.*, vol. 101, no. 36, pp. 13368–13373, Sep. 2004, doi: 10.1073/pnas.0403453101.

[219] D. Kerjaschki *et al.*, 'Transcellular transport and membrane insertion of the C5b-9 membrane attack complex of complement by glomerular epithelial cells in experimental membranous nephropathy', *J. Immunol.*, vol. 143, no. 2, pp. 546–552, Jul. 1989.

[220] G. Pocsfalvi, D. A. A. Raj, I. Fiume, A. Vilasi, F. Trepiccione, and G. Capasso, 'Urinary extracellular vesicles as reservoirs of altered proteins during the pathogenesis of polycystic kidney disease', *PROTEOMICS - Clinical Applications*, vol. 9, no. 5–6, pp. 552–567, Jun. 2015, doi: 10.1002/prca.201400199.

[221] S. Alvarez *et al.*, 'Urinary Exosomes as a Source of Kidney Dysfunction Biomarker in Renal Transplantation', *Transplantation Proceedings*, vol. 45, no. 10, pp. 3719–3723, Dec. 2013, doi: 10.1016/j.transproceed.2013.08.079.

[222] K. W. Witwer *et al.*, 'Standardization of sample collection, isolation and analysis methods in extracellular vesicle research', *Journal of Extracellular Vesicles*, vol. 2, no. 1, p. 20360, Jan. 2013, doi: 10.3402/jev.v2i0.20360.

[223] P. Saetun, T. Semangoen, and V. Thongboonkerd, 'Characterizations of urinary sediments precipitated after freezing and their effects on urinary protein and

chemical analyses', *American Journal of Physiology-Renal Physiology*, vol. 296, no. 6, pp. F1346–F1354, Jun. 2009, doi: 10.1152/ajprenal.90736.2008.

[224] H. Zhou *et al.*, 'Collection, storage, preservation, and normalization of human urinary exosomes for biomarker discovery', *Kidney international*, vol. 69, no. 8, pp. 1471–1476, 2006.

[225] A. R. Huebner *et al.*, 'Exosomes in Urine Biomarker Discovery', *Urine Proteomics in Kidney Disease Biomarker Discovery*. Springer Netherlands, Dordrecht, pp. 43–58, 2015, [Online]. Available: https://doi.org/10.1007/978-94-017-9523-4_5.

[226] M. Macías *et al.*, 'Comparison of six commercial serum exosome isolation methods suitable for clinical laboratories. Effect in cytokine analysis', *Clinical Chemistry and Laboratory Medicine (CCLM)*, vol. 57, no. 10, pp. 1539–1545, Sep. 2019, doi: 10.1515/cclm-2018-1297.

[227] R. J. Simpson and S. Mathivanan, 'Extracellular microvesicles: the need for internationally recognised nomenclature and stringent purification criteria.', 2012.

[228] M. L. Merchant, I. M. Rood, J. K. J. Deegens, and J. B. Klein, 'Isolation and characterization of urinary extracellular vesicles: implications for biomarker discovery', *Nature Reviews Nephrology*, vol. 13, no. 12, pp. 731–749, Dec. 2017, doi: 10.1038/nrneph.2017.148.

[229] A. Gámez-Valero, M. Monguió-Tortajada, L. Carreras-Planella, M. Franquesa, K. Beyer, and F. E. Borràs, 'Size-Exclusion Chromatography-based isolation minimally alters Extracellular Vesicles' characteristics compared to precipitating agents', *Scientific Reports*, vol. 6, no. 1, Dec. 2016, doi: 10.1038/srep33641.

[230] I. M. Rood *et al.*, 'Comparison of three methods for isolation of urinary microvesicles to identify biomarkers of nephrotic syndrome', *Kidney International*, vol. 78, no. 8, pp. 810–816, Oct. 2010, doi: 10.1038/ki.2010.262.

[231] H. Kalra *et al.*, 'Comparative proteomics evaluation of plasma exosome isolation techniques and assessment of the stability of exosomes in normal human blood plasma', *PROTEOMICS*, vol. 13, no. 22, pp. 3354–3364, Nov. 2013, doi: 10.1002/pmic.201300282.

[232] K. Brennan *et al.*, 'A comparison of methods for the isolation and separation of extracellular vesicles from protein and lipid particles in human serum', *Scientific Reports*, vol. 10, no. 1, Dec. 2020, doi: 10.1038/s41598-020-57497-7.

[233] R. J. Lobb *et al.*, 'Optimized exosome isolation protocol for cell culture supernatant and human plasma', *Journal of Extracellular Vesicles*, vol. 4, no. 1, p. 27031, Jan. 2015, doi: 10.3402/jev.v4.27031.

[234] L. Balaj *et al.*, 'Heparin affinity purification of extracellular vesicles', *Scientific Reports*, vol. 5, no. 1, Sep. 2015, doi: 10.1038/srep10266.

[235] W. Nakai *et al.*, 'A novel affinity-based method for the isolation of highly purified extracellular vesicles', *Scientific Reports*, vol. 6, no. 1, Dec. 2016, doi: 10.1038/srep33935.

[236] O. P. B. Wiklander *et al.*, 'Systematic Methodological Evaluation of a Multiplex Bead-Based Flow Cytometry Assay for Detection of Extracellular Vesicle Surface Signatures', *Frontiers in Immunology*, vol. 9, Jun. 2018, doi: 10.3389/fimmu.2018.01326.

[237] A. Cheruvanky *et al.*, 'Rapid isolation of urinary exosomal biomarkers using a nanomembrane ultrafiltration concentrator', *American Journal of Physiology-Renal Physiology*, vol. 292, no. 5, pp. F1657–F1661, May 2007, doi: 10.1152/ajprenal.00434.2006.

[238] K. C. Miranda *et al.*, 'Nucleic acids within urinary exosomes/microvesicles are potential biomarkers for renal disease', *Kidney International*, vol. 78, no. 2, pp. 191–199, Jul. 2010, doi: 10.1038/ki.2010.106.

[239] P. Gonzales, T. Pisitkun, and M. A. Knepper, 'Urinary exosomes: is there a future?', *Nephrology Dialysis Transplantation*, vol. 23, no. 6, pp. 1799–1801, Mar. 2008, doi: 10.1093/ndt/gfn058.

[240] M. L. Alvarez, M. Khosroheidari, R. Kanchi Ravi, and J. K. DiStefano, 'Comparison of protein, microRNA, and mRNA yields using different methods of urinary exosome isolation for the discovery of kidney disease biomarkers', *Kidney International*, vol. 82, no. 9, pp. 1024–1032, Nov. 2012, doi: 10.1038/ki.2012.256.

[241] A. Bobrie, M. Colombo, S. Krumeich, G. Raposo, and C. Théry, 'Diverse subpopulations of vesicles secreted by different intracellular mechanisms are present in exosome preparations obtained by differential ultracentrifugation', *Journal of Extracellular Vesicles*, vol. 1, no. 1, p. 18397, Jan. 2012, doi: 10.3402/jev.v1i0.18397.

[242] M. Monguió-Tortajada, M. Morón-Font, A. Gámez-Valero, L. Carreras-Planella, F. E. Borràs, and M. Franquesa, 'Extracellular-Vesicle Isolation from Different

Biological Fluids by Size-Exclusion Chromatography', *Current Protocols in Stem Cell Biology*, no. 49, p. e82, Jan. 2019, doi: 10.1002/cpsc.82.

[243] Z. Grubisic, P. Rempp, and H. Benoit, 'A universal calibration for gel permeation chromatography', *Journal of Polymer Science Part B: Polymer Letters*, vol. 5, no. 9, pp. 753–759, Sep. 1967, doi: 10.1002/pol.1967.110050903.

[244] S. I. Lozano-Ramos *et al.*, 'Molecular profile of urine extracellular vesicles from normo-functional kidneys reveal minimal differences between living and deceased donors', *BMC Nephrology*, vol. 19, no. 1, Dec. 2018, doi: 10.1186/s12882-018-0985-3.

[245] M. Monguió-Tortajada, C. Gálvez-Montón, A. Bayes-Genis, S. Roura, and F. E. Borràs, 'Extracellular vesicle isolation methods: rising impact of size-exclusion chromatography', *Cellular and Molecular Life Sciences*, vol. 76, no. 12, pp. 2369–2382, Jun. 2019, doi: 10.1007/s00018-019-03071-y.

[246] L. Carreras-Planella *et al.*, 'Characterization and proteomic profile of extracellular vesicles from peritoneal dialysis efflux', *PLOS ONE*, vol. 12, no. 5, p. e0176987, May 2017, doi: 10.1371/journal.pone.0176987.

[247] M. Rodríguez *et al.*, 'Identification of non-invasive miRNAs biomarkers for prostate cancer by deep sequencing analysis of urinary exosomes', *Molecular Cancer*, vol. 16, no. 1, Dec. 2017, doi: 10.1186/s12943-017-0726-4.

[248] D. Orton and A. Doucette, 'Proteomic Workflows for Biomarker Identification Using Mass Spectrometry — Technical and Statistical Considerations during Initial Discovery', *Proteomes*, vol. 1, no. 2, pp. 109–127, Aug. 2013, doi: 10.3390/proteomes1020109.

[249] K. Tanaka *et al.*, 'Protein and polymer analyses up tom/z 100 000 by laser ionization time-of-flight mass spectrometry', *Rapid Communications in Mass Spectrometry*, vol. 2, no. 8, pp. 151–153, Aug. 1988, doi: 10.1002/rcm.1290020802.

[250] X. Li, W. Wang, and J. Chen, 'Recent progress in mass spectrometry proteomics for biomedical research', *Science China Life Sciences*, vol. 60, no. 10, pp. 1093–1113, Oct. 2017, doi: 10.1007/s11427-017-9175-2.

[251] C. E. Parker and C. H. Borchers, 'Mass spectrometry based biomarker discovery, verification, and validation - Quality assurance and control of protein biomarker assays', *Molecular Oncology*, vol. 8, no. 4, pp. 840–858, Jun. 2014, doi: 10.1016/j.molonc.2014.03.006.

[252] E. C. Nice, 'The status of proteomics as we enter the 2020s: Towards personalised/precision medicine', *Analytical Biochemistry*, p. 113840, Jul. 2020, doi: 10.1016/j.ab.2020.113840.

[253] E. Borràs and E. Sabidó, 'What is targeted proteomics? A concise revision of targeted acquisition and targeted data analysis in mass spectrometry', *PROTEOMICS*, vol. 17, no. 17–18, p. 1700180, Sep. 2017, doi: 10.1002/pmic.201700180.

[254] S. J. T. Hidalgo *et al.*, 'A Master Pipeline for Discovery and Validation of Biomarkers', in *Machine Learning for Health Informatics*, vol. 9605, A. Holzinger, Ed. Cham: Springer International Publishing, 2016, pp. 259–288.

[255] S. S. Waikar, V. S. Sabbisetti, and J. V. Bonventre, 'Normalization of urinary biomarkers to creatinine during changes in glomerular filtration rate', *Kidney International*, vol. 78, no. 5, pp. 486–494, Sep. 2010, doi: 10.1038/ki.2010.165.

[256] M. Mussap *et al.*, 'Cystatin C is a more sensitive marker than creatinine for the estimation of GFR in type 2 diabetic patients', *Kidney International*, vol. 61, no. 4, pp. 1453–1461, Apr. 2002, doi: 10.1046/j.1523-1755.2002.00253.x.

[257] A. H. Gheinani *et al.*, 'Improved isolation strategies to increase the yield and purity of human urinary exosomes for biomarker discovery', *Scientific Reports*, vol. 8, no. 1, Dec. 2018, doi: 10.1038/s41598-018-22142-x.

[258] T. Pisitkun, M. T. Gandolfo, S. Das, M. A. Knepper, and S. M. Bagnasco, 'Application of systems biology principles to protein biomarker discovery: urinary exosomal proteome in renal transplantation', *Proteomics Clin Appl*, vol. 6, no. 5–6, pp. 268–278, Jun. 2012, doi: 10.1002/prca.201100108.

[259] P. Fernández-Llama, S. Khositseth, P. A. Gonzales, R. A. Star, T. Pisitkun, and M. A. Knepper, 'Tamm-Horsfall protein and urinary exosome isolation', *Kidney Int.*, vol. 77, no. 8, pp. 736–742, Apr. 2010, doi: 10.1038/ki.2009.550.

[260] F. Braun *et al.*, 'The proteome of small urinary extracellular vesicles after kidney transplantation as an indicator of renal cellular biology and a source for markers predicting outcome', *bioRxiv*, Nov. 2019, doi: 10.1101/845941.

[261] H.-Y. Jung *et al.*, 'Potential urinary extracellular vesicle protein biomarkers of chronic active antibody-mediated rejection in kidney transplant recipients', *Journal of Chromatography B*, vol. 1138, p. 121958, Feb. 2020, doi: 10.1016/j.jchromb.2019.121958.

[262] J. Park *et al.*, 'Integrated Kidney Exosome Analysis for the Detection of Kidney Transplant Rejection', *ACS Nano*, vol. 11, no. 11, pp. 11041–11046, Nov. 2017, doi: 10.1021/acsnano.7b05083.

[263] T. K. Sigdel *et al.*, 'Perturbations in the Urinary Exosome in Transplant Rejection', *Frontiers in Medicine*, vol. 1:57, Jan. 2015, doi: 10.3389/fmed.2014.00057.

[264] A. Kamińska *et al.*, 'Urinary Extracellular Vesicles: Potential Biomarkers of Renal Function in Diabetic Patients', *Journal of Diabetes Research*, vol. 2016, pp. 1–12, 2016, doi: 10.1155/2016/5741518.

[265] F. G. Cosio, H. Amer, J. P. Grande, T. S. Larson, M. D. Stegall, and M. D. Griffin, 'Comparison of low versus high tacrolimus levels in kidney transplantation: assessment of efficacy by protocol biopsies', *Transplantation*, vol. 83, no. 4, pp. 411–416, Feb. 2007, doi: 10.1097/01.tp.0000251807.72246.7d.

[266] H. Ekberg *et al.*, 'Cyclosporine, tacrolimus and sirolimus retain their distinct toxicity profiles despite low doses in the Symphony study', *Nephrol. Dial. Transplant.*, vol. 25, no. 6, pp. 2004–2010, Jun. 2010, doi: 10.1093/ndt/gfp778.

[267] N. Lynöe, M. Sandlund, G. Dahlqvist, and L. Jacobsson, 'Informed consent: study of quality of information given to participants in a clinical trial', *BMJ*, vol. 303, no. 6803, pp. 610–613, Sep. 1991.

[268] M. Puhka *et al.*, 'KeepEX, a simple dilution protocol for improving extracellular vesicle yields from urine', *European Journal of Pharmaceutical Sciences*, vol. 98, pp. 30–39, Feb. 2017, doi: 10.1016/j.ejps.2016.10.021.

[269] I. Lozano-Ramos *et al.*, 'Size-exclusion chromatography-based enrichment of extracellular vesicles from urine samples', *Journal of Extracellular Vesicles*, vol. 4, no. 1, p. 27369, Jan. 2015, doi: 10.3402/jev.v4.27369.

[270] The UniProt Consortium, 'UniProt: a worldwide hub of protein knowledge', *Nucleic Acids Research*, vol. 47, no. D1, pp. D506–D515, Jan. 2019, doi: 10.1093/nar/gky1049.

[271] J. Cox and M. Mann, 'MaxQuant enables high peptide identification rates, individualized p.p.b.-range mass accuracies and proteome-wide protein quantification', *Nat. Biotechnol.*, vol. 26, no. 12, pp. 1367–1372, Dec. 2008, doi: 10.1038/nbt.1511.

[272] L. Arike, K. Valgepea, L. Peil, R. Nahku, K. Adamberg, and R. Vilu, 'Comparison and applications of label-free absolute proteome quantification methods on

Escherichia coli', *J Proteomics*, vol. 75, no. 17, pp. 5437–5448, Sep. 2012, doi: 10.1016/j.jprot.2012.06.020.

[273] G. Stelzer *et al.*, 'The GeneCards Suite: From Gene Data Mining to Disease Genome Sequence Analyses', *Current Protocols in Bioinformatics*, vol. 54, no. 1, Jun. 2016, doi: 10.1002/cpbi.5.

[274] F. Desiere, 'The PeptideAtlas project', *Nucleic Acids Research*, vol. 34, no. 90001, pp. D655–D658, Jan. 2006, doi: 10.1093/nar/gkj040.

[275] B. MacLean *et al.*, 'Skyline: an open source document editor for creating and analyzing targeted proteomics experiments', *Bioinformatics*, vol. 26, no. 7, pp. 966–968, Apr. 2010, doi: 10.1093/bioinformatics/btq054.

[276] M. Pathan *et al.*, 'FunRich: An open access standalone functional enrichment and interaction network analysis tool', *PROTEOMICS*, vol. 15, no. 15, pp. 2597–2601, Aug. 2015, doi: 10.1002/pmic.201400515.

[277] M. Pathan *et al.*, 'A novel community driven software for functional enrichment analysis of extracellular vesicles data', *Journal of Extracellular Vesicles*, vol. 6, no. 1, p. 1321455, Dec. 2017, doi: 10.1080/20013078.2017.1321455.

[278] M. Ashburner *et al.*, 'Gene Ontology: tool for the unification of biology', *Nature Genetics*, vol. 25, no. 1, pp. 25–29, May 2000, doi: 10.1038/75556.

[279] The Gene Ontology Consortium, 'The Gene Ontology Resource: 20 years and still GOing strong', *Nucleic Acids Research*, vol. 47, no. D1, pp. D330–D338, Jan. 2019, doi: 10.1093/nar/gky1055.

[280] T. S. Keshava Prasad *et al.*, 'Human Protein Reference Database--2009 update', *Nucleic Acids Research*, vol. 37, no. Database, pp. D767–D772, Jan. 2009, doi: 10.1093/nar/gkn892.

[281] D. Maglott, J. Ostell, K. D. Pruitt, and T. Tatusova, 'Entrez Gene: gene-centered information at NCBI', *Nucleic Acids Research*, vol. 35, no. Database, pp. D26–D31, Jan. 2007, doi: 10.1093/nar/gkl993.

[282] The UniProt Consortium, 'The Universal Protein Resource (UniProt) in 2010', *Nucleic Acids Research*, vol. 38, no. suppl_1, pp. D142–D148, Jan. 2010, doi: 10.1093/nar/gkp846.

[283] H. Heberle, G. V. Meirelles, F. R. da Silva, G. P. Telles, and R. Minghim, 'InteractiVenn: a web-based tool for the analysis of sets through Venn diagrams',

BMC Bioinformatics, vol. 16:169, no. 1, Dec. 2015, doi: 10.1186/s12859-015-0611-3.

[284] S. Tyanova *et al.*, 'The Perseus computational platform for comprehensive analysis of (prote)omics data', *Nature Methods*, vol. 13, no. 9, pp. 731–740, Sep. 2016, doi: 10.1038/nmeth.3901.

[285] R Core Team, 'R: The R Project for Statistical Computing. R Foundation for Statistical Computing, Vienna, Austria.', 2017. https://www.r-project.org/ (accessed Jan. 17, 2020).

[286] IBM Corp., *IBM SPSS Statistics for Windows. Available from: https://hadoop.apache.org*. Armonk, NY: IBM Corp., 2017.

[287] A. Subramanian *et al.*, 'Gene set enrichment analysis: A knowledge-based approach for interpreting genome-wide expression profiles', *Proceedings of the National Academy of Sciences*, vol. 102, no. 43, pp. 15545–15550, Oct. 2005, doi: 10.1073/pnas.0506580102.

[288] A. Liberzon, A. Subramanian, R. Pinchback, H. Thorvaldsdottir, P. Tamayo, and J. P. Mesirov, 'Molecular signatures database (MSigDB) 3.0', *Bioinformatics*, vol. 27, no. 12, pp. 1739–1740, Jun. 2011, doi: 10.1093/bioinformatics/btr260.

[289] M. An, J. Wu, J. Zhu, and D. M. Lubman, 'Comparison of an Optimized Ultracentrifugation Method versus Size-Exclusion Chromatography for Isolation of Exosomes from Human Serum', *J. Proteome Res.*, vol. 17, no. 10, pp. 3599–3605, 05 2018, doi: 10.1021/acs.jproteome.8b00479.

[290] B. J. Benedikter *et al.*, 'Ultrafiltration combined with size exclusion chromatography efficiently isolates extracellular vesicles from cell culture media for compositional and functional studies', *Scientific Reports*, vol. 7, no. 1, pp. 1–13, Dec. 2017, doi: 10.1038/s41598-017-15717-7.

[291] A. Schwarz *et al.*, 'Biopsy-diagnosed renal disease in patients after transplantation of other organs and tissues', *Am. J. Transplant.*, vol. 10, no. 9, pp. 2017–2025, Sep. 2010, doi: 10.1111/j.1600-6143.2010.03224.x.

[292] X. Wang *et al.*, 'Unique molecular profile of exosomes derived from primary human proximal tubular epithelial cells under diseased conditions', *Journal of Extracellular Vesicles*, vol. 6, no. 1, p. 1314073, Dec. 2017, doi: 10.1080/20013078.2017.1314073.

[293] A. B. Farris and R. B. Colvin, 'Renal interstitial fibrosis: mechanisms and evaluation', *Curr. Opin. Nephrol. Hypertens.*, vol. 21, no. 3, pp. 289–300, May 2012, doi: 10.1097/MNH.0b013e3283521cfa.

[294] L. Gewin and R. Zent, 'How does TGF-β mediate tubulointerstitial fibrosis?', *Semin. Nephrol.*, vol. 32, no. 3, pp. 228–235, May 2012, doi: 10.1016/j.semnephrol.2012.04.001.

[295] I. Grgic, J. S. Duffield, and B. D. Humphreys, 'The origin of interstitial myofibroblasts in chronic kidney disease', *Pediatr. Nephrol.*, vol. 27, no. 2, pp. 183–193, Feb. 2012, doi: 10.1007/s00467-011-1772-6.

[296] R. M. Carew, B. Wang, and P. Kantharidis, 'The role of EMT in renal fibrosis', *Cell and Tissue Research*, vol. 347, no. 1, pp. 103–116, Jan. 2012, doi: 10.1007/s00441-011-1227-1.

[297] M. Puigmulé *et al.*, 'Differential proteomic analysis of cyclosporine A-induced toxicity in renal proximal tubule cells', *Nephrol. Dial. Transplant.*, vol. 24, no. 9, pp. 2672–2686, Sep. 2009, doi: 10.1093/ndt/gfp149.

[298] Z. Xiao *et al.*, 'Mechanisms of renal cell apoptosis induced by cyclosporine A: a systematic review of in vitro studies', *Am. J. Nephrol.*, vol. 33, no. 6, pp. 558–566, 2011, doi: 10.1159/000328584.

[299] D. Jenkins and A. S. Woolf, 'Uroplakins: New molecular players in the biology of urinary tract malformations', *Kidney International*, vol. 71, no. 3, pp. 195–200, Feb. 2007, doi: 10.1038/sj.ki.5002053.

[300] G. Min, H. Wang, T.-T. Sun, and X.-P. Kong, 'Structural basis for tetraspanin functions as revealed by the cryo-EM structure of uroplakin complexes at 6-Å resolution', *Journal of Cell Biology*, vol. 173, no. 6, pp. 975–983, Jun. 2006, doi: 10.1083/jcb.200602086.

[301] T. Karashima, 'Interaction of periplakin and envoplakin with intermediate filaments', *Journal of Cell Science*, vol. 115, no. 24, pp. 5027–5037, Dec. 2002, doi: 10.1242/jcs.00191.

[302] C. Ruhrberg, M. A. Hajibagheri, M. Simon, T. P. Dooley, and F. M. Watt, 'Envoplakin, a novel precursor of the cornified envelope that has homology to desmoplakin.', *The Journal of Cell Biology*, vol. 134, no. 3, pp. 715–729, Aug. 1996, doi: 10.1083/jcb.134.3.715.

[303] C. Ruhrberg, M. A. N. Hajibagheri, D. A. D. Parry, and F. M. Watt, 'Periplakin, a Novel Component of Cornified Envelopes and Desmosomes That Belongs to the Plakin Family and Forms Complexes with Envoplakin', *Journal of Cell Biology*, vol. 139, no. 7, pp. 1835–1849, Dec. 1997, doi: 10.1083/jcb.139.7.1835.

[304] M. Salih *et al.*, 'Proteomics of urinary vesicles links plakins and complement to polycystic kidney disease', *Journal of the American Society of Nephrology*, vol. 27, no. 10, pp. 3079–3092, Oct. 2016, doi: 10.1681/ASN.2015090994.

[305] T. K. Sigdel and M. M. Sarwal, 'Assessment of circulating protein signatures for kidney transplantation in pediatric recipients', *Frontiers in Medicine*, vol. 4, Jun. 2017, doi: 10.3389/fmed.2017.00080.

[306] E. Sarró, C. Jacobs-Cachá, E. Itarte, and A. Meseguer, 'A pharmacologically-based array to identify targets of cyclosporine A-induced toxicity in cultured renal proximal tubule cells', *Toxicology and Applied Pharmacology*, vol. 258, no. 2, pp. 275–287, Jan. 2012, doi: 10.1016/j.taap.2011.11.007.

[307] F. Lamoureux, E. Mestre, M. Essig, F. L. Sauvage, P. Marquet, and L. N. Gastinel, 'Quantitative proteomic analysis of cyclosporine-induced toxicity in a human kidney cell line and comparison with tacrolimus', *Journal of Proteomics*, vol. 75, no. 2, pp. 677–694, Dec. 2011, doi: 10.1016/j.jprot.2011.09.005.

[308] T. L. Williams, C. Bastos, N. Faria, and F. E. Karet Frankl, 'Making urinary extracellular vesicles a clinically tractable source of biomarkers for inherited tubulopathies using a small volume precipitation method: proof of concept', *J. Nephrol.*, vol. 33, no. 2, pp. 383–386, Apr. 2020, doi: 10.1007/s40620-019-00653-8.

[309] S. M. Meehan *et al.*, 'Platelets and capillary injury in acute humoral rejection of renal allografts', *Human Pathology*, vol. 34, no. 6, pp. 533–540, Jun. 2003, doi: 10.1016/S0046-8177(03)00189-8.

[310] Z. X. Yu *et al.*, 'Targeting Complement Pathways During Cold Ischemia and Reperfusion Prevents Delayed Graft Function', *American Journal of Transplantation*, vol. 16, no. 9, pp. 2589–2597, Sep. 2016, doi: 10.1111/ajt.13797.

[311] A. A. Nargesi, L. O. Lerman, and A. Eirin, 'Mesenchymal Stem Cell-derived Extracellular Vesicles for Renal Repair', *Current Gene Therapy*, vol. 17(1): 29–42, Jul. 2017, doi: 10.2174/1566523217666170412110724.

[312] F. Fatima *et al.*, 'Non-coding RNAs in Mesenchymal Stem Cell-Derived Extracellular Vesicles: Deciphering Regulatory Roles in Stem Cell Potency, Inflammatory Resolve, and Tissue Regeneration', *Frontiers in Genetics*, vol. 8:161, Oct. 2017, doi: 10.3389/fgene.2017.00161.

[313] V. Cantaluppi, L. Biancone, A. Quercia, M. C. Deregibus, G. Segoloni, and G. Camussi, 'Rationale of mesenchymal stem cell therapy in kidney injury', *Am. J. Kidney Dis.*, vol. 61, no. 2, pp. 300–309, Feb. 2013, doi: 10.1053/j.ajkd.2012.05.027.

[314] M. Monguió-Tortajada, R. Lauzurica-Valdemoros, and F. E. Borràs, 'Tolerance in organ transplantation: from conventional immunosuppression to extracellular vesicles', *Frontiers in Immunology*, vol. 4:1599–611matas, Sep. 2014, doi: 10.3389/fimmu.2014.00416.

[315] D. Zhang *et al.*, 'Dual sources of vitronectin in the human lower urinary tract: synthesis by urothelium vs. extravasation from the bloodstream', *American Journal of Physiology-Renal Physiology*, vol. 300, no. 2, pp. F475–F487, Feb. 2011, doi: 10.1152/ajprenal.00407.2010.

[316] J. Zhong, H.-C. Yang, V. Kon, A. B. Fogo, D. A. Lawrence, and J. Ma, 'Vitronectin-binding PAI-1 protects against the development of cardiac fibrosis through interaction with fibroblasts', *Laboratory Investigation*, vol. 94, no. 6, pp. 633–644, Jun. 2014, doi: 10.1038/labinvest.2014.51.

[317] J. Bariety, N. Hinglais, S. Bhakdi, C. Mandet, M. Rouchon, and M. D. Kazatchkine, 'Immunohistochemical study of complement S protein (Vitronectin) in normal and diseased human kidneys: relationship to neoantigens of the C5b-9 terminal complex', *Clin. Exp. Immunol.*, vol. 75, no. 1, pp. 76–81, Jan. 1989.

[318] A. Ravindran *et al.*, 'Proteomic Analysis of Complement Proteins in Membranous Nephropathy', *Kidney International Reports*, vol. 5, no. 5, pp. 618–626, May 2020, doi: 10.1016/j.ekir.2020.01.018.

[319] L. Mesnard *et al.*, 'Vitronectin dictates intraglomerular fibrinolysis in immune-mediated glomerulonephritis', *The FASEB Journal*, vol. 25, no. 10, pp. 3543–3553, Oct. 2011, doi: 10.1096/fj.11-180752.

[320] L. Peng, N. Bhatia, A. C. Parker, Y. Zhu, and W. P. Fay, 'Endogenous Vitronectin and Plasminogen Activator Inhibitor-1 Promote Neointima Formation in Murine Carotid Arteries', *Arteriosclerosis, Thrombosis, and Vascular Biology*, vol. 22, no. 6, pp. 934–939, Jun. 2002, doi: 10.1161/01.ATV.0000019360.14554.53.

[321] G. Otsuka, R. Agah, A. D. Frutkin, T. N. Wight, and D. A. Dichek, 'Transforming Growth Factor Beta 1 Induces Neointima Formation Through Plasminogen Activator Inhibitor-1–Dependent Pathways', *Arteriosclerosis, Thrombosis, and Vascular Biology*, vol. 26, no. 4, pp. 737–743, Apr. 2006, doi: 10.1161/01.ATV.0000201087.23877.e1.

[322] V. de Waard, E. K. Arkenbout, P. Carmeliet, V. Lindner, and H. Pannekoek, 'Plasminogen Activator Inhibitor 1 and Vitronectin Protect Against Stenosis in a Murine Carotid Artery Ligation Model', *Arteriosclerosis, Thrombosis, and Vascular Biology*, vol. 22, no. 12, pp. 1978–1983, Dec. 2002, doi: 10.1161/01.ATV.0000042231.04318.E6.

[323] J. M. López-Guisa, A. C. Rassa, X. Cai, S. J. Collins, and A. A. Eddy, 'Vitronectin accumulates in the interstitium but minimally impacts fibrogenesis in experimental chronic kidney disease', *American Journal of Physiology-Renal Physiology*, vol. 300, no. 5, pp. F1244–F1254, May 2011, doi: 10.1152/ajprenal.00701.2010.

[324] H. R. Lijnen, B. Van Hoef, K. Umans, and D. Collen, 'Neointima formation and thrombosis after vascular injury in transgenic mice overexpressing plasminogen activator inhibitor-1 (PAI-1)', *Journal of Thrombosis and Haemostasis*, vol. 2, no. 1, pp. 16–22, Jan. 2004, doi: 10.1111/j.1538-7836.2003.00533.x.

[325] K. T. Preissner, 'Structure and biological role of vitronectin', *Annu. Rev. Cell Biol.*, vol. 7, pp. 275–310, 1991, doi: 10.1146/annurev.cb.07.110191.001423.

[326] T. Takahashi, S. Inaba, and T. Okada, 'Vitronectin in children with renal disease-2 Examination of urinary vitronectin excretion', *The Japanese Journal of Nephrology*, vol. 37, no. 4, pp. 224–230, 1995, doi: 10.14842/jpnjnephrol1959.37.224.

[327] Z. Mohammed Ali *et al.*, 'Urine Angiotensin II Signature Proteins as Markers of Fibrosis in Kidney Transplant Recipients':, *Transplantation*, vol. 103:e146–e158, p. 1, Feb. 2019, doi: 10.1097/TP.0000000000002676.

[328] V. M. Weaver, D. J. Kotchmar, J. J. Fadrowski, and E. K. Silbergeld, 'Challenges for environmental epidemiology research: are biomarker concentrations altered by kidney function or urine concentration adjustment?', *Journal of Exposure Science & Environmental Epidemiology*, vol. 26, no. 1, pp. 1–8, Jan. 2016, doi: 10.1038/jes.2015.8.

[329] D. J. Greenblatt, B. J. Ransil, J. S. Harmatz, T. W. Smith, D. W. Duhme, and J. Koch-Weser, 'Variability of 24-Hour Urinary Creatinine Excretion by Normal Subjects', *The Journal of Clinical Pharmacology*, vol. 16, no. 7, pp. 321–328, Jul. 1976, doi: 10.1002/j.1552-4604.1976.tb01527.x.

[330] A. J. Matas *et al.*, 'Inflammation in areas of fibrosis: The DeKAF prospective cohort', *American Journal of Transplantation*, vol. 20:9, Apr. 2020, doi: 10.1111/ajt.15862.

[331] A. Øverbye *et al.*, 'Identification of prostate cancer biomarkers in urinary exosomes', *Oncotarget*, vol. 6, no. 30, pp. 30357–30376, Oct. 2015, doi: 10.18632/oncotarget.4851.

[332] L. F. Quintana *et al.*, 'Urine Proteomics to Detect Biomarkers for Chronic Allograft Dysfunction', *Journal of the American Society of Nephrology*, vol. 20, no. 2, pp. 428–435, Feb. 2009, doi: 10.1681/ASN.2007101137.

[333] T. K. Sigdel *et al.*, 'Mining the human urine proteome for monitoring renal transplant injury', *Kidney International*, vol. 89, no. 6, pp. 1244–1252, Jun. 2016, doi: 10.1016/j.kint.2015.12.049.

[334] L. Wang, T. Skotland, V. Berge, K. Sandvig, and A. Llorente, 'Exosomal proteins as prostate cancer biomarkers in urine: From mass spectrometry discovery to immunoassay-based validation', *European Journal of Pharmaceutical Sciences*, vol. 98, pp. 80–85, Feb. 2017, doi: 10.1016/j.ejps.2016.09.023.

[335] J. Kowal *et al.*, 'Proteomic comparison defines novel markers to characterize heterogeneous populations of extracellular vesicle subtypes', *Proceedings of the National Academy of Sciences*, vol. 113, no. 8, pp. E968–E977, Feb. 2016, doi: 10.1073/pnas.1521230113.

[336] J.-H. Lim *et al.*, 'Novel urinary exosomal biomarkers of acute T cell-mediated rejection in kidney transplant recipients: A cross-sectional study', *PLoS ONE*, vol. 13, no. 9, p. e0204204, 2018, doi: 10.1371/journal.pone.0204204.

SCIENTIFIC RECORD AND PHD ACTIVITIES

Name PhD candidate: Laura Carreras Planella

UAB department: Department of cell biology, physiology and immunology

PhD program: Advanced Immunology

Tutor: Dr. Francesc E. Borràs Serres

Directors: Dr. Francesc E. Borràs Serres and Dr. María Isabel Troya Saborido

Years: 2015-2020

1. LIST OF PUBLICATIONS DERIVED FROM THIS THESIS

1. Carreras-Planella L, Franquesa M, Lauzurica R, Borràs FE. *A brief history of kidney transplantation*. **Hektoen International** Journal, 2020 Sep. Summer 2020, Nephrology and Hypertension. ISSN 2155-3017.

2. Carreras-Planella L, Cucchiari D, Cañas L, Juega J, Franquesa M, Bonet J, Revuelta I, Diekmann F, Taco O, Lauzurica R, Borràs FE. *Urinary Vitronectin identifies patients with high levels of fibrosis in kidney grafts.* **Journal of Nephrology**. Accepted for publication.

3. Carreras-Planella L, Juega J, Taco O, Cañas L, Franquesa M, Lauzurica R, Borràs FE. *Proteomic Characterization of Urinary Extracellular Vesicles from Kidney-Transplanted Patients Treated with Calcineurin Inhibitors.* **International Journal of Molecular Sciences**. 2020 Oct, 21(20), 7569. Doi: 10.3390/ijms21207569.

2. LIST OF OTHER PUBLICATIONS DURING THE THESIS

1. Gámez-Valero A, Monguió-Tortajada M, Carreras-Planella L, Franquesa M, Beyer K, Borràs FE. *Size-Exclusion Chromatography-based isolation minimally alters Extracellular Vesicles' characteristics compared to precipitating agents.* **Scientific Reports**, 2016 Set, 6:33641. Doi: 10.1038/srep33641.

2. Carreras-Planella L, Borràs FE, Franquesa M. *Tolerance in transplantation: what's on the B side?.* **Mediators of Inflammation**, 2016 Nov. Doi: 10.1155/2016/8491956

3. Carreras-Planella L, Soler-Majoral J, Rubio-Esteve C, Lozano-Ramos SI, Franquesa M, Bonet J, Troya-Saborido MI, Borràs FE. *Characterization and proteomic profile of extracellular vesicles from peritoneal dialysis efflux.* **PLoS One**, 2017 May 10;12(5):e0176987. Doi: 10.1371/journal.pone.0176987.

4. Luk, F, Carreras-Planella L, Korevaar SS, de Witte SFH, Borràs FE, Betjes MG H, Baan CC, Hoogduijn MJ, Franquesa M. *Inflammatory Conditions Dictate the Effect of Mesenchymal Stem or Stromal Cells on B Cell Function.* **Frontiers in Immunology**, 2017 Aug 28;8:1042. Doi: 10.3389/fimmu.2017.01042.

5. Carreras-Planella L, Monguió-Tortajada M, Palma È, Borràs FE, Franquesa M. *Stem Cells: Immunotherapy in Solid Organ Transplantation*. Chapter in the book: **Encyclopedia of Tissue Engineering and Regenerative Medicine**, 2018. Doi: 10.1016/B978-0-12-801238-3.65441-7.

6. Lozano-Ramos SI, Bancu I, Carreras-Planella L, Monguió-Tortajada M, Cañas L, Juega J, Bonet J, Armengol MP, Lauzurica R, Borras FE. *Molecular profile of urine extracellular vesicles from normo-functional kidneys reveal minimal differences between living and deceased*

donors. **BMC Nephrology**, 2018 Jul 19(1):189. Doi: 10.1186/s12882-018-0985-3.

7. Carreras-Planella L, Monguió-Tortajada M, Borràs FE, Franquesa M. *Immunomodulatory Effect of MSC on B Cells Is Independent of Secreted Extracellular Vesicles.* **Frontiers in Immunology**, 2019 Jun 6;10:1288. Doi: 10.3389/fimmu.2019.01288.

8. Monguió-Tortajada M, Morón-Font M, Gámez-Valero A, Carreras-Planella L, Borràs FE, Franquesa M. *Extracellular-Vesicle Isolation from Different Biological Fluids by Size-Exclusion Chromatography*. **Current Protocols in Stem Cell Biology**, 2019 Jun;49(1):e82. Doi: 10.1002/cpsc.82.

9. Carreras-Planella L, Soler-Majoral J, Rubio-Esteve C, Morón-Font M, Franquesa M, Bonal J, Troya-Saborido MI, Borràs FE. *Proteomic profiling of peritoneal dialysis effluent-derived extracellular vesicles: a longitudinal study.* **Journal of Nephrology**, 2019 Dec;32(6):1021-1031. Doi: 10.1007/s40620-019-00658-3.

10. Bonomini M, Borras FE, Troya-Saborido M, Carreras-Planella L, Di Liberato L, Arduini A. *Proteomic Research in Peritoneal Dialysis*. **International Journal of Molecular Sciences**, 2020;21(15):E5489. 2020 Jul. Doi:10.3390/ijms21155489.

3. CONFERENCES AND PRESENTATIONS

Name	Type	Location	Year
RIKEN IMS-JSI International Symposium on Immunology	Oral and poster	Yokohama (Japan)	2016
23rd Annual Meeting of the Japanese Society for Peritoneal Dialysis	Oral	Kitakyushu (Japan)	2017
XI Catalan Society of Immunology Congress	Oral	Barcelona	2017
International Society for Extracellular Vesicles (ISEV) Annual Meeting	Poster	Barcelona	2018
B·DEBATE Clinical Proteomics: towards personalized medicine and health	Poster	Barcelona	2018
International Society for Extracellular Vesicles (ISEV) Annual Meeting	Oral	Kyoto (Japan)	2019

4. RESEARCH AND GENERAL ACADEMIC COURSES

Name	Location	Year
RIKEN IMS Summer Program (RISP) Lecture course	Yokohama (Japan)	2016
Course on R software programming	Badalona	2017
Practical Workshop: Bioinformatics Tools to study exosomes' effects	Derio (País Basc)	2017
Laboratory Animals Course for Researchers	Bellaterra	2018
La Caixa Foundation Technology Transfer seminars	Barcelona	2019

5. LECTURES

1. Practical lectures in the European Master in Vaccinology Erasmus + LIVE (Leading International Vaccinology Education). January 2020.
2. Practical lectures in Immunology in the Veterinary Medicine Grade. October 2020.